Molengraaffsingel 8
2629 JD DELFT
Postbus 6012
2600 JA DELFT

www.tno.nl

T +31 88 866 22 00

TNO-rapport

TNO 2022 R10283-A | Definitief rapport

Bepaling veiligheidsrisico in gebouwen bij mitigeren van uit-het-vlak bezwijken bij gebruik van de typologie-aanpak

Datum	26 september 2022
Auteur(s)	Prof.dr.ir. R.D.J.M. Steenbergen, Ir. J.P. Pru ksma, Ir. D. Moretti, Dr.ir. C.P.W.Geurts, Ir. N. Altinga
Exemplaarnummer	
Oplage	
Aantal pagina's	81 (incl. bijlagen)
Aantal bijlagen	
Opdrachtgever	Ministerie van EZK
Projectnaam	Adviesvragen EZK Bovengrond
Projectnummer	060.39973

Samenvatting

Dit rapport geeft een beschrijving van een onderzoek naar het effect dat uit-het-vlak versterkingsmaatregelen hebben op het individueel risico voor de typologieën METSELWERK1, METSELWERK2 en voor typologiegroep METSELWERK-C. Deze typologiegroep bestaat uit de typologieën METSELWERK5, METSELWERK6 en METSELWERK7. METSELWERK7 is de meest kwetsbare typologie uit deze typologiegroep en is als maatgevend beschouwd voor de gehele typologiegroep. De invloed van uit-het-vlak versterking op zowel lokaal bezwijken als op het globale gedrag (in de vorm van een toename van de verplaatsingscapaciteit) is meegenomen in de berekeningen. Het genoemde effect op het individuele risico is bepaald op basis van berekeningen met de TNO modelketen. Per locatie is bepaald of de typologie wel of niet voldoet aan de Meijdam norm nadat aangetoond is dat alle metselwerk wanden, eventueel na aanbrengen van versterkingsmaatregelen, voldoende bestand zijn tegen uit-het-vlak falen.

Voor de typologieën METSELWERK1 en METSELWERK2 volgt dat er een gebied is in Groningen waarbinnen nadat is aangetoond dat de metselwerk wanden, eventueel na aanbrengen van versterkingsmaatregelen, voldoende bestand zijn tegen uit-het-vlak falen, het risico niet voldoet aan de Meijdam norm. Dit gebied valt binnen de vlek zoals afgeleid in de rapporten [TNO, 2021b] en [TNO, 2021c], ook wel ‘vlek-in-vlek’ genoemd. In dit gebied moet ook in het vlak falen beoordeeld worden en moeten zo nodig versterkingsmaatregelen worden gerealiseerd.

In het randgebied binnen de vlek van typologie METSELWERK1 [TNO, 2021b] en typologie METSELWERK2 [TNO, 2021c], vallend buiten de genoemde vlek-in-vlek, behoeft uitsluitend te worden aangetoond dat de metselwerk wanden, eventueel na aanbrengen van versterkingsmaatregelen, voldoende bestand zijn tegen uit-het-vlak falen. Als dat het geval is, voldoet het risico aan de Meijdam norm. Voor de typologiegroep METSELWERK-C volgt dat binnen de vlek zoals afgeleid in [TNO, 2021d] uitsluitend moet worden aangetoond dat de metselwerk wanden, eventueel na aanbrengen van versterkingsmaatregelen, voldoende bestand zijn tegen uit-het-vlak falen. Als dat het geval is, voldoet het risico aan de Meijdam norm.

Inhoudsopgave

1 Inleiding

De gaswinning in Groningen leidt tot het ontstaan van ondiepe aardbevingen. Hoewel deze aardbevingen relatief licht zijn (in termen van Magnitudes op de Richterschaal), zijn de effecten aan het aardoppervlak door de relatief ondiepe locatie (3 km) van het hypocentrum aanzienlijk. Er is een grote opgave om het veiligheidsniveau voor de bewoners van Groningen te borgen.

In TNO Rapport 2020 R10628/A [TNO, 2021a] is een uniforme aanpak beschreven voor de beoordeling van de gebouwen in Groningen. Deze aanpak is erop gebaseerd dat gebouwen worden ingedeeld in een typologie. Per typologie worden de seismische kenmerken bepaald, rekening houdend met de variaties tussen gebouwen binnen die typologie. Op basis van deze kenmerken kan snel voor een gehele typologie worden bepaald of, en zo ja, waar deze voldoet aan de norm. De norm die bij de veiligheidsbeoordeling wordt gehanteerd is de Meijdam norm (het Individueel Risico per jaar moet gelijk aan of kleiner zijn dan 10^{-5}). TNO Rapport 2020 R10628/A zal vanaf nu worden aangeduid als het hoofdrapport [TNO, 2021a].

In voorliggend rapport wordt onderzocht wat het effect is van uit-het-vlak versterkingsmaatregelen van wanden op het risico voor typologieën METSELWERK1 en METSELWERK2 en voor typologiegroep METSELWERK-C. Voor de indeling in typologieën inclusief de bijbehorende kenmerken wordt verwezen naar het hoofdrapport en typologietoedelingsrapport [TNO, 2021a, 2022]. De uitwerking van bovengenoemde typologieën zonder versterking is beschreven in de typologiespecifieke rapporten [TNO, 2021b, 2021c, 2021d]. Het voorliggende rapport moet in samenhang met deze rapporten beschouwd worden.

Bij het faalmechanisme uit-het-vlak falen van metselwerkwanden kan dit het bezwijken betreffen van zowel dragende wanden als niet-dragende binnenwanden. Aan de hand van modelketenberekeningen voor typologieën METSELWERK1, METSELWERK2 en typologiegroep METSELWERK-C wordt onder voorwaarde dat aangetoond is dat alle metselwerk wanden, eventueel na aanbrengen van versterkingsmaatregelen, voldoende bestand zijn tegen uit-het-vlak falen, het individueel risico berekend per locatie in Groningen en wordt nagegaan of deze wel of niet voldoet aan de Meijdam norm.

De resultaten zijn gepresenteerd in de vorm van vlekkenkaarten. Deze kaarten tonen de vlek onder voorwaarde dat aangetoond is dat alle metselwerk wanden, eventueel na aanbrengen van versterkingsmaatregelen voldoende bestand zijn tegen uit-het-vlak falen. Voor deze kaarten geldt dat de berekende risico's inclusief de door het ACVG voorgestelde marge zijn zoals gerapporteerd in de respectievelijke typologiespecifieke rapporten [TNO, 2021b-d].

Leeswijzer

Dit rapport is als volgt opgebouwd. Hoofdstuk 2 omschrijft de methode en welke uitgangspunten zijn gekozen om het effect van uit-het-vlak versterking te bepalen. In hoofdstuk 3 worden de resultaten beschreven in de vorm van een vlekkenkaart voor typologie METSELWERK1. Hoofdstuk 4 behandelt typologie METSELWERK2 en hoofdstuk 5 behandelt typologiegroep METSELWERK-C. Ten slotte zijn in Hoofdstuk 6 de conclusies geformuleerd.

2 Afleiding van de vlekkenkaarten bij voldoende bestand zijn tegen uit-het-vlak falen

In de (typologiespecifieke) rapporten [TNO, 2021b, 2021c, 2021d] zijn de typologieën METSELWERK1 en METSELWERK2 en typologiegroep METSELWERK-C uitgewerkt en risicokaarten gepresenteerd. In deze kaarten is het gebied waar het risico voor deze typologieën boven de Meijdam norm uitkomt ingekleurd. Dit gebied wordt ook wel de vlek genoemd. Deze kaarten hebben betrekking op de niet-versterkte typologieën.

Om te beoordelen in welke mate versterkingsmaatregelen voor het uit-het vlak falen het individueel risico beïnvloeden, zijn modelketenberekeningen uitgevoerd voor de versterkte typologieën METSELWERK1 en METSELWERK2 en typologiegroep METSELWERK-C onder voorwaarde dat aangetoond is dat alle metselwerk wanden, eventueel na aanbrengen van versterkingsmaatregelen, voldoende bestand zijn tegen uit-het-vlak falen.

Ten behoeve van de risicoberekeningen zijn parameters voor het kwetsbaarheidsmodel en gevolgmodel afgeleid voor de typologieën onder voorwaarde dat aangetoond is dat alle metselwerk wanden, eventueel na aanbrengen van versterkingsmaatregelen, voldoende bestand zijn tegen uit-het-vlak falen. Deze parameters worden in dit hoofdstuk besproken.

Een uit-het-vlak versterking van niet-dragende en/of dragende wanden mag niet leiden tot verminderde weerstand (kracht en verplaatsing) tegen andere faalmechanismen. Ook mogen de globale dynamische eigenschappen niet significant zijn aangetast. Aangenomen wordt dat veel van de gebruikte oplossingen voor uit-het-vlak versterken zoals toepassen van voorzetwanden, het infrezen van strips en het aanbrengen van een koolstofnet met afwerklaag, alsmede gebruikelijke oplossingen voor versterken van verbindingen voldoen aan deze criteria.

2.1 Uit-het-vlak falen in relatie tot lokaal bezwijken (CS1 en CS2)

In paragraaf 3.5 van de typologiespecifieke rapporten [TNO, 2021b, 2021c, 2021d] is voor METSELWERK1, METSELWERK2 en METSELWERK-C beschreven dat uit-het-vlak bezwijken bij kan dragen aan de bezwijktoestanden CS1, CS2 en CS3. De bezwijktoestanden CS1 en CS2 worden gedomineerd door het uit-het-vlak falen van niet-dragende wanden. Lokaal bezwijken is in de risicoberekeningen meegenomen via een kwetsbaarheidskromme en een gevolgmodel bestaande uit overlijdenskansen corresponderend met de puinbedekkingsgraden voor bezwijktoestanden CS1 en CS2, zie bijlagen C en E van het hoofdrapport [TNO, 2021a].
Indien aangetoond is dat alle metselwerk wanden, eventueel na aanbrengen van versterkingsmaatregelen, voldoende bestand zijn tegen uit-het-vlak falen, betekent dit dat de bijdragen van de bezwijktoestanden CS1 en CS2 aan het risico ten minste een orde van grootte gereduceerd zijn. In de risicoberekening is dit in rekening gebracht door de overlijdenskansen voor CS1 en CS2 op nul in te stellen. Dit zijn de kansen Pd_inside|CS1, Pd_outside|CS1, Pd_inside|CS2 en

Pd_outside|CS2, zie bijlage E van het hoofdrapport [TNO, 2021a] en de tabel in hoofdstuk 6 van de typologiespecifieke rapporten.

2.2 Uit-het-vlak falen in relatie tot globaal bezwijken (CS3)

De bezwijktoestand CS3 kan worden gedomineerd door in-het-vlak falen van dragende metselwerk wanden of door uit-het-vlak falen van deze wanden of door een combinatie van deze twee bezwijkmechanismen. De mate waarin verschilt per typologie.

In paragraaf 3.5 van het typologiespecifieke rapport voor METSELWERK2 [TNO, 2021c] is beschreven dat CS3 falen van METSELWERK2 vooral gedomineerd wordt door in-het-vlak falen. Verwacht wordt daarom dat indien aangetoond is dat alle metselwerk wanden, eventueel na aanbrengen van versterkingsmaatregelen, voldoende bestand zijn tegen uit-het-vlak falen, er beperkt sprake is van een toename van de globale seismische weerstand. In hoofdstuk 4 wordt de keuze gemaakt voor de aan te houden parameterkeuzes voor de CS3 verplaatsingscapaciteit.

In paragraaf 3.5 van het typologiespecifieke rapport voor METSELWERK1 [TNO, 2021b] is beschreven dat CS3 falen van METSELWERK1 gedomineerd wordt door zowel in-het-vlak falen als uit-het-vlak falen. De typologie wordt beschreven aan de hand van 4 referentiegebouwen: soms is bij een gebouw uit-het-vlak falen maatgevend en soms in-het-vlak falen. Het is daarom niet zonder meer te zeggen dat er sprake zal zijn van een toename van de globale seismische weerstand voor de totale typologie, indien aangetoond is dat alle metselwerk wanden, eventueel na aanbrengen van versterkingsmaatregelen, voldoende bestand zijn tegen uit-het-vlak falen. In hoofdstuk 3 wordt hier verder op in gegaan en wordt de keuze gemaakt voor de aan te houden parameterkeuzes voor de CS3 verplaatsingscapaciteit.

In paragraaf 3.5 van het typologiespecifieke rapport voor METSELWERK-C [TNO, 2021d] wordt wel een toename verwacht van de globale seismische capaciteit indien aangetoond is dat alle metselwerk wanden, eventueel na aanbrengen van versterkingsmaatregelen, voldoende bestand zijn tegen uit-het-vlak falen. Dit omdat uit-het-vlak falen van metselwerk wanden het dominante faalmechanisme is bij deze typologie. In hoofdstuk 5 wordt hier verder op in gegaan en wordt de keuze gemaakt voor de aan te houden parameterkeuzes voor de CS3 verplaatsingscapaciteit.

In Bijlage A is via NLTH analyses voor enkele gebouwen behorende tot de typologie METSELWERK1 en typologiegroep METSELWERK-C bepaald wat de toename van de verplaatsingscapaciteit is onder de aanname dat alle metselwerk wanden, eventueel na aanbrengen van versterkingsmaatregelen, voldoende bestand zijn tegen uit-het-vlak falen. Voor typologiegroep METSELWERK-C is specifiek gekeken naar typologie METSELWERK7, de maatgevende typologie binnen deze typologiegroep.

Figuur 2.1 vat de studie uit Bijlage A samen. De volgende drie gebouwen zijn onderzocht:

- ‘Bleeksteen’ behorende tot de typologie METSELWERK1; hier is uit-het-vlak falen maatgevend.
- EUC-BUILD2 en LNEC-BUILD-3 behorende tot METSELWERK7 en variaties op deze modellen; ook hier is uit-het-vlak falen maatgevend.

De horizontale as van de grafiek is de limiet voor de lokale uit-het-vlak verplaatsing van een wand in mm, ‘No OOP’ betekent dat andere mechanismen, zoals in-het-vlak falen, dominant zijn ten opzichte van uit-het-vlak falen. Benadrukt wordt dat ‘OOP limits’ een indirect criterium zijn voor de werkelijke faalgrens van een metselwerk wand uit-het-vlak: de faalgrens is zowel gerelateerd aan kracht- als vervormingscapaciteit.
De verticale as toont de verplaatsingscapaciteit in mm voor globaal bezwijken.

De grafiek voor Bleeksteen betreft één referentiegebouw, terwijl de grafieken voor EUC-BUILD2 en LNEC-BUILD-3 de mediane toename in verplaatsingscapaciteit beschrijven voor respectievelijk 9 en 7 variaties in de gebruikte referentiegebouwen. In deze simulaties zijn gevelopeningen, metselwerkeigenschappen, vloermateriaal en de geometrie van de plattegrond gevarieerd, zie Bijlage A voor details.

Uit Figuur 2.1 volgt dat er een toename is in globale verplaatsingscapaciteit bij toenemende limietverplaatsing voor uit-het-vlak falen van wanden. In de uitwerking van de typologieën is uitgegaan van 100 mm limietverplaatsing voor uit-het-vlak falen, zie [TNO, 2021b, 2021d]. Bij ‘No OOP’ is de grens bereikt dat het maatgevende faalmechanisme van uit-het-vlak naar in-het-vlak verschuift. Dit levert de toename in verplaatsingscapaciteit zoals weergegeven in Tabel 2.1. Zoals aangegeven zijn dit de mediane waarden voor de variaties voor EUC-BUILD2 en LNEC-BUILD-3 en de specifieke waarde voor Bleeksteen.

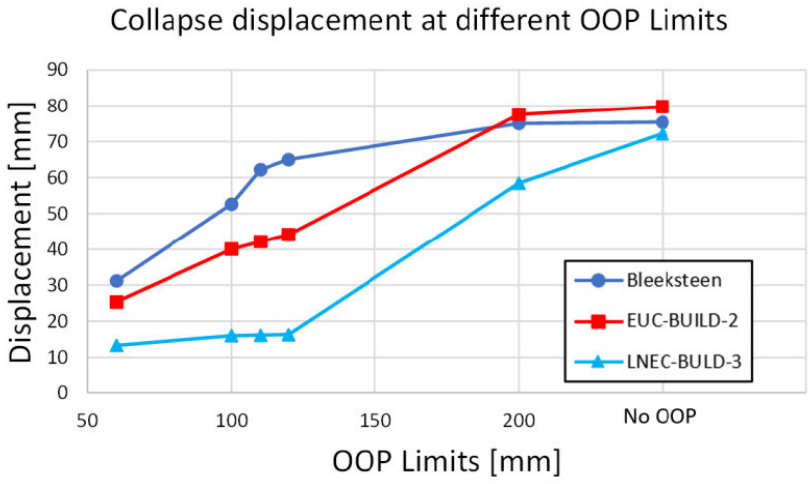

Figuur 2.1 Mediane toename verplaatsingscapaciteit (verticale as) bij mitigeren lokaal uit-het-vlak falen van 60 mm tot geen uit het vlak falen (horizontale as) voor de drie onderzochte gebouwen.

Tabel 2.1. Toename van de verplaatsingscapaciteit op basis van de berekeningen voor de 3 referentiegebouwen. De getallen kunnen afgelezen worden uit Figuur 2.1, en zijn expliciet gegeven in [Messali & Longo, 2022].

Referentiegebouw	**Globale verplaatsings-capaciteit bij 100 mm OOP limiet [mm]**	**Verplaatsings-capaciteit op de grens van het maatgevend worden van in-het vlak falen [mm]**	**Toename verplaatsings-capaciteit [%]**
Bleeksteen	52	75	44
EUC-BUILD2	40	80	100
LNEC-BUILD-3	16	72	350

Tabel 2.1 laat zien dat de globale verplaatsingscapaciteit bij onversterkte gebouwen waarbij het faalgedrag wordt gedomineerd door uit-het-vlak falen een grote mate van spreiding kent vanwege het lokale gedrag van metselwerk wanden op verschillende plaatsen in die gebouwen. Onder de aanname dat alle metselwerk wanden, eventueel na aanbrengen van versterkingsmaatregelen, voldoende bestand zijn tegen uit-het-vlak falen is de globale verplaatsingscapaciteit nagenoeg hetzelfde voor alle onderzochte gebouwen omdat er sprake is van hetzelfde globale in-het-vlak faalmechanisme. In deze situatie is er dus sprake van een grotere verplaatsingscapaciteit en naar verwachting minder spreiding in de seismische weerstand van de typologie.

2.3 Uitgangspunten berekening vlekkenkaarten bij mitigeren uit-het-vlak falen en implementatie

Op basis van de uitkomsten van de berekeningen zoals beschreven in 2.1 en 2.2 zijn de volgende uitgangspunten gehanteerd voor de typologieën METSELWERK1, METSELWERK2 en typologiegroep METSELWERK-C voor de berekening van de vlekkenkaarten onder voorwaarde dat aangetoond is dat alle metselwerk wanden, eventueel na aanbrengen van versterkingsmaatregelen, voldoende bestand zijn tegen uit-het-vlak falen.

1. In het gevolgmodel zijn de overlijdenskansen voor CS1 en CS2 op nul gesteld, zie paragraaf 2.1.
2. De verplaatsingscapaciteit voor globaal bezwijken (de kwetsbaarheidskromme parameter DL_CS3) is vergroot daar waar van toepassing; zie hiervoor de hoofdstukken 3, 4 en 5 voor respectievelijk METSELWERK1, METSELWERK2 en METSELWERK-C.
3. De overige parameters in de TNO modelketen zijn gelijk gehouden. Dit betreft o.a. de gebouw tot gebouw variatie en de modelonzekerheid.
4. De door het ACVG voorgestelde marge zoals beschreven in [TNO, 2021b, 2021d] is in rekening gebracht.

Ad 1 en 2:
De kwetsbaarheidskrommen voor typologieën METSELWERK2 en METSELWERK-C zijn afgeleid voor een enkel maatgevend referentiegebouw, zie [TNO, 2021c, 2021d]. Het doorvoeren van punt 1) is direct geïmplementeerd door de overlijdenskansen voor bezwijktoestanden CS1 en CS2 op nul te zetten in het gevolgmodel. Dit betreft het op nul zetten van de kansen Pd_inside|CS1, Pd_outside|CS1, Pd_inside|CS2 en Pd_outside|CS2 in plaats van de getallen zoals

gegeven in tabel 6 in paragraaf 4.6 van de rapporten [TNO, 2021c, 2021d]. De vergroting van de verplaatsingscapaciteit is geïmplementeerd door de limietverplaatsing DL_CS3 daar waar van toepassing te vergroten conform punt 2.

Voor METSELWERK1 zijn er meerdere referentiegebouwen gebruikt in de afleiding van de kwetsbaarheidskrommen. Om punten 1 en 2 te implementeren zijn de oorspronkelijke kwetsbaarheidskrommen voor de individuele referentiegebouwen als uitgangspunt genomen. Vervolgens is voor ieder referentiegebouw de overlijdenskans voor CS1 en CS2 op nul gesteld en vervolgens is de gecombineerde kwetsbaarheidskromme bepaald. Daarna zijn, om aan punt 3 te voldoen, de mediaanverschuiving, modelonzekerheid, gebouw-gebouw variatie weer toegevoegd zoals beschreven in [TNO, 2021b].

Ad 3:
Het niet aanpassen van de overige parameters in de modelketen betreft hoofdzakelijk de volgende punten:

a) In de berekening van het risico bij de grens van in-het-vlak falen is in de globale *backbone curve* alleen de verplaatsingscapaciteit opgehoogd daar waar dit van toepassing is. In bijlage A is te zien dat de *base shear* capaciteit ook (iets) groter wordt; ook zal de demping naar verwachting toenemen door de grotere hysterese-loop. In de gevolgde aanpak is de vorm van de backbone curve ongewijzigd en is de demping niet aangepast. De aanpak is daarom naar verwachting conservatief.
b) De gebouw tot gebouw variatie is dezelfde gehouden (bij METSELWERK7 inclusief de vergroting conform (ACVG, 2021)). Zoals in paragraaf 2.2 toegelicht zal naar verwachting de gebouw tot gebouw variatie afnemen doordat er sprake is van nog slechts één faalmechanisme. Dit faalmechanisme betreft het in-het-vlak falen; ook dit faalmechanisme kent spreiding maar minder dan voor twee gemengde faalmechanismen in-het-vlak en uit-het vlak falen. Het toepassen van de oorspronkelijke gebouw tot gebouw variatie is naar verwachting conservatief.
c) De in het hoofdrapport [TNO, 2021a] in bijlage C.4 voorgestelde verlaging van de mediane seismische capaciteit van 15% is gehandhaafd. Deze was afgeleid op basis van studies waarin kwetsbaarheidskrommen zijn afgeleid op basis van een volledige MDOF (NLTH) benadering. Een belangrijke reden voor de aanpassing van de kwetsbaarheidskromme in de vorm van een verlaging van de mediane seismische capaciteit van 15% was dat voor verschillende tijdsignalen en bij verschillende gebouwen er een plotselinge overgang tussen faalmechanismen optrad. In het geval dat alle metselwerk wanden, eventueel na aanbrengen van versterkings-maatregelen, voldoende bestand zijn tegen uit-het-vlak falen vervalt grotendeels de reden voor deze aanpassing met 15% omdat er sprake is van een éénduidig maatgevend faalmechanisme. Naar verwachting is een eventueel benodigde aanpassing minder dan deze 15%. De gevolgde aanpak is op dit punt daarom conservatief.
d) De modelonzekerheid is dezelfde gehouden. Dit is een conservatieve keuze omdat het mitigeren van een faalmechanisme met veel modelonzekerheid (uit-het-vlak falen met sterke afhankelijkheid van lokale (rand)condities) tot gevolg heeft dat een beter uit experimenten bekend faalmechanisme (in-het-vlak falen) dominant wordt.

De gevolgde implementatie is daarmee op bovenstaande punten a) t/m d) naar alle waarschijnlijkheid conservatief.

3 Vlekkenkaart typologie METSELWERK1

Voor METSELWERK1 is het risico berekend volgens de uitgangspunten beschreven in hoofdstuk 2.

Voor METSELWERK1 zijn er meerdere referentiegebouwen gebruikt in de afleiding van de kwetsbaarheidskrommen. De oorspronkelijke kwetsbaarheidskrommen voor de individuele referentiegebouwen zijn als uitgangspunt genomen om te bezien of en hoeveel de verplaatsingscapaciteit DL_CS3 vergroot kan worden als in-het-vlak falen maatgevend wordt.

In Tabel 3.1 is de waarde voor de verplaatsingscapaciteit DL_CS3 voor de 4 gebruikte referentiegebouwen weergegeven.

Tabel 3.1: Verplaatsingscapaciteit DL_CS3

Referentiegebouw	**DL_CS3 [m]**
Julianalaan 52	0,051
E45 Schildwolde	0,098
Wilgenbos	0,161
Oostergoweg	0,123

Het blijkt dat alleen referentiegebouw ‘Julianalaan 52’ een verplaatsingscapaciteit heeft die kleiner is dan verwacht mag worden uit de drift limieten voor in-het-vlak falen conform NPR 9998. In de risicobepaling is echter het referentiegebouw ‘E45 Schildwolde’ dominant, zie Bijlage B.3 van [TNO, 2021b]. Dit betekent dat vergroting van de verplaatsingscapaciteit DL_CS3 voor ‘Julianalaan 52’ geen significante invloed heeft op het berekende risico voor de gehele typologie METSELWERK1. Daarom wordt voor de typologie METSELWERK1 de verplaatsingscapaciteit voor globaal bezwijken (de kwetsbaarheidskromme parameter DL_CS3) niet vergroot.

Figuur 3.1 toont de resulterende vlekkenkaart. Voor de seismische dreiging zijn dezelfde uitgangspunten gebruikt als in de huidige beschikbare NPR webtool, voor periode t5, [NEN, 2021] (voor details zie het hoofdrapport [TNO, 2021a]).

In de blauwe vlek-in-vlek van Figuur 3.1 is de veiligheid noch lokaal, noch globaal aangetoond met de typologie-aanpak. In het roze deel van de vlek behoeft alléén het uit-het-vlak bezwijken van dragende en niet-dragende wanden te worden gecontroleerd en waar nodig worden versterkt; in de roze vlek is versterken voor globaal bezwijken niet nodig.

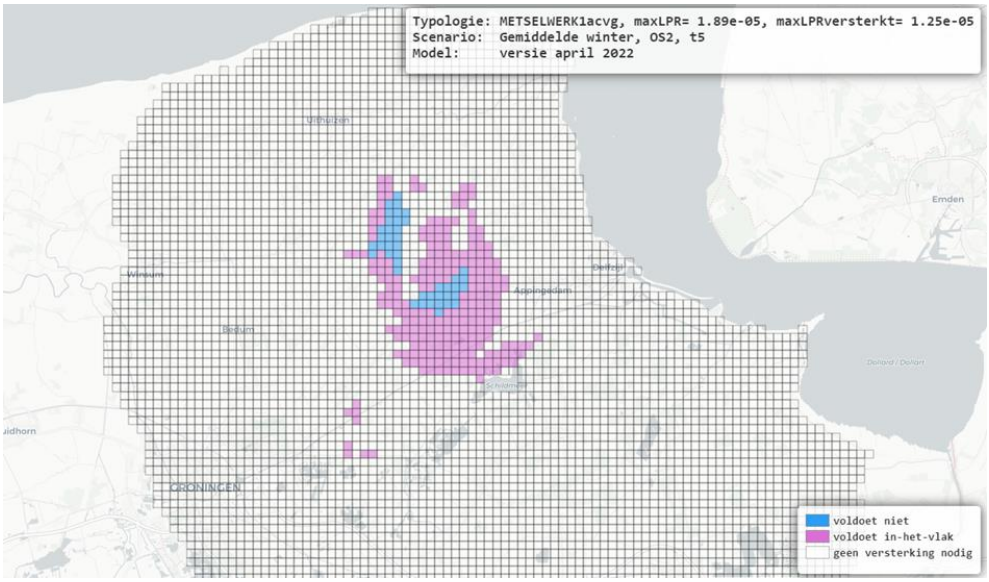

Figuur 3.1 Vlekkenkaart voor METSELWERK1 bij voldoende bestand zijn tegen uit-het-vlak falen.

4 Vlekkenkaart typologie METSELWERK2

Voor METSELWERK2 is het risico berekend volgens de uitgangspunten beschreven in hoofdstuk 2.

In paragraaf 3.5 van het typologiespecifieke rapport voor METSELWERK2 [TNO, 2021c] is beschreven dat CS3 falen van METSELWERK2 vooral gedomineerd wordt door in-het-vlak falen. Daarom wordt voor METSELWERK2 de verplaatsingscapaciteit voor globaal bezwijken (de kwetsbaarheidskromme parameter DL_CS3) niet vergroot.

Figuur 4.1 toont (in blauw) de resulterende vlek-in-vlek. In roze is de vlek van de onversterkte typologie uit [TNO, 2021c] weergegeven.

Voor de seismische dreiging zijn dezelfde uitgangspunten gebruikt als in de huidige beschikbare NPR webtool, voor periode t5 [NEN, 2021] (voor details zie het hoofdrapport [TNO, 2021a]).

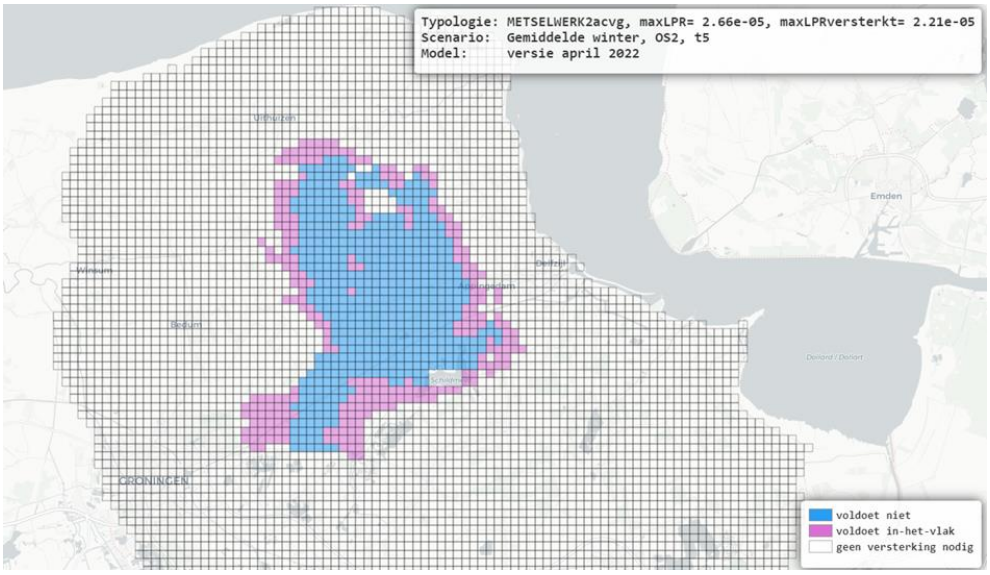

Figuur 4.1 Vlekkenkaart voor METSELWERK2 bij voldoende bestand zijn tegen uit-het-vlak falen (blauw), getoond op de vlekkenkaart van de onversterkte typologie (roze).

In de blauwe vlek-in-vlek van Figuur 4.1 is de veiligheid noch lokaal als globaal aangetoond met de typologie-aanpak. In het roze deel van de vlek behoeft alléén het uit-het-vlak bezwijken van dragende en niet-dragende wanden te worden gecontroleerd en waar nodig worden versterkt; in de roze vlek is versterken voor globaal bezwijken niet nodig.

5 Vlekkenkaart typologiegroep METSELWERK-C

De risicobeoordeling van de hele typologiegroep METSELWERK-C wordt gedaan op basis van de eigenschappen van typologie METSELWERK7 die als maatgevend voor de hele groep is beschouwd, zie [TNO, 2021d]. Voor deze typologie is het risico berekend volgens de uitgangspunten beschreven in hoofdstuk 2.

Voor METSELWERK7 is er één maatgevend referentiegebouw gebruikt in de afleiding van de kwetsbaarheidskrommen. De oorspronkelijke kwetsbaarheidskromme voor dit referentiegebouw is als uitgangspunt genomen om te bezien of en hoeveel de verplaatsingscapaciteit DL_CS3 vergroot kan worden als in-het-vlak falen maatgevend wordt.

In Tabel 5.1 is weergegeven welke de verplaatsingscapaciteit DL_CS3 is voor het gebruikte referentiegebouw.

Tabel 5.1: Verplaatsingscapaciteit DL_CS3

Referentiegebouw	**DL_CS3 [m]**
Badweg 12	0,02

Uit de studie in Bijlage A blijkt dat de verplaatsingscapaciteit bij het maatgevend worden van in-het-vlak falen aanzienlijk groter is dan de waarde weergegeven in Tabel 5.1. In Bijlage A wordt hiervoor de NPR 9998:2020 drift limiet voor ductiel of bros bezwijken genomen. Voor ductiel gedrag bedraagt de drift-limiet op effectieve hoogte 0,8% en 0,4% voor bros falen; bij een effectieve hoogte van ca. 5 m betreft dit 0,04 m en 0,02 m respectievelijk. Dit betreft rekenwaarden, de gemiddelde waarden liggen hoger, namelijk 0,07 m en 0,035 m (zie ook Bijlage A). Het is voor in-het-vlak falen niet a priori bekend of het faalmechanisme ductiel dan wel bros zal zijn, dit hangt van de eigenschappen van de betreffende wand. Als conservatieve waarde wordt daarom 0,035 m aangehouden voor de gemiddelde drift-limiet voor bros bezwijken. De spreiding in deze drift-limiet komt tot uitdrukking in de gebouw-tot-gebouw variatie die ook conservatief is gekozen (zie hoofdstuk 2). Dit betekent dat in een conservatieve benadering de verplaatsingscapaciteit voor globaal bezwijken (de kwetsbaarheidskromme parameter DL_CS3) is vergroot met 75% voor METSELWERK-C (METSELWERK7).

Figuur 5.1 toont de resulterende vlekkenkaart. Voor de seismische dreiging zijn dezelfde uitgangspunten gebruikt als in de huidige beschikbare NPR webtool, voor periode t5 [NEN, 2021] (voor details zie het hoofdrapport [TNO, 2021a]).

In Figuur 5.1 is te zien dat er geen vlek aanwezig is in de kaart. Dit betekent dat met betrekking tot in-het-vlak falen in het geval dat aangetoond is dat alle metselwerk wanden, eventueel na aanbrengen van versterkingsmaatregelen voldoende bestand zijn tegen uit-het-vlak falen met de typologie-aanpak de veiligheid is aangetoond voor METSELWERK-C. Met betrekking tot uit-het-vlak falen is met de typologie-aanpak de veiligheid niet aangetoond voor METSELWERK-C binnen de oorspronkelijke vlek uit [TNO, 2021d]. Deze oorspronkelijke vlek is weergegeven in Figuur 5.2.

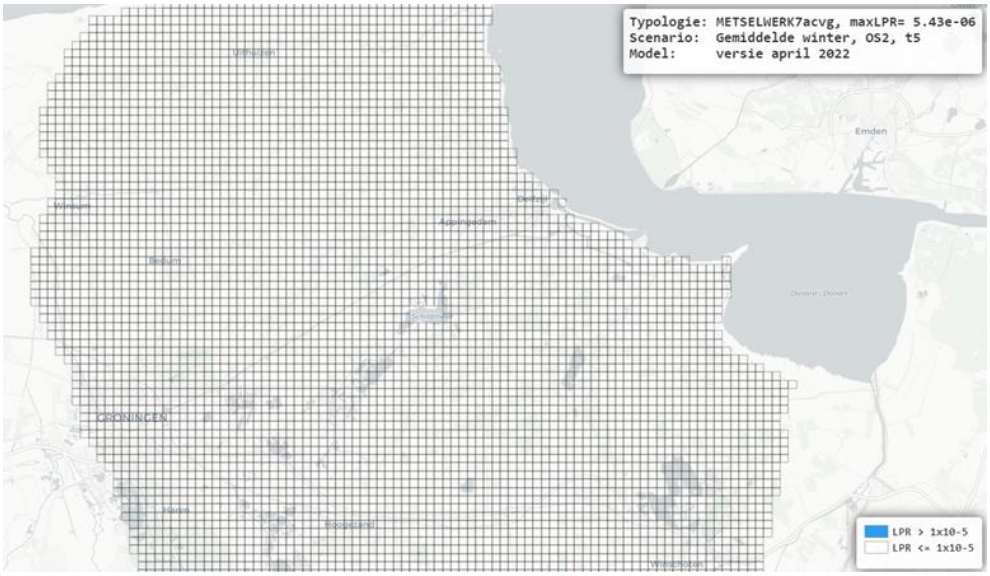

Figuur 5.1 Vlekkenkaart voor METSELWERK7 bij voldoende bestand zijn tegen uit-het-vlak falen.

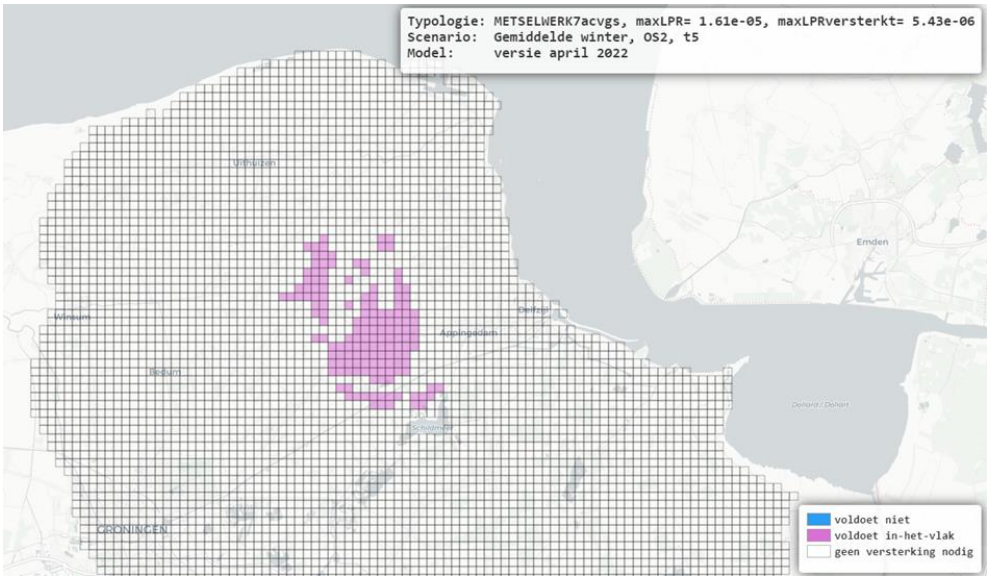

Figuur 5.2 Oorspronkelijke vlekkenkaart voor METSELWERK7 uit [TNO, 2021d]. Binnen deze vlek hoeft alleen het uit-het-vlak falen beoordeeld te worden.

6 Conclusies

Dit rapport beschrijft het onderzoek naar het effect dat uit-het-vlak versterkingsmaatregelen hebben op het individueel risico voor de typologieën METSELWERK1, METSELWERK2 en voor typologiegroep METSELWERK-C. Hiertoe zijn risicoberekeningen uitgevoerd voor deze typologieën voor de situatie dat is aangetoond dat alle metselwerk wanden, eventueel na aanbrengen van versterkingsmaatregelen, voldoende bestand zijn tegen uit-het-vlak falen.

Voor de typologiegroep METSELWERK-C geldt het volgende:

- Indien aangetoond is dat alle metselwerk wanden, eventueel na aanbrengen van versterkingsmaatregelen voldoende bestand zijn tegen uit-het-vlak falen, is de veiligheid aangetoond in geheel Groningen.
- Indien niet aangetoond is dat alle metselwerk wanden voldoende bestand zijn tegen uit-het-vlak falen is met de typologie-aanpak de veiligheid niet aangetoond binnen de vlek die is afgeleid en weergegeven in de typologiespecifieke rapporten [TNO, 2021b] en [TNO, 2021d].
- Binnen de vlek in de rapporten [TNO, 2021b] en [TNO, 2021d] is het alleen noodzakelijk het uit-het vlak falen te beoordelen en indien nodig het aanbrengen van versterkingsmaatregelen om dit uit-het vlak falen te voorkomen.

Voor de typologieën METSELWERK1 en METSELWERK2 geldt het volgende:

- Er kan onderscheid gemaakt worden binnen de vlek uit het typologiespecifieke rapport [TNO, 2021b] en [TNO, 2021c] tussen enerzijds een buitenrand waarin alleen de veiligheid met betrekking tot uit-het-vlak falen niet is aangetoond en anderzijds een vlek-in-vlek waarin de veiligheid noch voor in-het-vlak noch voor uit-het-vlak falen is aangetoond.

Voor de typologiegroep METSELWERK-C dient binnen de vlek in de rapporten [TNO, 2021b] en [TNO, 2021d] uitsluitend gecontroleerd te worden of de gebouwen voldoen aan de eisen in NPR 9998 voor uit-het-vlak falen van dragende en niet-dragende metselwerk wanden. Bij niet voldoen dienen de betreffende wanden versterkt te worden.

Voor de typologieën METSELWERK1 en METSELWERK2 dient in de getoonde vlek-in-vlek een controle te worden uitgevoerd met het betrekking tot de eisen in de NPR 9998 voor zowel in-het-vlak falen als uit-het-vlak falen. In de resterende buitenring dient alleen gecontroleerd te worden of de gebouwen voldoen aan de eisen in NPR 9998 voor uit-het-vlak falen van niet dragende metselwerk binnenwanden. Bij niet voldoen dient versterkt te worden.

Bij het ontwerp van versterkingsmaatregelen moet worden aangetoond dat het pand in de versterkte toestand in zijn geheel voldoet aan de veiligheidseisen. Een uit-het-vlak versterking van niet-dragende en/of dragende wanden mag niet leiden tot verminderde weerstand (kracht en verplaatsing) tegen andere faalmechanismen. Ook mogen de globale dynamische eigenschappen niet significant zijn aangetast. Aangenomen wordt dat veel van de gebruikte oplossingen voor uit-het-vlak versterken zoals toepassen van voorzetwanden, het infrezen van strips en het

aanbrengen van een koolstofnet met afwerklaag, alsmede gebruikelijke oplossingen voor versterken van verbindingen voldoen aan deze criteria.

7 Referenties

[ACVG, 2021]
Beoordeling aanvullingen TNO op typologie-aanpak. ACVG 202105-01. Brief aan de ministers Ollongren en Blok, 27 mei 2021

[Luco et al 2007]
Luco N, Ellingwood BR, Hamburger RO, Hooper JD, Kimball JK, Kircher CA (2007), “Risk targeted versus current seismic design maps for the conterminous United States”, SEAOC 2007 convention proceedings

[Martins et al. 2015]
Martins, L., Silva, V., Crowley, H., Bazzurro, P., Marques, M. (2015), Investigation of Structural Fragility for Risk-targeted Hazard Assessment, 12th International Conference on Applications of Statistics and Probability in Civil Engineering, ICASP12.

[Messali, Longo, 2022]
Messali, F., Longo, M., Influence of the local out-of-plane collapse of URM walls on the global performance of buildings of typologies ‘Metselwerk 1’ and ‘Metselwerk 7’. Delft University of Technology. Report number 11, Version 02 (draft), 01 April 2022.

[Steenbergen, 2021]
Reliability based code making for seismic assessment under gas extraction, R.D.J.M. Steenbergen, Heron Volume 66 (2021), issue 1

[TNO, 2021a]
TNO Rapport 2020 R10628/A: Typologie-gebaseerde beoordeling van de veiligheid bij aardbevingen in Groningen1 - Achtergrond bij de methode, TNO, 2021

[TNO, 2021b]
TNO Rapport 2020 R10699A: Typologie-gebaseerde beoordeling van de veiligheid bij aardbevingen in Groningen - Uitwerking van typologie METSELWERK1, TNO 2021

[TNO, 2021c]
TNO 2020 R10700A: Typologie-gebaseerde beoordeling van de veiligheid bij aardbevingen in Groningen - Uitwerking van typologie METSELWERK2

[TNO, 2021d]
TNO 2020 R10966A: Typologie-gebaseerde beoordeling van de veiligheid bij aardbevingen in Groningen - Uitwerking van typologiegroep METSELWERK-C (typologieën METSELWERK5+6+7)

[TNO, 2022a]
TNO Rapport 2021 R11002/C: Typologie-gebaseerde beoordeling van de veiligheid bij aardbevingen in Groningen – Typologisch toedelen, TNO, 2022

8 Ondertekening

Delft, september 2022 TNO

Dr.ir. M.R. de Rooij
Project Manager

Ir. A.D. Pikaart
Research Manager Structural Reliability

A Influence of the local out-of-plane collapse of URM walls on the global performance of buildings of typologies ‘Metselwerk 1’ and ‘Metselwerk 7’

Project	Typology – B2B variability
Report number	11
Internal Reference	B2B-R11
Date	April 1, 2022
Version	02
Status	Draft

INFLUENCE OF THE LOCAL OUT-OF-PLANE COLLAPSE OF URM WALLS ON THE GLOBAL PERFORMANCE OF BUILDINGS OF TYPOLOGIES 'METSELWERK 1' AND 'METSELWERK 7'

A quick, safe and validated typology based seismic assessment of buildings

Client: Ministerie van Economische Zaken en Klimaat (EZK)

Authors Francesco Messali
F.Messali@tudelft.nl
Michele Longo
M.Longo@tudelft.nl

Address Delft University of Technology
Faculty of Civil Engineering and Geosciences
Stevinweg 1, 2628 CN, Delft

TU Delft Delft University of Technology

Faculty of Civil Engineering and Geosciences
Stevinweg 1
2628 CN Delft
PO 5048
2600 GA Delft
www.citg.tudelft.nl

Report

Title:
Influence of the local out-of-plane collapse of URM walls on the global performance of buildings of typologies 'Metselwerk 1' and 'Metselwerk 7'

Author(s):
Francesco Messali
Michele Longo

Date:
01/04/2022

Client(s): Ministerie van Economische Zaken en Klimaat (EZK)	*Version:* 02	*Status:* Draft
Project number: B2B	*Project name:* A quick, safe and validated typology based seismic assessment of buildings	*File reference:* B2B-R11

Cite as:
Messali, F., Longo, M. (2022). Influence of the local out-of-plane collapse of URM walls on the global performance of buildings of typologies 'Metselwerk 1' and 'Metselwerk 7'. Delft University of Technology. Report number 11, Version 02 (draft), 01 April 2022.

Table of Contents

1 Introduction

The work described in this document focuses on the effect of local out-of-plane failure of masonry walls (analysed via an indirect approach for which the failure is achieved at the exceedance of a pre-determined threshold value) on the global response of buildings classified under the typology 'Metselwerk 1' or 'Metselwerk 7'. The former typology consist of terraced and semi-detached houses with two-storeys plus attic. The latter corresponds to one- and two-storey detached houses, with cavity unreinforced masonry (URM) walls, timber floor and roof structure. 'Metselwerk 1' buildings are usually governed by a combination of in-plane (IP) and out-of-plane (OOP) failure. The predominance of one or the other depends on the building geometry. The seismic behaviour of 'Metselwerk 7' buildings is governed by the OOP failure of the loadbearing walls.

Since the behaviour at near collapse of both typologies involves the local OOP of the walls, these can be strengthened to improve the global building performance. A short description of few strengthening methods whose effectiveness has been tested experimentally is provided in Appendix A.

In order to determine the global capacity of the strengthened buildings, first the numerical models should be validated against experimental tests at both wall and building level. Only then the results of the analyses can be considered representative of the behaviour of real buildings. However, first the number of experimental tests available is limited and, second and most important, such process requires long time to be carried out, while the time frame available for the project requires a quicker solution. For this reason, the effect of the local strengthening on the global behaviour is studied by considering the outcomes of already available nonlinear time history (NLTH) analyses, and modifying the definition of the OOP displacement capacity of the walls. Since the global capacity curve of the building is limited at the point where the OOP displacement of one loadbearing wall exceeds a specific value, the increase of such value modifies also as a consequence the global performance. On the other hand, any contribution of the strengthening measure to increase the OOP force and/or the IP force and displacement capacity of the wall is conservatively neglected.

Also the selection of the reference buildings is mainly based on the opportunity to re-use available material. For the typology 'Metselwerk 1', a two-storey (plus attic) semi-detached houses (twee-onder-een-kapwoning) is selected as reference. The structure is made of two building units and appendixes and it is located in Bleeksteen 1-3, Delfzijl. For sack of simplicity, it is simply named as 'Bleeksteen'.

For the typology 'Metselwerk 7', two main buildings are considered. Since this typology is characterized by large variations of the buildings in terms of geometry, several variants of the two different reference buildings are considered in this study. The buildings considered as reference are EUC-BUILD-2 and LNEC-BUILD-3, which were tested in dynamic conditions on shake tables at the laboratory of EUCENTRE (Pavia, Italy) and LNEC (Lisbon, Portugal), respectively.

A short description of the three buildings is provided in Section 2 and more details can be found in the assessment reports [1] [2] and testing reports [3] [4].

A detailed description of the methodology used to determine the performance of the buildings with an increased OOP wall capacity is described in Section 3. The procedure can be summarized as follows. For each set of analyses, the corresponding hysteresis curves are evaluated. Each curve is limited at the point where a specific failure criteria is reached (either OOP or IP). Different values of OOP displacement threshold limit are selected as alternative failure criteria, in addition to the in-plane displacement limit. Such OOP limits represent the displacement capacity of the strengthened wall. This criteria is applied to all load-bearing walls of the building. The selected OOP displacement limits are equal to 60%, 100%, 110%, 120% and 200% the wall thickness (taken equal to 100 mm). A case in which the OOP failure is completely prevented and the global capacity is governed by the IP resistance is also investigated. For each analysed building a mean backbone curve (for each of the OOP limit) is computed.

The updated post-processing of the numerical simulation results and the comparison between the obtained backbone curves is presented in Section 4, and the conclusions in Section 5.

2 Reference buildings and variations

2.1 Reference buildings

As introduced in Section 1, the study presented in this report refers to one building belonging to typology 'Metselwerk 1' and a set of variations of two different reference buildings to typology 'Metselwerk 7'. For the latter, the variations (in terms of geometry and material properties) are introduced to capture the high variability between detached houses. A description of the three case studies is presented in the next sub-sections.

2.1.1 Bleeksteen

The Bleeksteen building is a two-storey (plus attic) semi-detached house (twee-onder-een-kapwoning) made of two building units and appendixes, built in 1967 and belonging to the typology 'Metselwerk 1'. The building is made of unreinforced masonry (URM) cavity walls. A picture and a plan section of the building is shown in Figure 1. The building is made with a cavity wall system with clay bricks for the outer leaf and calcium silicate bricks for the inner load bearing leaf. It has a height of 8.3 m measured at the ridge beam. The ground floor of the main building is made of concrete beams and concrete panels (combinatievloer), whereas the ground floor of the appendixes is made of concrete. The 1st floor consists of a NeHoBo floor spanning in the North-South direction. At the attic floor, timber beams spanning in the North-South direction are connected with chipboard panels. The roof is composed by timber purlins, connected with chipboard panels. A dormer is present at the West side of the roof. A more detailed description is provided in [1].

Figure 1. Bleeksteen building semi-detached house. South-East façade view (left) and plan view (right).

The Bleeksteen building is characterized by large openings in the longitudinal façades. The percentage of openings at the East façade is equal to 75% at ground storey level. The openings on the ground floor of the West façade are equal to the 52% of the length of the facade. Due to such opening percentages, the building belongs to typology 'Metselwerk 1'.

2.1.2 EUC-BUILD-2

The first case study for typology 'Metselwerk 7' refers to a specimen tested on a shake table at the laboratory of EUCENTRE (Pavia, Italy) and named EUC-BUILD-2 [11]. The specimen was designed to resemble a typical one-storey detached house with a pitched roof (Figure 2). The house is composed of a first-floor timber diaphragm and of a pitched timber roof finished with clay tiles. The timber floor and roof framing members are supported by double-wythe solid clay URM walls. A gable is present on the front (north) and back (south)

façade, as shown in Figure 3. More details about the considered specimen are provided in the testing report [3].

Figure 2: Buildings with construction details similar to those adopted for the shake-table test specimen (from [3]), and actual specimen tested at the laboratory of EUCENTRE (from [11]).

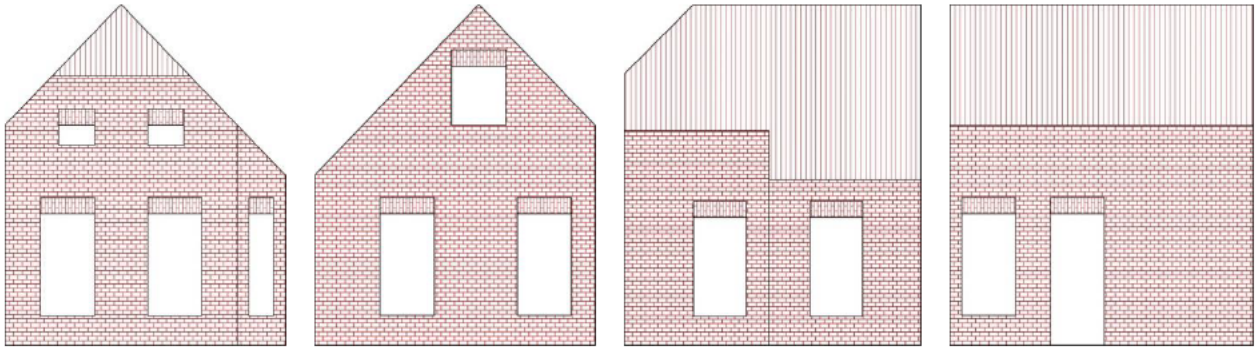

Figure 3: Layout of the façades of reference building EUC-BUILD-2, as studied in the current work.

2.1.3 LNEC-BUILD-3

Similarly to EUC-BUILD-2, this case study considers a specimen, named LNEC-BUILD3, which was tested on a shake table at the laboratory facilities of the Laboratório Nacional de Engenharia Civil (LNEC, Lisbon, Portugal). Also this specimen was built to resemble a typical pre-1940 Dutch detached house in the Groningen area (Figure 4). As shown in Figure 5, the specimen is composed of a high symmetrical gambrel roof finished with clay tiles; a vertical chimney is found on the west façade. The east and the west walls extend above the timber floor in gables, weakly connected to the floor and the roof framing. The load-bearing structural system consists of 208 mm thick double-wythe solid clay URM walls in three out of the four perimeter walls. A 100 mm thick interior wall runs parallel to the shaking direction, longwise the centreline of the building plan. The east façade consists of single wythe wall with 10 cm thickness.
More details about the considered specimen are provided in the testing report [4].

Figure 4: Building views, a) North-East view, b) South-East view (from [4]).

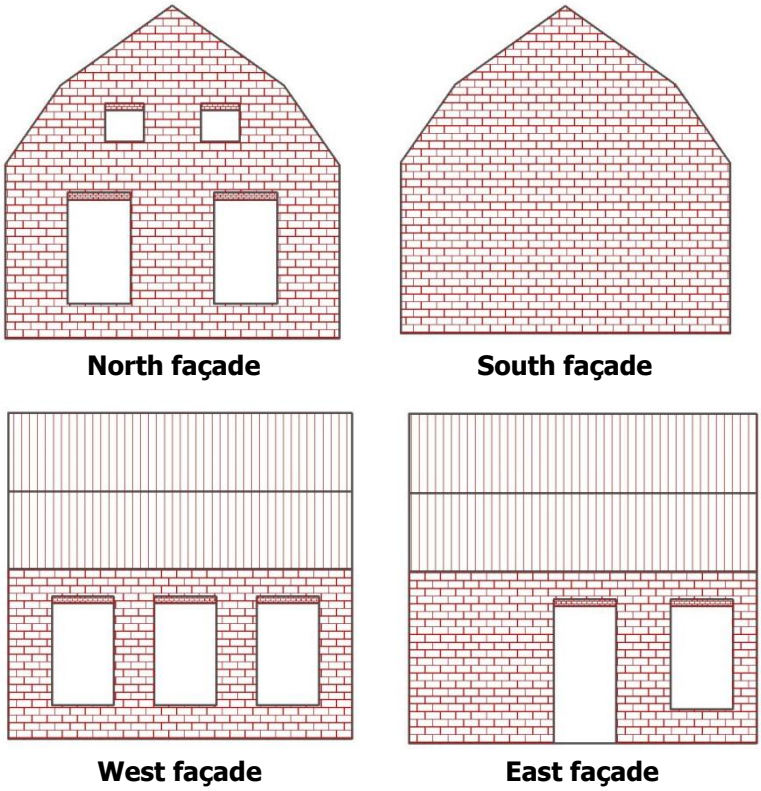

Figure 5: Layout of the façades of reference building LNEC-BUILD-3, as studied in the current work.

2.2 'Metselwerk 7' variations and ground motions

For all the 'Metselwerk 7' variations, cavity walls made of solid clay bricks (for both the inner loadbearing leaves and the external veneers) are considered in place of the original double-wythe URM walls.

The following variations of the two 'Metselwerk 7' reference buildings are considered in this study:

- **Building plan regularity (only for EUC-BUILD-2).** EUC-BUILD-2 has a L-shaped plan, with a re-entrant corner. The length of this portion of the building is doubled (increasing the torsional effects), or zeroed resulting in a regular shape (and hence decreasing the torsional effects). LNEC-BUILD-3 is

characterised by a rectangular plan and no variations are considered. The three plan variations are shown in Table 1.

- **Layout of a façade**. Three different layouts of a façade are considered for each building, the east and the west façade for EUC-BUILD-2 and LNEC-BUILD-3, respectively. The considered combinations are shown in Table 1.

- **Masonry material properties**. Two different sets of material properties for the URM are considered: clay brick brickwork pre-1945 (CL1) and post-1945 (CL2). The material properties are defined according to Table F.2 of NPR 9998 [12].

- **Timber material properties**. Two different sets of material properties for the timber structures are considered. The set T1 is defined after experimental tests [13] and past numerical studies performed by TU Delft to predict the experimental behaviour of shake table tests [14]. The same values are adopted for both the buildings. The set T2 is characterised by halved values of the material properties.

A summary of all the variations is listed in Table 2.

For each model, seven different ground motions are applied at the base of the structure. The number of ground motions is reduced to four for Bleeksteen due to the extremely high computational burden of the model. The ground motions are part of those used for the Hazard and Risk study [15], and especially for the NLTHA performed by ARUP [16]. Only the stronger motions (M08 to M11 for 'Metselwerk 1' and M05 to M11 for 'Metselwerk 7') have been considered to have more information of the behaviour of the building at collapse. Each ground motion consists of three orthogonal components, one parallel to the façades, one to the transversal walls and one vertical component. The component in the transversal direction for the Bleeksteen model is removed to provide numerical stability without affecting the global failure mechanism of the structure. Few considered signals were unable to cause the collapse of the building at specific displacement limits (as defined in section 3). For those cases, few motions are scaled by a factor two (or one and a half) in order to reach a specific failure criteria.
A summary of the ground motions is included in Table 3 (extract from Table 2 of [16]). Additional information about the ground motions can be found in Appendix B.

In total, 8 NLTH analyses for 'Metselwerk 1' and 126 NLTH analyses for 'Metselwerk 7' have been performed. The complete and detailed results of the finite element models can be find in the assessment reports [1] [2].

Table 1. Summary of the geometrical variations of the 'Metselwerk 7' reference buildings.

	EUC-BUILD-2		LNEC-BUILD-3
	Plan (P) variations	**Façade (F) variations**	
1	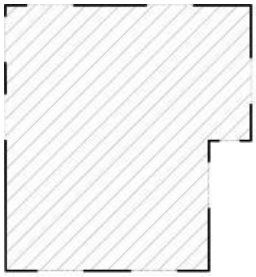	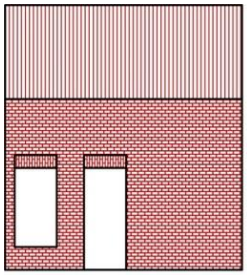	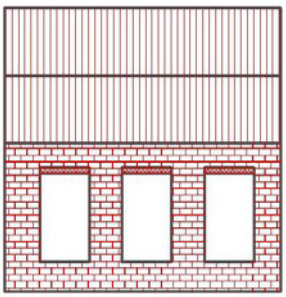
2		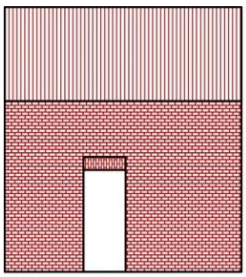	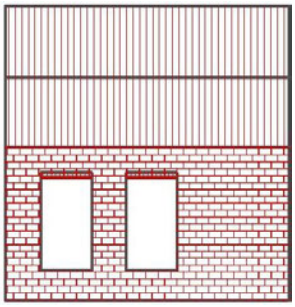
3	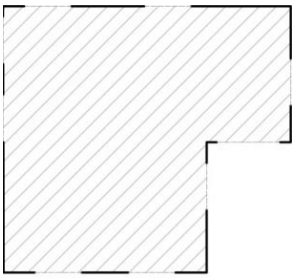	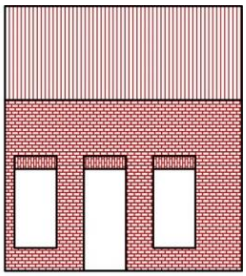	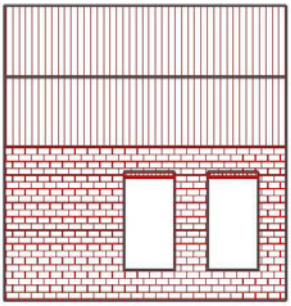

Table 2. List of the 16 variations of 'Metselwerk 7' considered.

No.	Ref. building	Timber properties	Masonry properties	Floor shape	Façade layout
#1	EUC-BUILD-2	T1	CL1	P1	F1
#2	EUC-BUILD-2	T2	CL1	P1	F1
#3	EUC-BUILD-2	T1	CL2	P1	F1
#4	EUC-BUILD-2	T1	CL1	P1	F2
#5	EUC-BUILD-2	T1	CL1	P1	F3
#6	EUC-BUILD-2	T1	CL2	P1	F3
#7	EUC-BUILD-2	T1	CL1	P2	F1
#8	EUC-BUILD-2	T1	CL1	P3	F1
#9	EUC-BUILD-2	T1	CL2	P3	F1
#10	LNEC-BUILD-3	T1	CL1	-	F1
#11	LNEC-BUILD-3	T1	CL2	-	F1
#12	LNEC-BUILD-3	T2	CL2	-	F1
#13	LNEC-BUILD-3	T1	CL1	-	F2
#14	LNEC-BUILD-3	T1	CL2	-	F2
#15	LNEC-BUILD-3	T1	CL1	-	F3
#16	LNEC-BUILD-3	T1	CL2	-	F3

Table 3. Summary of the ground motions applied for the NLTHA (from [16]). Values refer to the main horizontal motion direction.

Ground motion	Label of first component	AvgSa (g)	Arias intensity (m/s)	PGA (g)	Sa(0.1s) (g)
M05	N_00147T	0.27	0.51	0.25	0.67
M06	N_00250L	0.34	1.53	0.88	0.87
M07	E_17167_EW	0.40	1.20	0.53	0.72
M08	N_00415L	0.46	1.74	0.70	1.02
M09	N_00569T	0.46	2.25	0.52	0.68
M10	N_00407L	0.57	3.54	0.82	1.26
M11	N_00451T	0.74	3.85	1.25	1.49

3 Methodology

3.1 Model Description

The three buildings are numerically model by means of the software Diana FEA version 10.4. The model approach is based on the assumptions already employed in similar studies of the same project ([2], [17], [18], [19]) and it is described in the current section. The complete description and results of the three buildings here investigate can be found in [1] [2].

Quadratic 8-noded curved shell elements (CQ40S and CT30S) are used to model walls, floors and roof. The irregular and complex roof and floor framings, made by timber beams, are modelled with linear Class-III beam element (CL18B). A non-linear constitutive behaviour is considered for the masonry walls, while the rest of the elements are linear elastic. The Engineering Masonry Model [20] is selected as material model for the two different clay masonry types (before and after 1945) and for the calcium silicate brick masonry. The material properties of masonry are taken from Table F.2 of NPR 9998:2020 [12]. An orthotropic behaviour, whose properties are calibrated according to the laboratory experiment [13] and on the basis of previous simulations [14], is assigned to timber planks of floors and roof. The outer leaves are not explicitly modelled and they do not contribute to the global stability of the walls, but their mass is included in the numerical model via mass elements acting in the horizontal direction perpendicular to the wall plane. This implies the assumption that the wall ties are unable to transfer any shear force. Such modelling choice is supported by outcomes of the study reported in [21]. Non-linear point interfaces are used to model the pocket connections between the beams of the timber floor and the masonry walls, and between the purlins and the masonry gables. A coulomb-friction model is employed for the interfaces. This last assumption is not employed in the Bleeksteen building in order to reduce computational time. A comparison between this conservative choice and the model with interfaces is described in section 4. Expansion joints are modelled as physical gap in the party walls at ground and first floor level. The joints are located at a distance of approximately 1 m from the two façades. Additionally, the connections between the internal non-loadbearing partition walls and the party wall at first floor level are modelled as a row of elements with rotated local axes and reduced material properties. Both elastic properties and tensile/shear parameters are reduced by 30%, whereas the compressive parameters are unchanged. These last two details are shown in Figure 6. More details on the constitutive models and the material properties used for the simulations are provided in Appendix C. The model is restrained at the bottom from translations and rotations. The elements are meshed with an average size of 200x200 mm. Pictures of the FE models are depicted in Figure 6 and Figure 7.

Before performing the NLTH analyses, an eigenvalue analyses is run to define the two modes with the highest mass participation. The two corresponding eigenvalues are used to calculate the Rayleigh damping coefficients, whose value is updated with the global stiffness matrix at each step. A damping ratio equal to 2% is assumed, compliant with the recommendations of NPR 9998 [12]. The gravity load is initially applied in ten equal steps. Then each component of the triaxial (biaxial for Bleeksteen) ground motion is applied simultaneously as prescribed acceleration at the nodes at the base of the building with a time step of 2.5 ms. The Newmark-Beta method is used for the time integration ($\beta = 0.25$, $\gamma = 0.5$). The Secant BFGS (Quasi-Newton) method is adopted as iterative method. Energy norm with a tolerance of 0.01% is employed. The Parallel Direct Sparse method is employed to solve the system of equations. The second order effects are considered via the Total Lagrange geometrical nonlinearity.

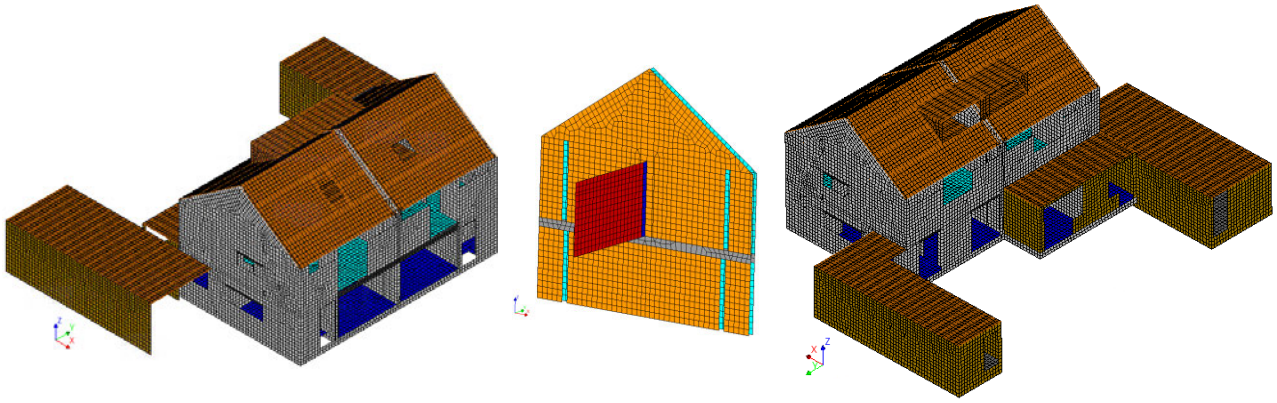

South-East view | Party walls detail | North-West view

Figure 6. FE models adopted for the simulation of 'Metselwerk 1' Bleeksteen building.

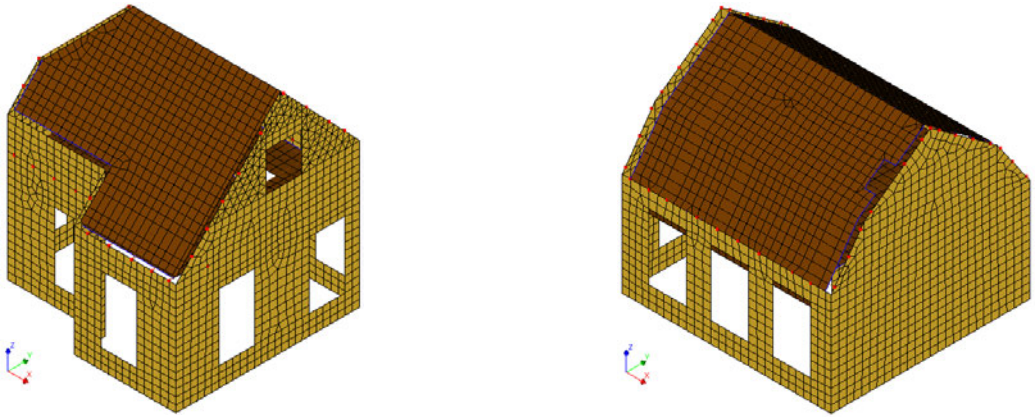

EUC-BUILD-2 | LNEC-BUILD-3

Figure 7. FE models adopted for the simulation of 'Metselwerk 7' buildings.

3.2 Failure (stop) criteria

The outputs of the NLTH analyses are shown and discussed mainly in terms of normalised base shear (i.e. the measured base shear normalised by the effective mass of the building) vs the displacement at attic level. The attic displacement is computed as the average of the displacements measured for different points at the attic level: the four corner points of each floor and the four points in the middle of the floor/walls (as shown for the three buildings in Figure 8).

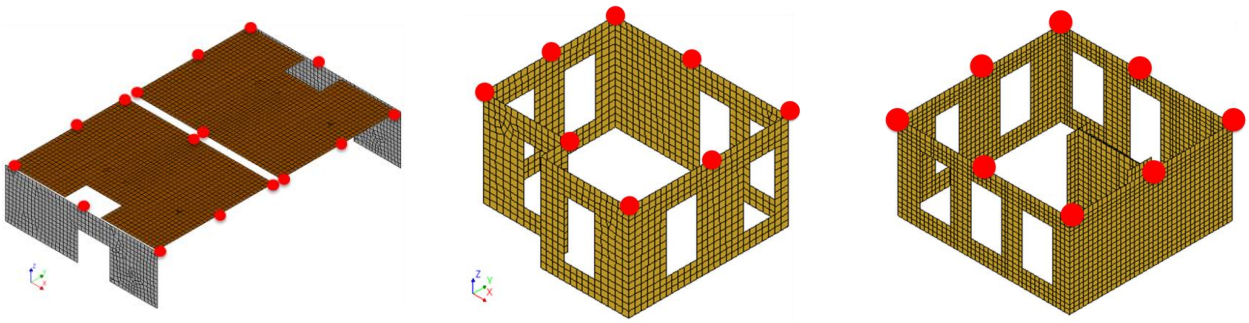

Bleeksteen | EUC-BUILD-2 | LNEC-BUILD-3

Figure 8. Points considered to define the attic displacement.

The ultimate displacement capacity of the building (i.e. the displacement at collapse of the building) is computed by considering both a global in-plane drift limit and a local out-of-plane maximum displacement for the walls.

NPR 9998:2020 [12] sets the maximum interstorey drift for a URM building in the in-plane direction equal to 1.5% for ductile mechanisms and to 0.6% for a brittle (shear type) failure. The average drift at the effective height is set equal to 0.8% for ductile mechanisms and 0.4% for a brittle failure at the effective height. These values refers to the characteristic capacity of the building. A correction factor of 1.6/0.9 (about 1.77) (similar to that used in [17] and [19] for the SLaMA analyses) is then applied to the in-plane limits to obtain the mean IP displacement capacity.

The implicit out-of-plane (OOP) failure criterion relates the global failure of the building to the local OOP collapse of a single loadbearing wall. Such conservative method is used since the analyses are unable to describe explicitly the OOP collapse of the walls and, therefore, the progressive collapse of the whole building. In order to identify the point of collapse of a wall, a maximum OOP displacement is defined. This value is varied in order to investigate the sensitivity of such parameter on the global response of the buildings. The chosen OOP displacement limits are equal to 0.6, 1.0, 1.1, 1.2 and 2.0 times the thickness of the internal loadbearing leaf (i.e. 100 mm). It should be noted that the values 0.6 and 1.0 are alternative representative values for URM walls, whereas 2.0 is selected as representative of the performance of a strengthened wall (a description of possible strengthening measures can be find in Appendix A). The values 1.1 and 1.2 are also considered to study the sensitivity of the criterion to small variations of the local OOP capacity. Finally, a case in which the OOP failure is assumed to be completely prevented is also investigated. The average attic displacement at collapse is then computed as the average between the displacement of the different floor points when a wall exceeds for the first time in the analysis the maximum OOP displacement.
A summary of the OOP and IP failure criteria is reported in Table 4.

The hysteretic curves defined for each analysis (according to the corresponding failure criteria) are used to determine the global backbone capacity curve of the building according to the procedure described in [2].
An example of backbone curve, defined for variation #01 of EUC-BUILD-2, is shown in Figure 9.

Table 4. Failure (stop) criteria of the three buildings.

Failure (stop) criteria	**Bleeksteen**	**EUC-BUILD-2**	**LNEC-BUILD-3**
OOP-060	60 mm		
OOP-100	100 mm		
OOP-110	110 mm		
OOP-120	120 mm		
OOP-200	200 mm		
IP	1st Floor DUC: 72.0 mm 1st Floor BRI: 28.8 mm Attic DUC: 76.8 mm Attic BRI: 38.4 mm	Attic DUC: 82.9 mm Attic BRI: 33.2 mm	Attic DUC: 72.5 mm Attic BRI: 29.0 mm

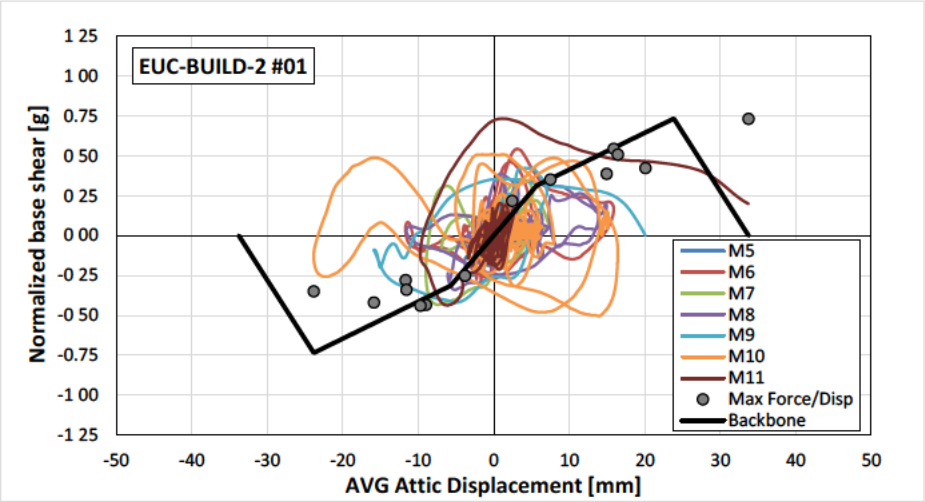

Figure 9. Example of a backbone curve defined for the model EUC-BUILD-2 - variation #01.

4 Results

This section presents the backbone curves computed starting from the analyses performed on the 'Metselwerk 1' reference building and on the variations of the 'Metselwerk 7' reference buildings EUC-BUILD-2 and LNECBUILD-3. Different backbone curves are computed depending on the considered local OOP failure criterion, and then compared one another.

4.1 Bleeksteen

Eight NLTH analyses are performed by applying different motions at the base of the Bleeksteen model. The selected motions are M08, M09, M10 and M11, either employing the original base acceleration or an amplified acceleration (two times the original acceleration for motions M08, M09 and M10 and 1.5 times for M11). This choice is made in order to overcome, at least in one analysis, the maximum OOP displacement at near collapse defined for the failure criteria (i.e. 2 times the wall thickness).
First of all, a comparison with the modelling approach used in a previous study [1] (with nonlinear floors and timber-masonry interface elements) is provided. This check is meant to validate the changes made to the model of Bleeksteen, modelled with linear elastic floor and rigid timber-masonry connections to save computational time. A comparison between the normalized force-displacement of the two modelling approaches for motions M09 and M11 are depicted in Figure 10. The model with linear floors and no interface elements has equivalent force capacity than the model with nonlinear floors and interface elements. The lower flexibility at the attic and roof level provided by the rigid connections conservatively reduces the maximum achieved displacement up to about 20%. Additionally, it should be taken into account that the models from the previous study [1] were run with a triaxial set of motions (instead of two) able to produce additional damage and increase the overall flexibility of the building. Given the fact that the updated model approach results much lighter in terms of computational effort, more stable numerically and without large differences in both damage pattern and global behaviour, the approach is considered valid for the investigation reported in this document.

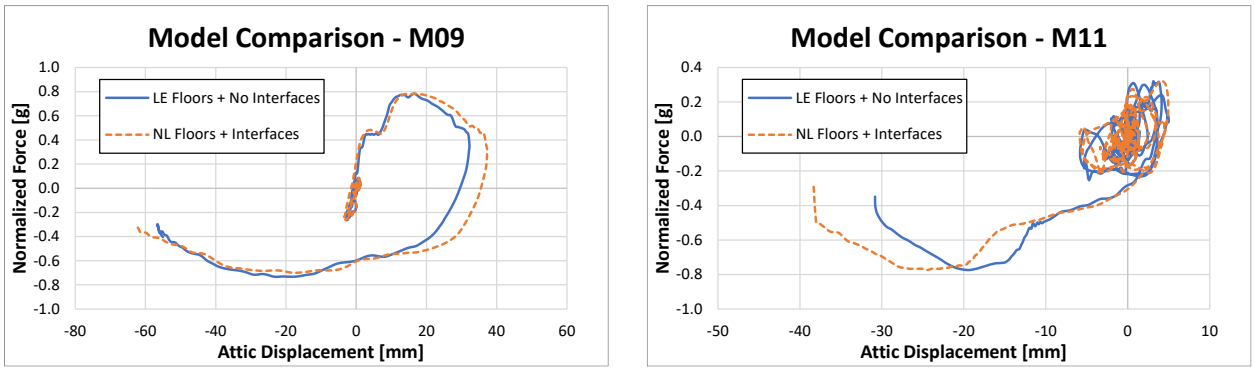

(a) (b)

Figure 10. Comparison of hysteresis curve of Bleeksteen building using different modelling assumptions. Motion M09 (a) and M11 (b).

The hysteretic curves of the different floors of the Bleeksteen model subjected to the amplified M08 are plotted in Figure 11. The global in-plane mechanism involves both first and attic storey in a ductile manner (mainly flexural failures are detected in the masonry piers). Roof displacement does not differ much to the one at the attic level. The inter-storey drift is for all cases larger at the ground level, with values almost double respect to the first level. However, the IP failure criteria is never reached at the ground floor but at the attic level, thus referring to the drift limit at effective-height (76.8 mm as indicated in Table 4). The IP failure criteria is exceeded only for three out of the eight analyses (M08, M09 and M10 amplified). In the other cases the in-

plane displacements do not exceed the limit by the end of the applied motion. One-way OOP bending failure of the party walls at the ground floor is observed. In a few cases, also the party walls at the first floor undergo large displacements which lead to collapse. The maximum OOP displacement of the ground floor party wall for the analyses with the original (not amplified) accelerations is about 150 mm (M09). Larger OOP displacements are reached by the model for the amplified motions, with a max OOP displacement above 200 mm for amplified M08 and M09. The exceedance point of each failure criterion is marked on the normalized force-attic displacement curve of amplified M08 in Figure 11b and on the attic displacement-time curve in Figure 12. Large differences are observed, from an attic displacement of 28 mm when the party wall exceeds an OOP displacement of 60 mm up to a max attic displacement of almost 75 mm for a 200 mm OOP displacement. Eventually, the IP limit of 76.8 mm is also exceeded. The OOP failure mechanism is shown for the case M10 as maximum displacement contour plot in Figure 13a.
Both OOP(-200) and IP failure criteria of the analysis with amplified M08 are depicted in Figure 13b.

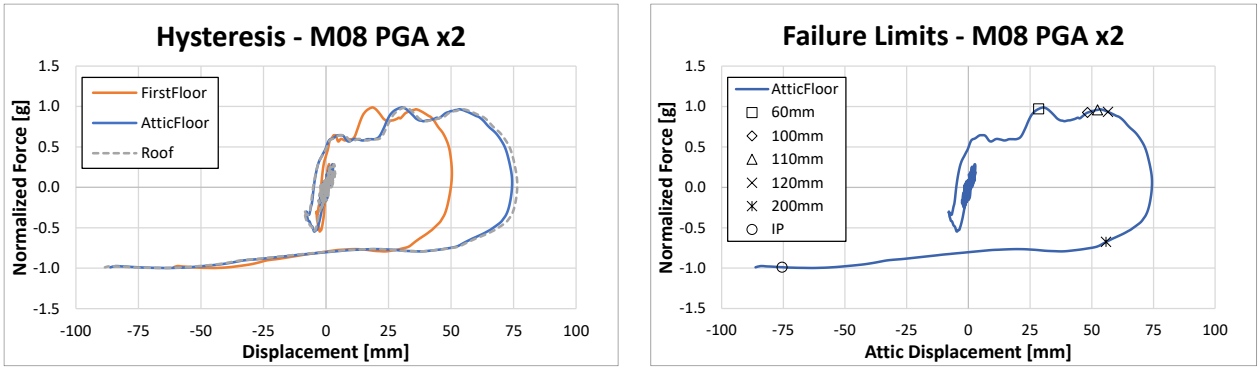

(a) (b)

Figure 11. Hysteresis curve of Bleeksteen building for M08 motion amplified by 2 times. Comparison between the displacement at different floor levels (a) and exceedance of the considered failure criteria (b).

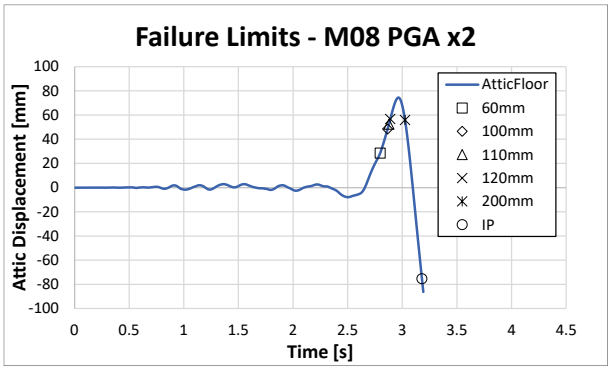

Figure 12. Time-displacement curve of Bleeksteen building for M08 motion amplified by 2 times. The exceedance of the failure criteria is reported on the curve.

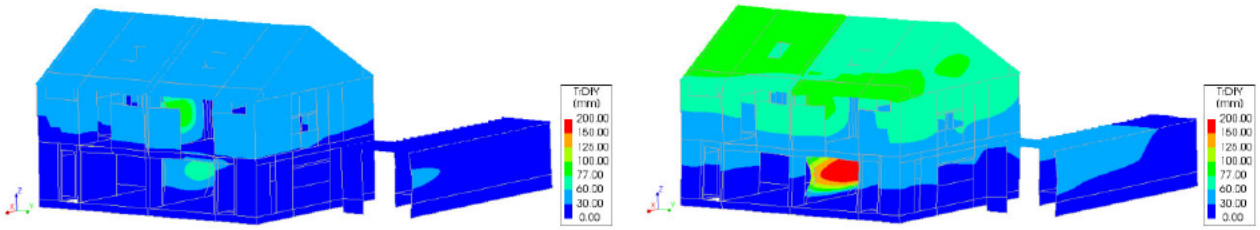

(a) (b)

Figure 13. Max/Min longitudinal displacement of Bleeksteen building. Picture taken after reaching criteria OOP-100 of M10 (a) and OOP-200 and IP for M08 PGA x2 (b).

A single backbone per failure criteria is computed following the methodology described in [2]. The main output is reported in Table 5 and plotted in Figure 14. The results are compared with the reference case (OOP 100, max OOP displacement of 100 mm) as reported in Table 6. When the OOP displacement is limited to 60 mm, both peak and collapse displacement are about 40% lower than those with the OOP limit of 100 mm, with values of 17.9 and 31.1 mm, respectively. When increasing the OOP limit to 110 mm and 120 mm, the high IP displacement of analysis M11, which does not show any failure, comes into play increasing the peak displacement of about 93%. Collapse displacement for these limits increases by about 20%. When the OOP displacement is further increased to 200 mm, the peak displacement increase to 67 mm (+130% with respect to OOP-100) and the collapse displacement increases to 75 mm (+42% with respect to OOP-100). These last results are almost the same as the ones obtained when no OOP failure (but only IP) is considered.

All the overall results of the Bleeksteen calculations are presented in Appendix F.

Table 5. Main outputs of the backbone curves of Bleeksteen for each stop criteria.

OOP-060		OOP-100		OOP-110		OOP-120		OOP-200		No OOP	
d [mm]	v_a [g]	d [mm]	v_a [g]	d [mm]	v_a [g]	d [mm]	v_a [g]	d [mm]	v_a [g]	d [mm]	v_a [g]
-31.16	0.00	-52.67	0.00	-62.21	0.00	-65.00	0.00	-75.03	0.00	-75.37	0.00
-17.86	-0.86	-29.26	-0.98	-56.48	-1.10	-56.48	-1.11	-67.44	-1.14	-67.44	-1.19
-3.99	-0.29	-6.45	-0.43	-8.36	-0.50	-8.36	-0.50	-8.36	-0.50	-9.27	-0.46
0.00	0.00	0.00	0.00	0.00	0.00	0.00	0.00	0.00	0.00	0.00	0.00
3.99	0.29	6.45	0.43	8.36	0.50	8.36	0.50	8.36	0.50	9.27	0.46
17.86	0.86	29.26	0.98	56.48	1.10	56.48	1.11	67.44	1.14	67.44	1.19
31.16	0.00	52.67	0.00	62.21	0.00	65.00	0.00	75.03	0.00	75.37	0.00

Table 6. Average peak and collapse displacement of Bleeksteen and difference respect to OOP-100 case.

		OOP-060	OOP-100	OOP-110	OOP-120	OOP-200	No OOP
Peak	Value	17.89	29.26	56.48	56.48	67.44	67.44
	Difference	-39%	0%	+93%	+93%	+130%	+130%
Collapse	Value	31.16	52.67	62.21	65.00	75.03	75.37
	Difference	-41%	0%	+18%	+23%	+42%	+43%

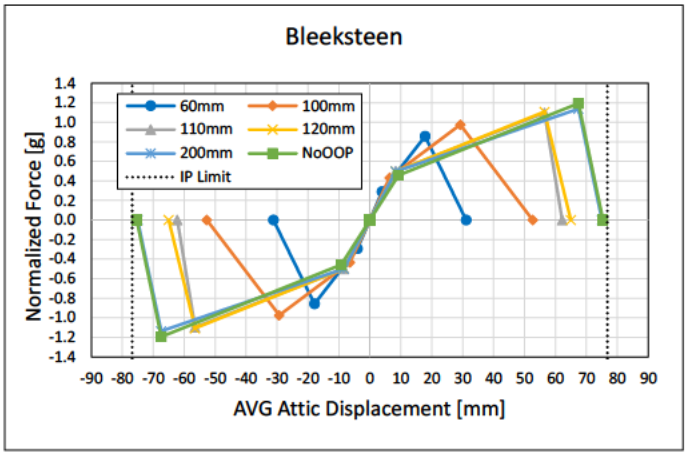

Figure 14. Bleeksteen backbone curves for each failure criteria. IP limits at 76.8 mm.

4.2 EUC-BUILD-2

Sixty-nine NLTH analyses were performed on nine variations of EUC-BUILD-2, which represent a building belonging to the 'Metselwerk 7' typology. These analyses are all characterized by large OOP displacements of the North and South building façades (Figure 15), whereas the in-plane deformation of the East and West façades is relatively small. The largest deformations are observed just below the attic level and are obtained for ground motions M10 and M11. The displacements larger than the thickness of the inner loadbearing leaf are shown in orange-red in Figure 15.

In general, even if the failure mechanism is the same for all the buildings, the effect of the variations on the structural response of the building is evident. Specifically:

- Stronger masonry (clay brickworks post 1945) allows the structure to reach higher normalised base shear and global displacements at near collapse;
- The presence of additional openings, which reduce the length of the piers, determines lower normalised base shear at peak but it contributes to attain larger displacements at near collapse (conversely, when an opening is removed, the structure is stronger but less ductile);
- Plan irregularities have limited effects on the normalised base shear and peak/collapse displacement.

Sixty-nine NLTH analyses were performed on nine variations of EUC-BUILD-2, which represent a building under the 'Metselwerk 7' category. These analyses are all characterized by large OOP displacements of the North and South building façades (Figure 15), whereas the in-plane deformation of the East and West façades is small. The largest deformations are observed just below the attic level and are obtained for ground motions M10 and M11. The displacements larger than the thickness of the inner loadbearing leaf are shown in orange-red in Figure 15.

Table 7, Table 8 and Table 9 report the main outputs of the backbone curves defined for each variation in terms of attic displacement (d) and normalised base shear (v_a) at the points of cracking, peak and collapse as defined in section 3 and [1]. The results are expressed by considering different stop criteria of the OOP displacement.

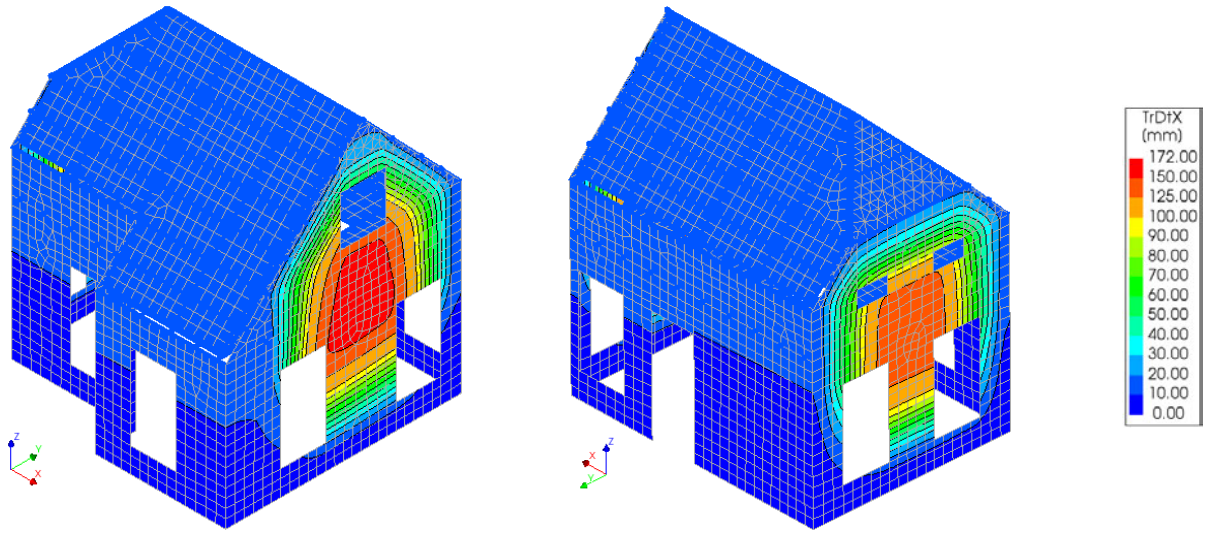

South-West view North-East view

Figure 15. Maximum OOP displacement of the North-South façades of EUC-BUILD-2 #01 for motion M11.

Table 7. Main outputs of the backbone curves for each variation of EUC-BUILD-2. OOP stop criteria equal to 60 and 100 mm.

Variation	OOP-060						OOP-100					
	Cracking		Peak		Collapse		Cracking		Peak		Collapse	
	d	v_a	d	v_a	d	v_a	d	v_a	d	v_a	d	v_a
	[mm]	[g]	[mm]	[g]	[mm]	[g]	[mm]	[g]	[mm]	[g]	[mm]	[g]
#01	5.69	0.31	15.77	0.73	24.29	0.0	5.69	0.31	23.85	0.73	33.75	0.0
#02	5.80	0.31	15.81	0.74	25.28	0.0	5.80	0.31	23.85	0.74	33.34	0.0
#03	4.10	0.32	19.08	0.85	23.17	0.0	4.10	0.32	27.55	0.85	43.25	0.0
#04	5.57	0.31	14.59	0.79	20.16	0.0	5.57	0.31	22.95	0.79	30.06	0.0
#05	3.56	0.24	21.47	0.51	32.52	0.0	3.56	0.24	27.93	0.51	44.70	0.0
#06	5.49	0.30	17.23	0.66	29.84	0.0	5.49	0.30	41.27	0.66	62.76	0.0
#07	6.32	0.29	15.32	0.71	21.26	0.0	6.32	0.29	21.32	0.71	31.01	0.0
#08	3.25	0.25	16.18	0.72	25.94	0.0	3.25	0.25	23.86	0.72	36.10	0.0
#09	4.21	0.34	19.93	0.81	25.75	0.0	4.21	0.34	29.92	0.84	45.44	0.0
AVG	**4.89**	**0.30**	**17.26**	**0.72**	**25.36**	**0.00**	**4.89**	**0.30**	**26.94**	**0.73**	**40.05**	**0.00**
CV	**23%**	**11%**	**14%**	**14%**	**15%**	**-**	**23%**	**11%**	**22%**	**14%**	**26%**	**-**

Table 8. Main outputs of the backbone curves for each variation of EUC-BUILD-2. OOP stop criteria equal to 110 and 120 mm.

Variation	OOP-110						OOP-120					
	Cracking		Peak		Collapse		Cracking		Peak		Collapse	
	d	v_a	d	v_a	d	v_a	d	v_a	d	v_a	d	v_a
	[mm]	[g]	[mm]	[g]	[mm]	[g]	[mm]	[g]	[mm]	[g]	[mm]	[g]
#01	5.69	0.31	23.85	0.73	35.38	0.0	5.69	0.31	23.85	0.73	36.73	0.0
#02	5.80	0.31	23.85	0.74	35.21	0.0	5.80	0.31	23.85	0.74	36.45	0.0
#03	4.10	0.32	30.69	0.85	45.78	0.0	4.40	0.32	31.82	0.85	48.85	0.0
#04	5.57	0.31	22.95	0.79	31.63	0.0	5.57	0.31	22.95	0.79	33.00	0.0
#05	3.56	0.24	28.96	0.51	47.12	0.0	3.56	0.24	30.25	0.51	48.77	0.0
#06	5.49	0.30	41.27	0.66	65.83	0.0	5.49	0.30	41.31	0.66	68.76	0.0
#07	6.52	0.29	21.32	0.71	32.54	0.0	6.52	0.29	21.32	0.71	34.11	0.0
#08	3.25	0.25	23.86	0.72	37.75	0.0	3.25	0.25	23.86	0.72	39.15	0.0
#09	4.21	0.34	31.83	0.84	48.12	0.0	4.21	0.34	33.44	0.84	51.34	0.0
AVG	**4.91**	**0.30**	**27.62**	**0.73**	**42.15**	**0.00**	**4.94**	**0.30**	**28.07**	**0.73**	**44.13**	**0.00**
CV	**23%**	**11%**	**23%**	**14%**	**26%**	**-**	**23%**	**11%**	**23%**	**14%**	**26%**	**-**

Table 9. Main outputs of the backbone curves for each variation of EUC-BUILD-2. OOP stop criteria equal to 200 mm and no out-of-plane criteria.

Variation	OOP-200						NO-OOP					
	Cracking		Peak		Collapse		Cracking		Peak		Collapse	
	d	v_a	d	v_a	d	v_a	d	v_a	d	v_a	d	v_a
	[mm]	[g]	[mm]	[g]	[mm]	[g]	[mm]	[g]	[mm]	[g]	[mm]	[g]
#01	5.69	0.31	23.85	0.73	79.78	0.0	5.69	0.31	23.85	0.73	79.78	0.0
#02	5.80	0.31	23.85	0.74	79.78	0.0	5.80	0.31	23.85	0.74	79.78	0.0
#03	4.10	0.32	31.82	0.85	67.36	0.0	4.10	0.32	31.82	0.85	79.78	0.0
#04	5.57	0.31	22.95	0.79	79.78	0.0	5.57	0.31	22.95	0.79	79.78	0.0
#05	3.56	0.24	30.25	0.51	79.78	0.0	3.56	0.24	30.25	0.51	79.78	0.0
#06	5.49	0.30	41.51	0.66	79.78	0.0	5.49	0.30	61.26	0.66	79.78	0.0
#07	6.52	0.29	21.32	0.71	79.78	0.0	6.52	0.29	21.32	0.71	79.78	0.0
#08	3.25	0.25	23.86	0.72	79.78	0.0	3.25	0.25	23.86	0.72	79.78	0.0
#09	4.21	0.34	33.44	0.84	71.96	0.0	4.21	0.34	38.80	0.84	79.78	0.0
AVG	**4.91**	**0.30**	**28.09**	**0.73**	**77.53**	**0.00**	**4.91**	**0.30**	**30.88**	**0.73**	**79.78**	**0.00**
CV	**23%**	**11%**	**24%**	**14%**	**6%**	**-**	**23%**	**11%**	**41%**	**14%**	**0%**	**-**

The significant points of the backbone curves computed for each failure criterion are listed in Table 12 and the curves are plotted in Figure 16. The in-plane failure (79.78 mm) is observed in the model for variation #06 and #09 only. In the former it is reached before that the OOP maximum displacement exceeds the value 200 mm (and hence the IP criteria is normative). Lower and upper bounds of the average backbone curves taking into account the CV are drawn and depicted in Figure 17.

The difference in terms of peak and collapse displacement for the different failure criteria with respect to the OOP-100 limit case are reported in Table 11. When the OOP displacement is limited to 60 mm, both peak and collapse displacement are about 36% lower than the ones with the OOP limit of 100 mm, with values of 17.3 and 25.4 mm, respectively. When the OOP limit is increased to 110 mm and 120 mm, just a small increment

is detected in both peak and collapse displacement, not higher than 10%. Also the peak displacement increases less than 15%. With an OOP limitation of 200 mm, the collapse displacement shows a large increment (94%), almost equal to the maximum possible IP displacement. The peak force remains substantially unchanged for all the different OOP failure criteria.

The overall results of the EUC-BUILD-2 calculations are fully presented in Appendix D.

Table 10. Average backbone curves of EUC-BUILD-2 for each stop criteria.

OOP-060		OOP-100		OOP-110		OOP-120		OOP-200		No OOP	
d [mm]	v_a [g]	d [mm]	v_a [g]	d [mm]	v_a [g]	d [mm]	v_a [g]	d [mm]	v_a [g]	d [mm]	v_a [g]
-25.36	0.00	-40.05	0.00	-42.15	0.00	-44.13	0.00	-77.53	0.00	-79.78	0.00
-17.26	-0.72	-26.94	-0.73	-27.62	-0.73	-28.07	-0.73	-28.09	-0.73	-30.88	-0.73
-4.89	-0.30	-4.89	-0.30	-4.91	-0.30	-4.91	-0.30	-4.91	-0.30	-4.91	-0.30
0.00	0.00	0.00	0.00	0.00	0.00	0.00	0.00	0.00	0.00	0.00	0.00
4.89	0.30	4.89	0.30	4.91	0.30	4.91	0.30	4.91	0.30	4.91	0.30
17.26	0.72	26.94	0.73	27.62	0.73	28.07	0.73	28.09	0.73	30.88	0.73
25.36	0.00	40.05	0.00	42.15	0.00	44.13	0.00	77.53	0.00	79.78	0.00

Table 11. Average peak and collapse displacement of EUC-BUILD-2 and difference respect to OOP-100 case.

		OOP-060	OOP-100	OOP-110	OOP-120	OOP-200	No OOP
Peak	AVG	17.26	26.94	27.62	28.07	28.09	30.88
	Difference	-36%	0%	+3%	+4%	+4%	+15%
Collapse	AVG	25.36	40.05	42.15	44.13	77.53	79.78
	Difference	-37%	0%	+5%	+10%	+94%	+99%

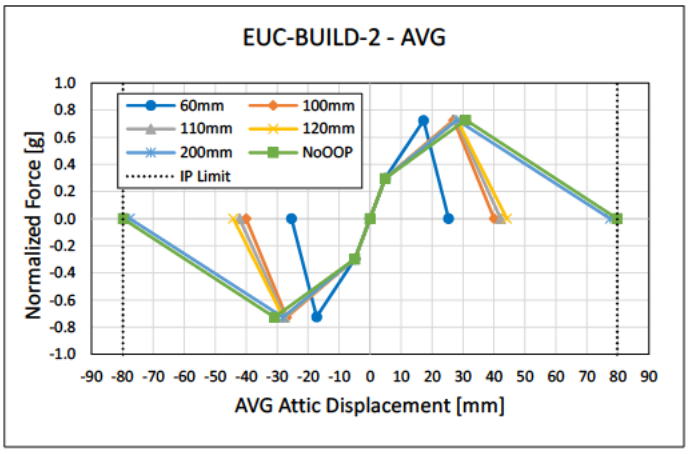

Figure 16. EUC-BUILD-2 average backbone curves for each failure criteria. IP limits at 79.8 mm.

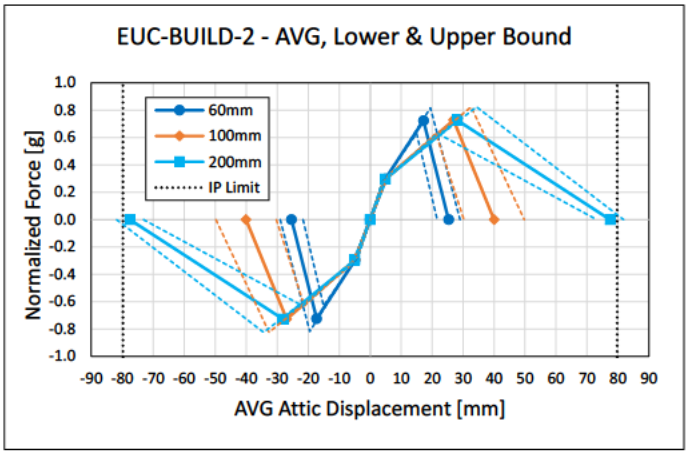

Figure 17. EUC-BUILD-2 average, lower and upper backbone curves for three failure criteria. IP limits at 79.8 mm.

4.3 LNEC-BUILD-3

Fifty-seven NLTH analyses were performed on seven variations of LNEC-BUILD-3, which represent a building belonging to the 'Metselwerk 7' typology. These analyses are all characterized by large OOP displacements of the South façade (Figure 18), a large wall with no openings disconnected from the internal walls, whereas the OOP deformations of the North façade, with four openings, are much smaller. The in-plane deformations of the East and West façades are small, with limited flexural and shear cracking of the piers: the West wall is characterized by rocking of the short piers, while a diagonal shear crack is observed in the long wall of the East façade. The irregularity of the openings also determines the torsion of the building, with displacements of the West façade at the attic level almost double than those of the East façade.
The largest deformations are obtained for ground motions M10 and M11. The displacements larger than the thickness of the inner load bearing leaf, in the middle of the South façade at the attic level, are shown in orange/red in Figure 18.

For this set of analyses, the effect of the variations introduced for the sensitivity study on the structural response of the building is limited. The variations affect more the global in-plane but they do not impact the OOP collapse of the South wall and, consequently, the performance of the building at failure.

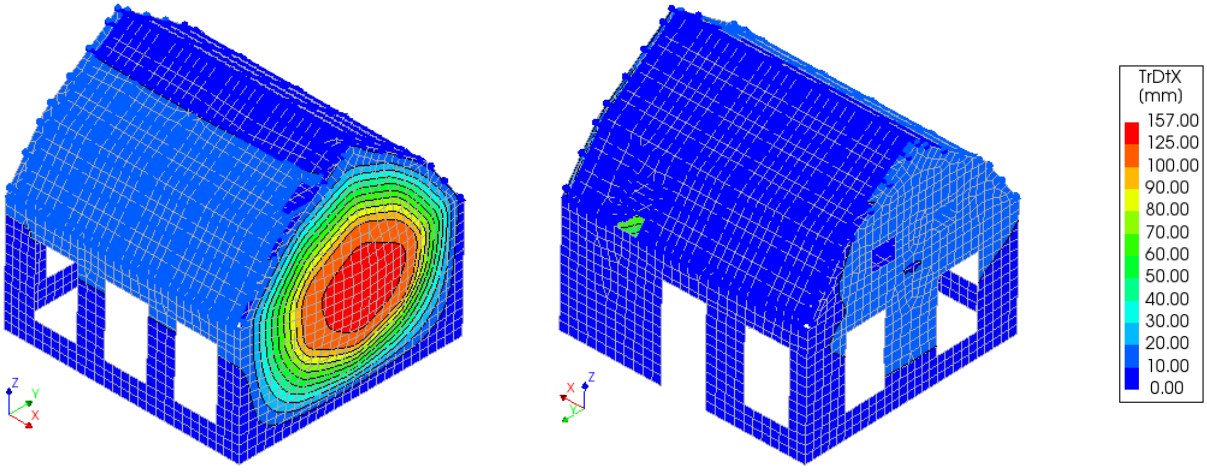

South-West view North-East view

Figure 18. Deformations in the North-South direction of LNEC-BUILD-3 #11 for motion M11 after the collapse of the South wall.

Table 12, Table 13 and Table 14 report the main outputs of the backbone curves defined for each variation in terms of attic displacement (d) and normalised base shear (v_a) at the points of cracking, peak and collapse as defined in section 3 and [2]. The results are expressed by considering different stop criteria of the OOP displacement.

Table 12. Main outputs of the backbone curves for each variation of LNEC-BUILD-3. OOP stop criteria equal to 60 and 100 mm.

Variation	OOP-060						OOP-100					
	Cracking		Peak		Collapse		Cracking		Peak		Collapse	
	d	v_a	d	v_a	d	v_a	d	v_a	d	v_a	d	v_a
	[mm]	[g]	[mm]	[g]	[mm]	[g]	[mm]	[g]	[mm]	[g]	[mm]	[g]
#10	2.06	0.32	8.61	0.88	19.57	0.0	2.06	0.32	13.85	0.88	21.55	0.0
#11	1.53	0.33	9.01	1.01	13.63	0.0	1.53	0.33	10.12	1.01	17.78	0.0
#12	1.56	0.33	9.23	1.00	14.01	0.0	1.56	0.33	10.27	1.00	17.80	0.0
#13	1.61	0.31	6.75	0.94	12.27	0.0	1.61	0.31	10.63	0.94	13.53	0.0
#14	1.37	0.31	6.70	1.06	9.96	0.0	1.37	0.31	7.61	1.06	12.74	0.0
#15	1.80	0.33	7.15	0.97	13.60	0.0	1.80	0.33	9.94	0.97	15.67	0.0
#16	1.41	0.33	6.50	1.04	10.37	0.0	1.41	0.33	8.12	1.04	13.27	0.0
AVG.	**1.62**	**0.32**	**7.71**	**0.99**	**13.34**	**0.00**	**1.62**	**0.32**	**10.08**	**0.99**	**16.05**	**0.00**
CV	**15%**	**3%**	**15%**	**6%**	**24%**	**-**	**15%**	**3%**	**20%**	**6%**	**20%**	**-**

Table 13. Main outputs of the backbone curves for each variation of LNEC-BUILD-3. OOP stop criteria equal to 110 and 120 mm.

Variation	OOP-110						OOP-120					
	Cracking		Peak		Collapse		Cracking		Peak		Collapse	
	d	v_a	d	v_a	d	v_a	d	v_a	d	v_a	d	v_a
	[mm]	[g]	[mm]	[g]	[mm]	[g]	[mm]	[g]	[mm]	[g]	[mm]	[g]
#10	2.06	0.32	13.85	0.88	21.76	0.0	2.06	0.32	13.85	0.88	21.97	0.0
#11	1.53	0.33	10.12	1.01	17.80	0.0	1.53	0.33	10.12	1.01	17.80	0.0
#12	1.56	0.33	10.27	1.00	17.84	0.0	1.56	0.33	10.27	1.00	17.84	0.0
#13	1.61	0.31	10.63	0.95	13.81	0.0	1.61	0.31	11.90	0.95	14.40	0.0
#14	1.37	0.31	7.61	1.06	12.76	0.0	1.37	0.31	7.61	1.06	12.76	0.0
#15	1.80	0.34	9.94	0.97	15.86	0.0	1.80	0.34	12.64	0.97	16.11	0.0
#16	1.41	0.33	8.12	1.06	13.32	0.0	1.41	0.33	8.12	1.06	13.32	0.0
AVG.	**1.62**	**0.32**	**10.08**	**0.99**	**16.16**	**0.00**	**1.62**	**0.32**	**10.64**	**0.99**	**16.31**	**0.00**
CV	**15%**	**3%**	**20%**	**6%**	**20%**	**-**	**15%**	**3%**	**22%**	**6%**	**20%**	**-**

Table 14. Main outputs of the backbone curves for each variation of LNEC-BUILD-3. OOP stop criteria equal to 200 mm and no out-of-plane criteria.

Variation	OOP-200						NO-OOP					
	Cracking		Peak		Collapse		Cracking		Peak		Collapse	
	d	v_a	d	v_a	d	v_a	d	v_a	d	v_a	d	v_a
	[mm]	[g]	[mm]	[g]	[mm]	[g]	[mm]	[g]	[mm]	[g]	[mm]	[g]
#10	2.06	0.32	13.85	0.88	25.52	0.0	2.06	0.32	25.64	0.88	72.22	0.0
#11	1.53	0.33	17.80	1.01	72.22	0.0	1.53	0.33	17.80	1.01	72.22	0.0
#12	1.56	0.33	17.74	1.00	72.22	0.0	1.56	0.33	17.74	1.00	72.22	0.0
#13	1.61	0.31	20.62	0.95	72.22	0.0	1.61	0.31	20.62	0.95	72.22	0.0
#14	1.37	0.31	14.88	1.06	72.22	0.0	1.37	0.31	14.88	1.06	72.22	0.0
#15	1.80	0.34	12.64	0.97	22.78	0.0	1.80	0.34	23.58	0.97	72.22	0.0
#16	1.41	0.33	15.15	1.06	72.22	0.0	1.41	0.33	15.15	1.06	72.22	0.0
AVG.	**1.62**	**0.32**	**16.10**	**0.99**	**58.49**	**0.00**	**1.62**	**0.32**	**19.34**	**0.99**	**72.22**	**0.00**
CV	**15%**	**3%**	**17%**	**6%**	**40%**	**-**	**15%**	**3%**	**21%**	**6%**	**0%**	**-**

The computed average values of each variation and for each OOP limit are summarised in Table 15 and plotted in Figure 19. The in-plane attic displacement at NC (72.2 mm) is not achieved for any simulation, but it is nevertheless considered as an upper limit. Lower and upper bounds of the average backbone curves taking into account the CV are depicted in Figure 20.

The difference in terms of peak and collapse displacement for the different failure criteria with respect to the OOP-100 limit case are reported in Table 16. When the OOP displacement is limited to 60 mm, a reduction of 24% and 17% for the peak and collapse displacement, respectively, are obtained with respect to the OOP limit of 100 mm. When the OOP limit is increased to 110 mm and 120 mm, no major difference is detected for both peak and collapse displacement (+6%). For OOP-200, the peak displacement increases to 16.1 mm (+60%), and the collapse displacement to 58.5 mm (+264%). When the OOP is assumed to be completely prevented, an increase to 19.3 mm (+92%) for the peak displacement and to 72.2 mm (+350%) for the collapse displacement, respectively, is achieved.

The overall results of the LNEC-BUILD-3 calculations are described and reported in Appendix E.

Table 15. Average backbone curves of LNEC-BUILD-3 for each stop criteria.

OOP-060		OOP-100		OOP-110		OOP-120		OOP-200		No OOP	
d [mm]	v_a [g]	d [mm]	v_a [g]	d [mm]	v_a [g]	d [mm]	v_a [g]	d [mm]	v_a [g]	d [mm]	v_a [g]
-13.34	0.00	-16.05	0.00	-16.16	0.00	-16.31	0.00	-58.49	0.00	-72.22	0.00
-7.88	-0.99	-10.08	-0.99	-10.08	-0.99	-10.64	-0.99	-16.10	-0.99	-19.34	-0.99
-1.62	-0.32	-1.62	-0.32	-1.62	-0.32	-1.62	-0.32	-1.62	-0.32	-1.62	-0.32
0.00	0.00	0.00	0.00	0.00	0.00	0.00	0.00	0.00	0.00	0.00	0.00
1.62	0.32	1.62	0.32	1.62	0.32	1.62	0.32	1.62	0.32	1.62	0.32
7.71	0.99	10.08	0.99	10.08	0.99	10.64	0.99	16.10	0.99	19.34	0.99
13.34	0.00	16.05	0.00	16.16	0.00	16.31	0.00	58.49	0.00	72.22	0.00

Table 16. Average peak and collapse displacement of LNEC-BUILD-3 and difference respect to OOP-100 case.

		OOP-060	OOP-100	OOP-110	OOP-120	OOP-200	No OOP
Peak	AVG	7.71	10.08	10.08	10.64	16.10	19.34
	Difference	-24%	0%	0%	+6%	+60%	+92%
Collapse	AVG	13.34	16.05	16.16	16.31	58.49	72.22
	Difference	-17%	0%	+1%	+2%	+264%	+350%

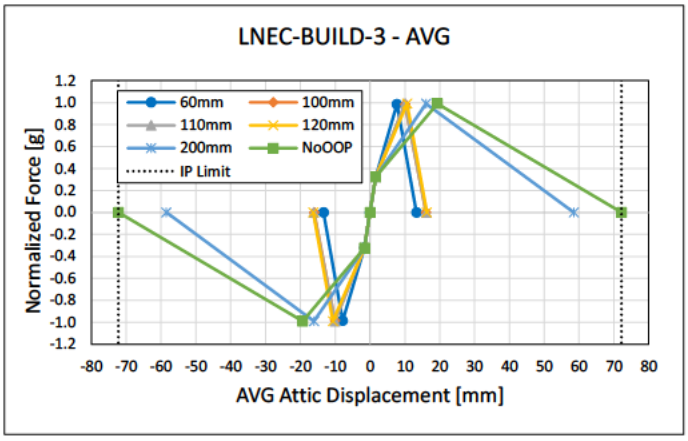

Figure 19. LNEC-BUILD-3 average backbone curves for each failure criteria. IP limits at 72.2 mm.

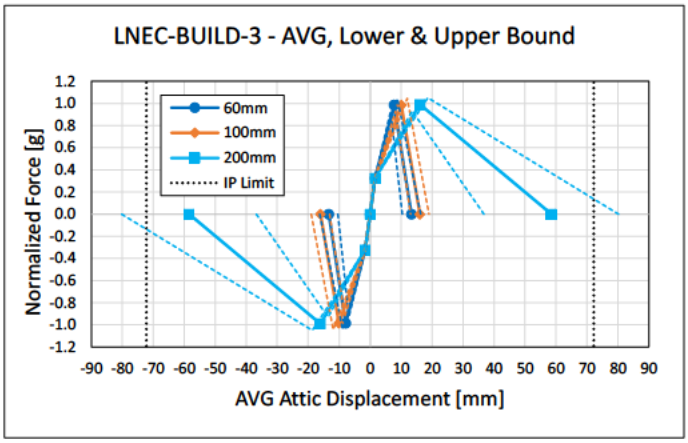

Figure 20. LNEC-BUILD-3 average, lower and upper backbone curves for three failure criteria. IP limits at 72.2 mm.

5 Conclusions

The work described in this document focuses on the effect of local out-of-plane failure of masonry walls (analysed via an indirect approach for which the failure is achieved at the exceedance of a pre-determined threshold value) on the global response of buildings classified under the typology 'Metselwerk 1' or 'Metselwerk 7'. Since the behaviour at near collapse of both typologies involves the local OOP of the walls, these can be strengthened to delay or even prevent the OOP collapse and hence improve the global building performance. In this study, the effect of the OOP strengthening applied locally on the global building performance is analysed via an indirect approach for which the failure is achieved at the exceedance of a pre-determined threshold value of already available nonlinear time history (NLTH) analyses. For the typology 'Metselwerk 1', a two-storey (plus attic) semi-detached houses (twee-onder-een-kapwoning) is selected as reference, named as 'Bleeksteen'. For the typology 'Metselwerk 7', two main buildings and their additional variations are considered. The buildings considered as reference are EUC-BUILD-2 and LNEC-BUILD-3.
The hysteresis curves obtained for each set of analyses are evaluated at the point where a specific failure criteria is exceeded (either OOP or IP). The OOP limit displacements represent the displacement capacity of the strengthened wall. The selected OOP displacement limits are equal to 60% and 100% the wall thickness (taken equal to 100 mm) for URM, and 110%, 120% and 200% the wall thickness for the strengthened walls. Additionally, a case in which the OOP failure is assumed to be completely prevented, so that the global structural behaviour is governed by the IP failure criterion, is also investigated. For each analysed building a mean backbone curve is computed for each failure criterion. An overview of the displacement at near collapse computed for each of the three buildings is shown in Figure 21.

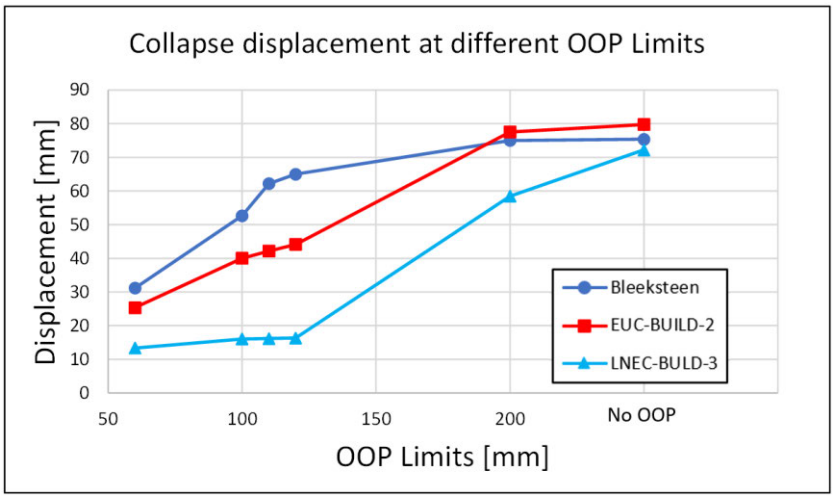

Figure 21. Peak and collapse displacement for different OOP limits for the three investigated buildings.

Since no clear definition of the dynamic OOP displacement limit for URM walls is available, two values (60 mm and 100 mm, taken as reference) are considered. When the OOP displacement is limited to 60% of the wall thickness:

- Peak and collapse displacement of Bleeksteen and EUC-BUILD-2 are about 40% lower with respect to the case when OOP is limited to 100 mm.
- In LNEC-BUILD-3 the reduction of the peak displacement is about 24% while the collapse one is 17% with respect to the case when OOP is limited to 100 mm.

When strengthening methods are applied (with respect to the reference case – 100 mm of maximum OOP displacement):

- The collapse displacement of Bleeksteen (Metselwerk 1) increases more than 40% when the OOP displacement is limited to 200% of the wall thickness. The collapse displacement is equal in this case to 75 mm, close to the value that can be achieved in case the OOP failure is completely prevented.
- For the two buildings belonging to 'Metselwerk 7', a typology for which the OOP failure is predominant, strengthening the walls against OOP failure has an even larger impact: the displacement at near collapse increases of more than 100% for the EUC-BUILD-2 building and even 350% for the LNEC-BUILD-3 building.

In addition, the following is observed:

- The increment of the collapse displacement of the Bleeksteen building when 120% the wall thickness is considered as OOP limit is 23% larger than that obtained for the reference 100 mm limit. This difference is much larger for the peak displacement of Bleeksteen building (+93% with respect to the reference case): this is mainly due to the excellent performance of the building for one motion (M11) for which large in-plane displacements are achieved with no exceedance of the OOP failure criteria.
- The peak and collapse displacements of the 'Metselwerk 7' buildings have low sensibility to small changes to the OOP limits, from 100% to 110% or 120% the wall thickness. A maximum variation of 10% is found in these cases.

Finally, it should be noted that any increment of the building normalized base shear due to the application of the strengthening methods (which affect also the in-plane behaviour of the walls, as shown in [22]) is conservatively not taken into account and goes beyond the scope and the possibility of the current study.

References

[1] Messali, F., Longo, M., Singla, A. (2021). Seismic performance of a semi-detached house: case study Bleeksteen 1-3, Delfzijl. Delft University of Technology. Report number 07, Version 03, 26 May 2021

[2] Messali, F., Longo, M., Singla, A. (2020). A numerical investigation of building typology 'Metselwerk 7'. Delft University of Technology. Report number 03, Version 02 (final), 04 June 2021

[3] Graziotti, F., Tomassetti, U., Rossi, A., Marchesi, B., Kallioras, S., Mandirola, M, Fragomeli, A., Mellia, E., Peloso, S., Cuppari, F., Guerrini, G., Penna, A., Magenes, G. (2016). Shaking table tests on a full-scale clay-brick masonry house representative of the Groningen building stock and related characterization tests. Report EUC128/2016U, EUCENTRE, Pavia, IT

[4] Kallioras, S., Correia, A.A., Marques, A.I., Bernardo, V., Candeias, P.X., Graziotti, F. (2018). LNEC-BUILD-3: an incremental shake-table test on a Dutch URM detached house with chimneys. Report EUC203/2018U, EUCENTRE, Pavia, IT

[5] Graziotti, F., Tomassetti, U., Rossi, A., Kallioras, S., Mandirola, M., Cenja, E., Penna, A., Magenes G. (2015). Experimental campaign on cavity-wall systems representative of the Groningen building stock. Report, EUC318/2015U, EUCENTRE, Pavia, Italy

[6] Graziotti, F., Tomassetti, U., Penna, A., & Magenes, G. (2016). Out-of-plane shaking table tests on URM single leaf and cavity walls. Engineering Structures, 125, 455-470

[7] Türkmen, Ö.S. (2020). Seismic retrofitting of masonry walls with flexible deep mounted CFRP strips. Technische Universiteit Eindhoven

[8] Giaretton, M., Dizhur, D., Ingham, J.M. (2016). Shaking table testing of as-built and retrofitted clay brick URM cavity-walls. Engineering Structures 125 (2016) 70–79

[9] Cassol, D., Giongo, I., Ingham, J.M., Dizhur, D. (2021). Seismic out-of-plane retrofit of URM walls using timber strong-backs. Construction and Building Materials 269 (2021) 121237

[10] Damiani, N., Miglietta, M., Mazzella, L., Grottoli, L., Guerrini, G., Graziotti, F. (2019). Full-scale shaking table test on a dutch URM cavity-wall terraced-house end unit a retrofit solution with strong-backs and OSB boards. EUC-BUILD-7. Research Report EUC052/2019U, V1.0, 07/03/2019

[11] Kallioras, S., Guerrini, G., Tomassetti, U., Peloso, S., & Graziotti, F. (2018). Dataset from the dynamic shake-table test of a full-scale unreinforced clay-masonry building with flexible timber diaphragms. Data in brief, 18, 629-640

[12] NEN, Nederlands Normalisatie Instituut (2020). NPR 9998:2020 nl. Beoordeling van de constructieve veiligheid van een gebouw bij nieuwbouw, verbouw en afkeuren - Geïnduceerde aardbevingen - Grondslagen, belastingen en weerstanden. Delft, the Netherlands (in Dutch)

[13] Ravenshorst, G., & Mirra, M. (2017). Test report on cyclic behaviour of replicated timber diaphragms representing a detached house. Delft University of Technology

[14] Messali, F., Rots, J.G. (2018). EUC-BUILD-6: post-test refined predictions (TU Delft – DIANA 10.2). TU Delft Report, 28 October 2018

[15] Crowley, H., Pinho, R. (2020). Report on the Fragility and Consequence Models for the Groningen Field (Version 7). NAM report, March 2020

[16] Merczel, D., Abeysekera, I., McVitty, W., Grant, D., Kluwer, R., (2017). Typology Modelling: Analysis Results in Support of Fragility Functions – 2017 Batch Results. NAM report, October 2017

[17] Messali, F., Longo, M. (2021). Study of a median backbone curve and of the building to building variability for typology 'Metselwerk 1'. Delft University of Technology. Report number 02, Final Version, 11 June 2021

[18] Singla, A., Longo, M., Messali, F. (2020). Influence of the floor type at first storey level on the seismic behaviour of a terraced house. Memorandum, Delft University of Technology. 09 June 2020

[19] Messali, F., Longo, M. (2020). Definition of a consistent backbone curve for typology 'Metselwerk 2'. Delft University of Technology. Report number 01, Version 02, 14 April 2020

[20] Schreppers, G.M.A., Garofano, A., Messali, F., Rots, J.G. (2017). DIANA Validation report for Masonry modelling. Report *DIANA FEA BV & TU Delft*, 15 February 2017

[21] Longo, M., Messali, F. (2022). Calibration against shake table tests of a FE model for URM cavity walls subjected to out-of-plane dynamic loads. Report number 10, Draft version 02, 21 March 2022

[22] Guerrini, G., Damiani, N., Miglietta, M., Graziotti, F. (2021). Cyclic response of masonry piers retrofitted with timber frames and boards. Proceedings of the Institution of Civil Engineers-Structures and Buildings, 174(5), 372-388

[23] Crowley, H., Pinho, R., Cavalieri, F. (2019). Report on the v6 Fragility and Consequence Models for the Groningen Field. NAM report, March 2019

Appendix A – Experimental background of strengthening methods

Strengthening of cavity walls via anchors

A series of shake table tests have been performed at the laboratories of EUCENTRE (Pavia, Italy) in 2015 [5] [6]. The experimental campaign considered the one way bending performance of both single leaf and cavity walls. In total, four tests were carried out, one on a single leaf wall, and three on cavity walls. Two different levels of pre-compression for the loadbearing walls were applied. Additionally, also the number of wall ties connecting the two leaves in the cavity walls was varied. The characteristics of the four tested specimens are reported in Table A1. A complete and detailed description of the tests and of the specimens is provided in [5].

Table A1. Properties of the specimens tested at EUCENTRE (2015).

Specimen name	Wall type	L (m)	t (m)	H (m)	σ_v (MPa)	No. ties
EC_COMP_4	Single-leaf wall	1.438	0.102	2.754	0.3 – 0.1	-
EC_COMP_5	CS inner wall	1.438	0.102	2.754	0.1	2/m^2
	Clay outer wall	1.425	0.100	2.700	-	
EC_COMP_6	CS inner wall	1.438	0.102	2.754	0.3	2/m^2
	Clay outer wall	1.425	0.100	2.700	-	
EC_COMP_7	CS inner wall	1.438	0.102	2.754	0.1	4/m^2
	Clay outer wall	1.425	0.100	2.700	-	

Figure A1 to Figure A4 report the performance of the specimens up to failure of the four tested specimens in terms of maximum mid-height displacements reached during each motion against the measured PGA. It should be noted that two figures are presented for EC_COMP_4 (the single leaf wall) because the wall was tested under two different levels of pre-compression. However, no collapse was found for the highest level of vertical pre-compression (σ_v = 0.3 MPa).
Table A2 summarizes the value of the maximum PGA reached for each tested specimens.
The authors of the experimental campaign noted that [6]:

- the wall ties ensured a horizontally coupled response in the cavity walls, even for the specimens containing only 2 ties/m^2;
- the number of ties connecting the two leaves affects the cavity wall response;
- the capacity of cavity walls is strongly influenced by the vertical stress acting on the loadbearing leaf (similar to single leaf walls);
- all the tested cavity wall specimens showed lower capacities when compared to the single-leaf specimen loaded with the same axial force.

As regards the last remark, it is observed that for a low pre-compression level similar performance between the single leaf and the cavity walls is obtained whit 4 ties/m^2, whereas a reduced capacity (-20% PGA) is achieved in case of 2 ties/m^2. For a higher compression, the cavity wall reaches a higher value of PGA with respect to the corresponding single leaf wall. However, the latter is not pushed up to failure, so that a similar final performance between the two typologies of walls is expected. Finally, also the displacements reached at failure by single leaf and the CS loadbearing inner leaf of the cavity walls are comparable, although the latter wall typology shows slightly larger ductility.
In general, a cavity wall for which the two leaves are strongly coupled is not able to achieve better performance than a corresponding single leaf wall. In other terms, the coupling of the veneer to the loadbearing inner leaf does not significantly improve the performance of the cavity wall as a whole, although it is essential to avoid the collapse of the veneer (which is the most vulnerable part of a cavity wall due to the cantilever static scheme and the reduced vertical loads). For this reason, the displacement capacity of cavity walls strengthened by the application of anchors which couple the two leaves is maintained equal to the thickness of the inner leaf in the numerical simulations presented in the main report.

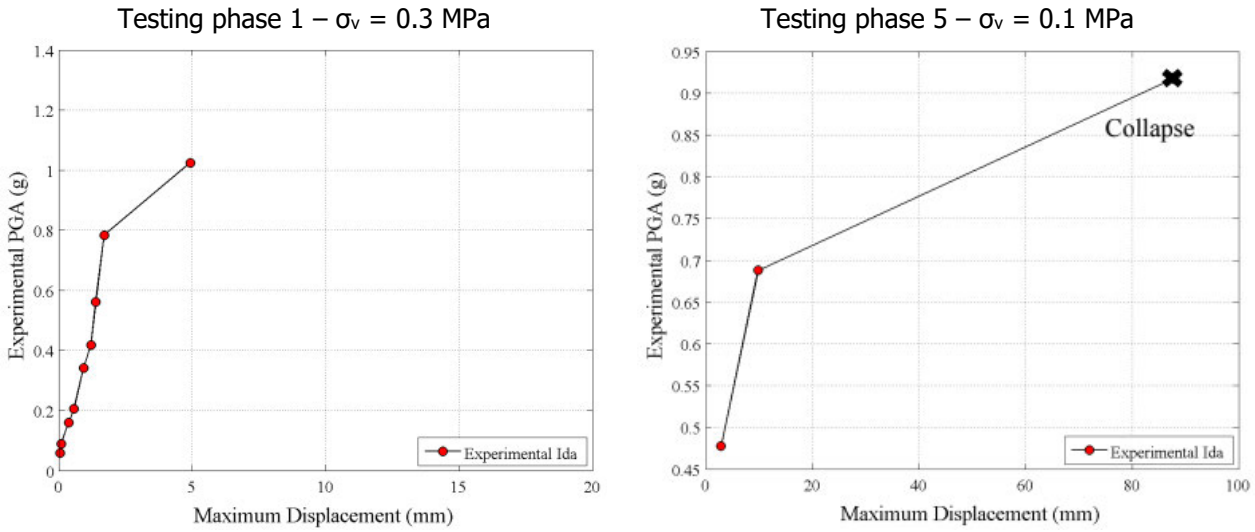

Figure A1. Performance of specimen EC_COMP_4 for incremental out-of-plane loading up to collapse [5].

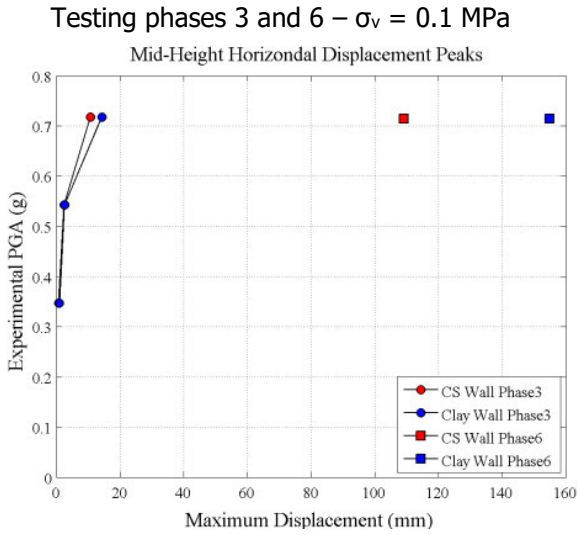

Figure A2. Performance of specimen EC_COMP_5 for incremental out-of-plane loading up to collapse [5].

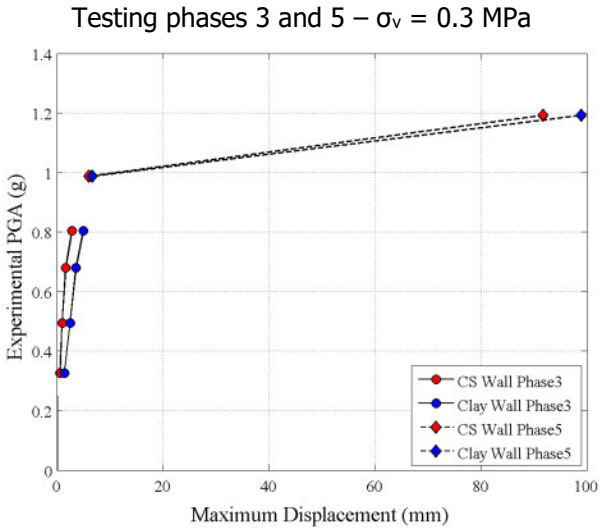

Figure A3. Performance of specimen EC_COMP_6 for incremental out-of-plane loading up to collapse [5].

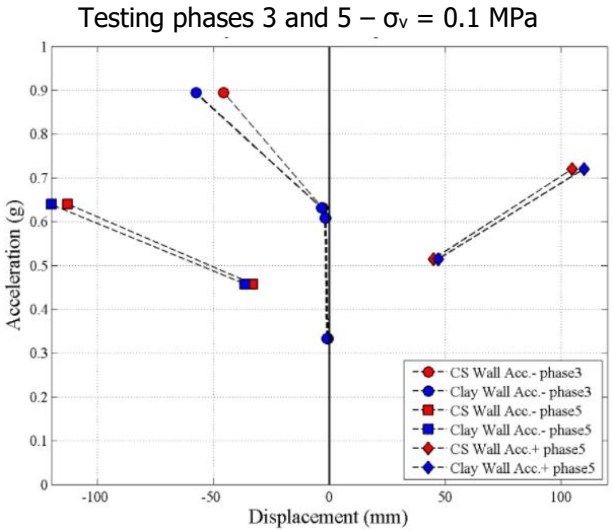

Figure A4. Performance of specimen EC_COMP_7 for incremental out-of-plane loading up to collapse [5].

Table A2. Summary of the maximum PGA reached during the tests for each specimen.

Precompression	σ_v = 0.1 MPa			σ_v = 0.3 MPa	
Type of wall	Single leaf wall	Cavity wall	Cavity wall	Single leaf wall	Cavity wall
Name of wall	EC_COMP_4	EC_COMP_5	EC_COMP_7	EC_COMP_4	EC_COMP_6
No. of ties	-	2/m^2	4/m^2	-	2/m^2
Max PGA	0.92	0.72	0.90	1.05 (no collapse)	1.20

Application of FDM CFRP strips

Flexible deep mounted carbon FRP (FDM CFRP) strips to masonry using a flexible adhesive is a retrofitting technique developed to improve the out-of-plane seismic behaviour of URM walls. The performance of strengthened masonry walls was tested in an experimental campaign carried out at TU Eindhoven [7], alone and in combination with a single-sided fabric reinforced cementitious matrix (FRCM) overlay to form a hybrid retrofit solution. The FRCM system consists of a carbon fiber mesh embedded in a polymer-modified mortar. In the following only the improvement of the OOP performance of the walls due to the application of the CFRP strips is considered and concisely summarized.

To test the performance of the strengthened walls, nine full scale walls were tested under quasi-dynamic cyclic lateral loading: three unreinforced reference specimens, and six walls reinforced with two FDM CFRP strips each, as shown in Figure A5. A vertical load was applied at the top of the walls and maintained constant throughout the experiment, whereas a cyclic lateral load was applied by means of four horizontal steel beams. The plot of the moment - mid span displacements for the unreinforced and the strengthened specimens is shown in Figure A6 and Figure A7, respectively. A comparison between the backbone curves of the lateral moment - mid span displacement for both unreinforced and strengthened specimens is displayed in Figure A8. Specimens URM-1 are STRIP-6 are not included in the comparison: the former due to an unexpected asymmetric behaviour, the latter because a higher compressive axial load was applied compared to all the other tests.

The following is observed by the author of the tests:

- Compared to the URM specimens, the application of the FDM CFRP strips determine smaller multiple cracks in the mortar joints rather than a single wide open crack;
- The moment capacity of the URM wall is increased with 133% with the installation of the FDM CFRP strips.
- As for the mid-span displacement, the instability displacement was approximately equal to the wall thickness for the URM specimens. For the FDM CFRP retrofitted specimen with high axial load, the instability displacement was estimated at 200 mm, whereas the limit is even higher in case of low axial load (it was not obtained due to the stroke limits of the used actuator).

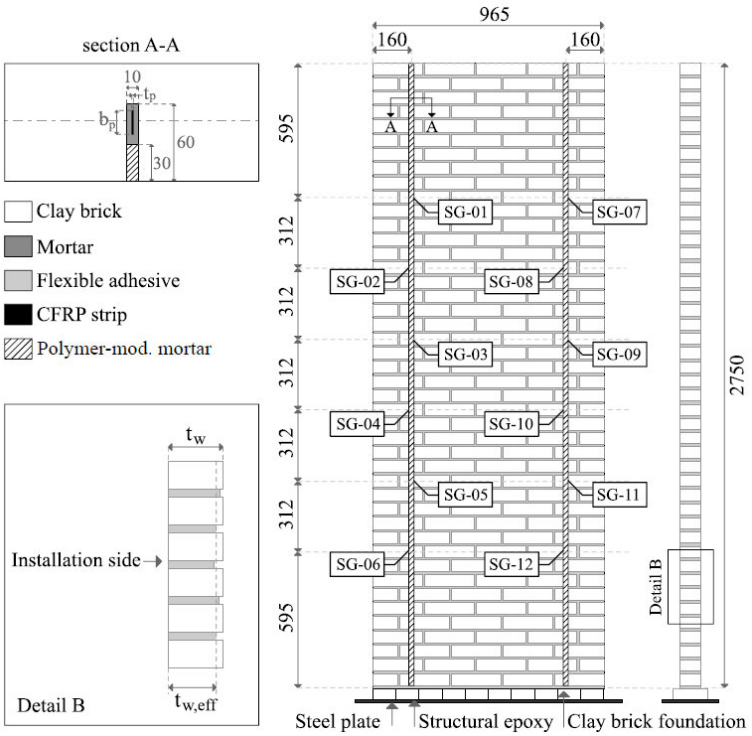

Figure A5. Schematic overview of a FDM CFRP strip retrofitted specimen (from [7]).

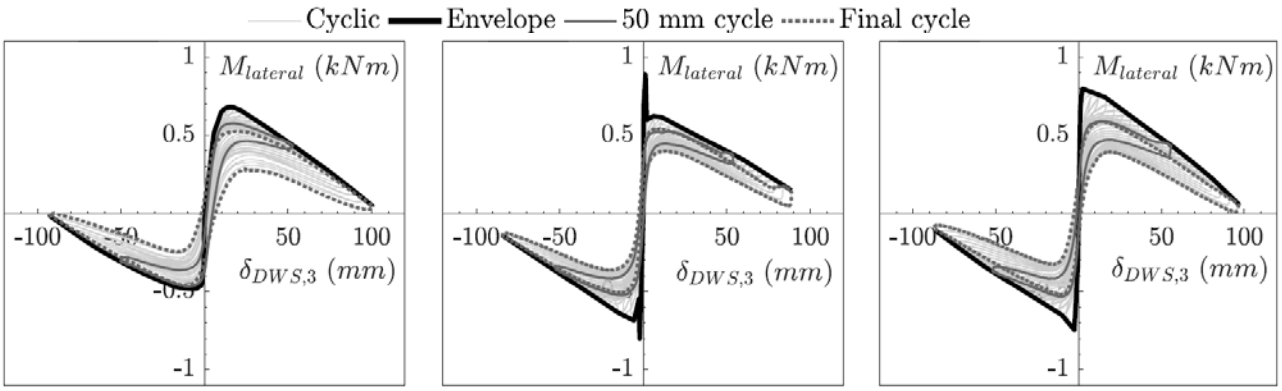

Figure A6. Moment – mid span displacement plots of unreinforced reference specimens (from [7]).

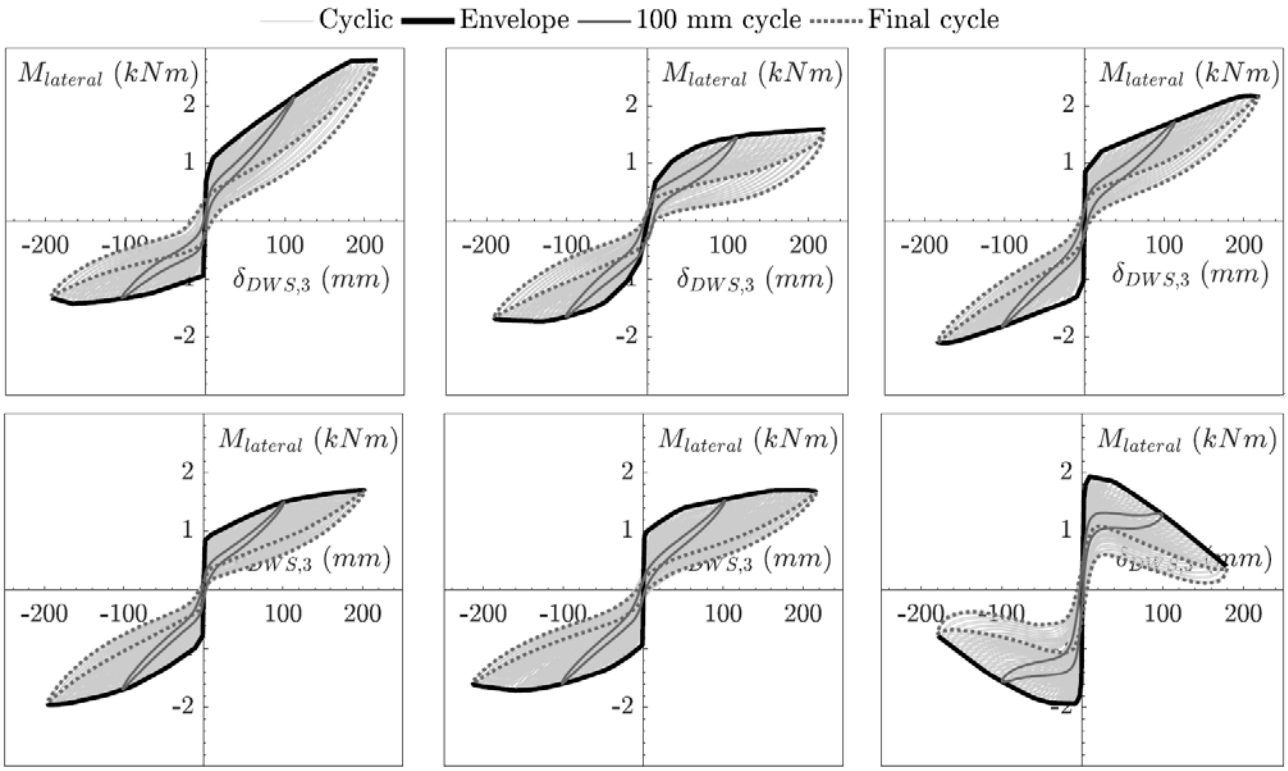

Figure A7. Moment – mid span displacement plots of the strengthened specimens (from [7]).

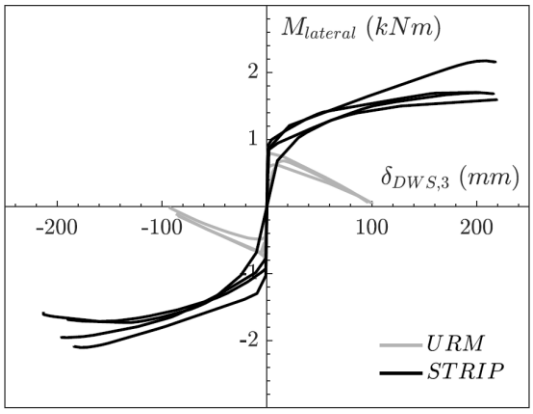

Figure A8. Backbone lateral moment – mid span displacement plots of all URM and strengthened specimens (from [7]).

Application of timber strong-backs

The out-of-plane performance of URM cavity walls can be improved by connecting vertical timber elements (strong-backs) to the interior surface of the walls using mechanical screws or bolts. This retrofitting technique has been studied experimentally at the University of Auckland (New Zealand) [8] [9] and at EUCENTRE (Pavia, Italy) [10]. In the first case, both shake table tests and quasi-static pushover tests have been performed on single walls whereas in the latter case the retrofitting solution has been applied to a full scale complete building, which was tested on a shake table. Also the type of masonry differs between the two studies. The cavity walls investigated at the University of Auckland are made of solid clay bricks for both the inner and the outer leaf,

with strong-backs made of radiate pine purlins of 45 x 90 mm section (Figure A9a). The walls studied at EUCENTRE are built to resemble traditional Dutch cavity walls, made of calcium silicate bricks and perforated clay bricks for the inner and the outer leaf, respectively, and the timber purlins have a section of 80x60 mm, where 60 mm was the dimension perpendicular to masonry walls (Figure A9b).

(a) (b)

Figure A9. Specimens tested at the University of Auckland (a) [9] and at EUCENTRE (b) [10].

The shake table tests performed at the University of Auckland [8] show that the addition of timber strong-backs allow the walls to withstand motions with a maximum PGA more than twice higher than that achieved by the unreinforced reference specimens, as shown in Figure A10. On the other hand, no increase in terms of displacement capacity is reported. When quasi-static tests are performed by means of airbags [8], the capacity of the retrofitted walls was found largely increased when compared to that of the URM walls (3.5 times when the strong-back is on the compression side and 5.6 times when the strong-back is on the tension side, respectively). Again, no increase in terms of displacement capacity is reported.

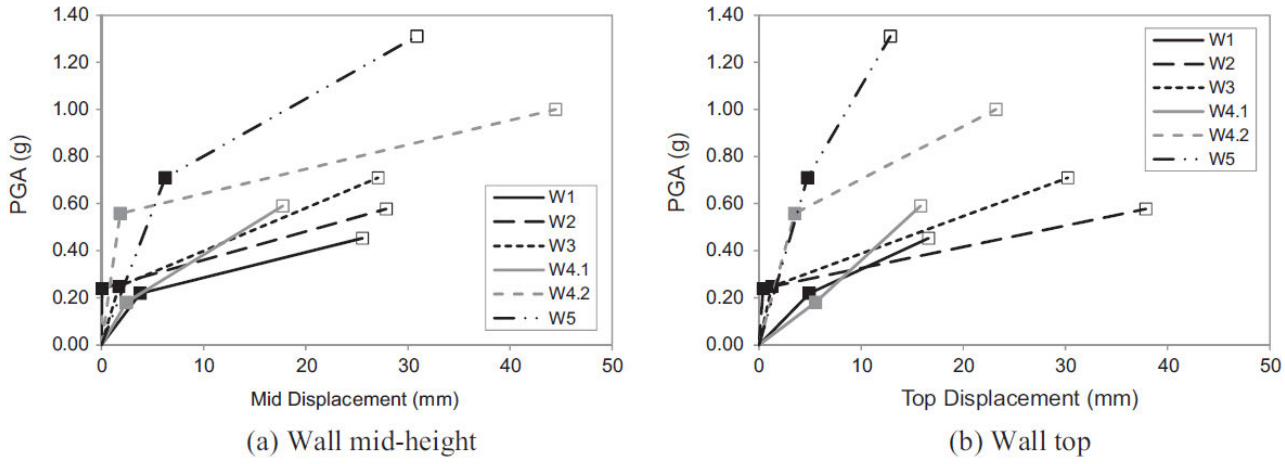

Figure A10. PGA versus maximum displacement recorded in the walls: W1, W4 are the unreinforced specimens, whereas W5 is the specimen strengthened with the addition of strong-backs (from [8]).

The shake table test performed at building level at EUCENTRE was carried out on a building strengthened by means of the application of timber strong-backs to the walls and OSB panels to the timber floors. A building having the same characteristics, but unreinforced, had been previously tested and considered as benchmark (EUC-BUILD-6). It should be noted that collapse of EUC-BUILD-6 was mainly governed by the in-plane failure of the piers at the first storey level. Indeed, the strengthening measure aimed to improve not only the OOP but also the IP performance of the single structural elements, as documented by the IP tests performed at the wall scale [10], for which both the force and displacement capacity increased largely after the application of the strong-backs.

The results of the incremental dynamic test show that the strengthened specimen is able to withstand motions having a maximum PGA twice as high as that found for the URM specimen (Figure A11a), in line with the results presented in [8]. A similar increase of base shear is observed (Figure A11b). However, such improvement of the performance is determined also by the additional stiffness provided to the floors by the OSB panels and, especially, by the increased in-plane capacity of the masonry piers. Also at the building level, the maximum achieved displacement does not increase in comparison with the URM case, although the residual force at the maximum displacement is significantly larger in case of the strengthened building.

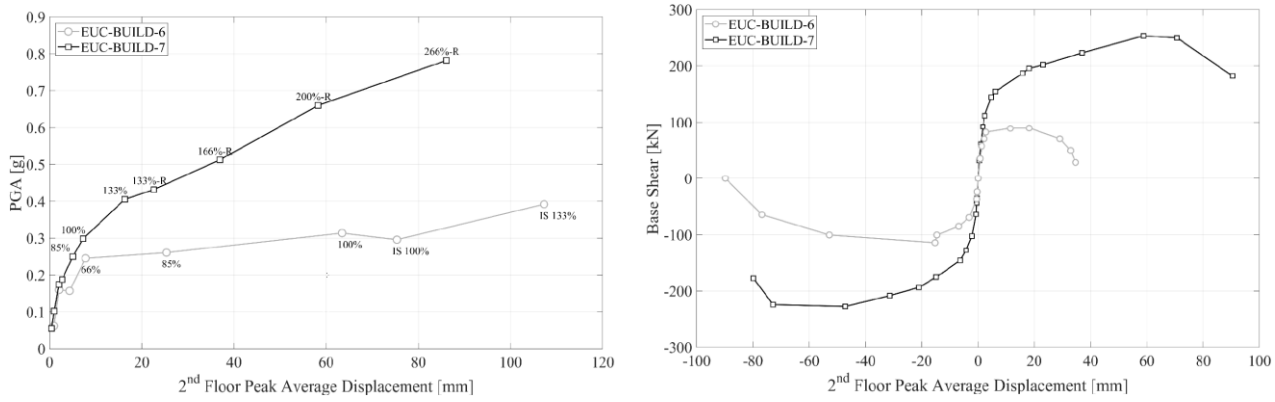

(a) (b)

Figure A11. Comparison between the performance of the URM specimen (EUC-BUILD-6) and strengthened specimen (EUC-BUILD-7): PGA (a) and base shear (b) vs attic floor displacement (from [10])

The application of the timber strong-backs significantly improve the OOP capacity of the masonry walls, but the experimental tests do not document an increase of the displacement at near collapse. Besides, the modified in-plane behaviour of the walls too should be considered in order to accurately estimate the performance of a building strengthened with the application of strong-backs, which goes beyond the scope of the current study as defined in Section 1 of the main report.

Appendix B – Ground motions

The seven ground motions used are selected from [16] and adopted in this study and they are listed in Table 3. Each motion contains three components, two horizontal and one vertical. The accelerogram of the each motion is plotted in Figure B1. The response spectra of the motions are shown in Figure B2.

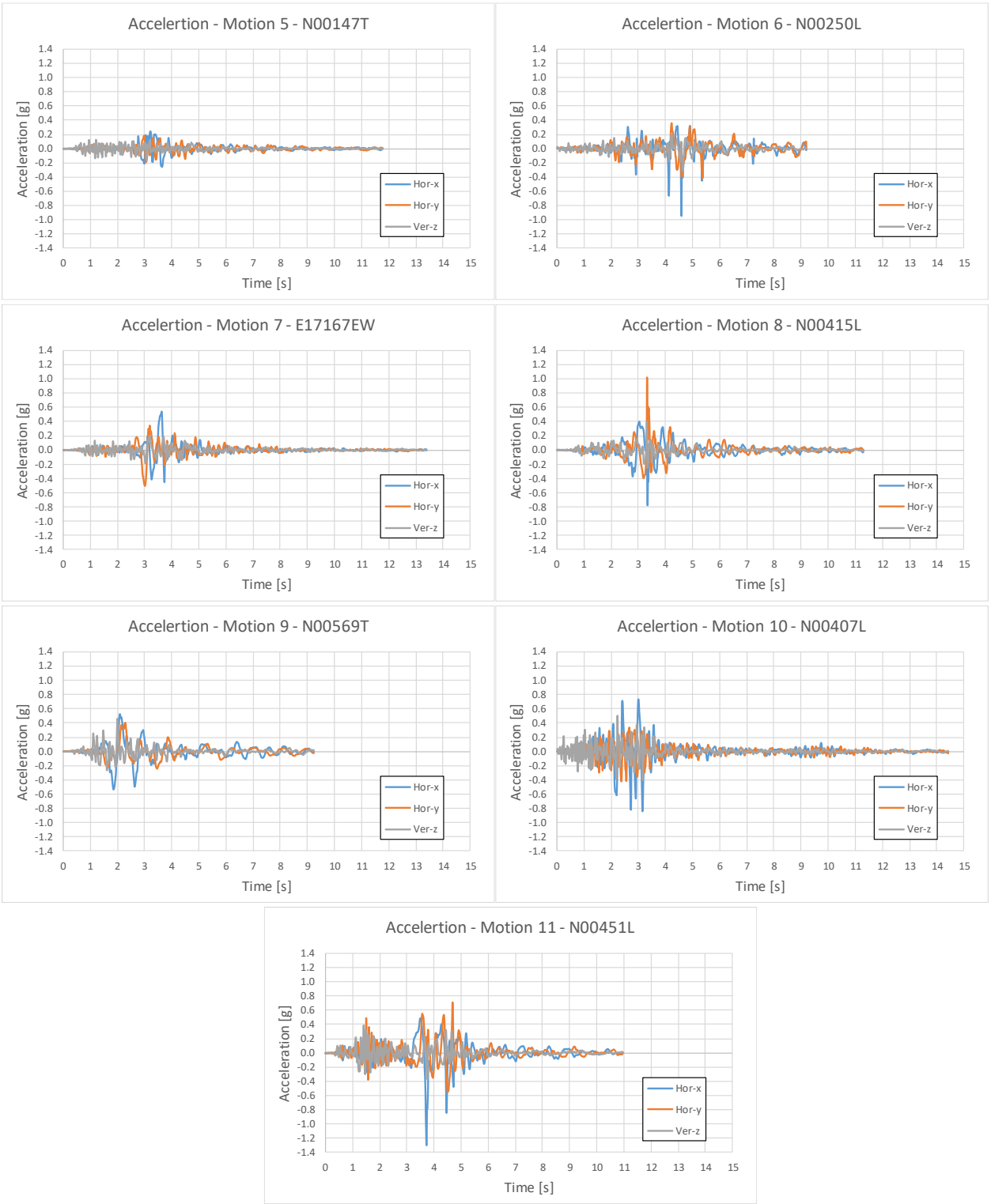

Figure B1. Accelerograms of the seven applied ground motions.

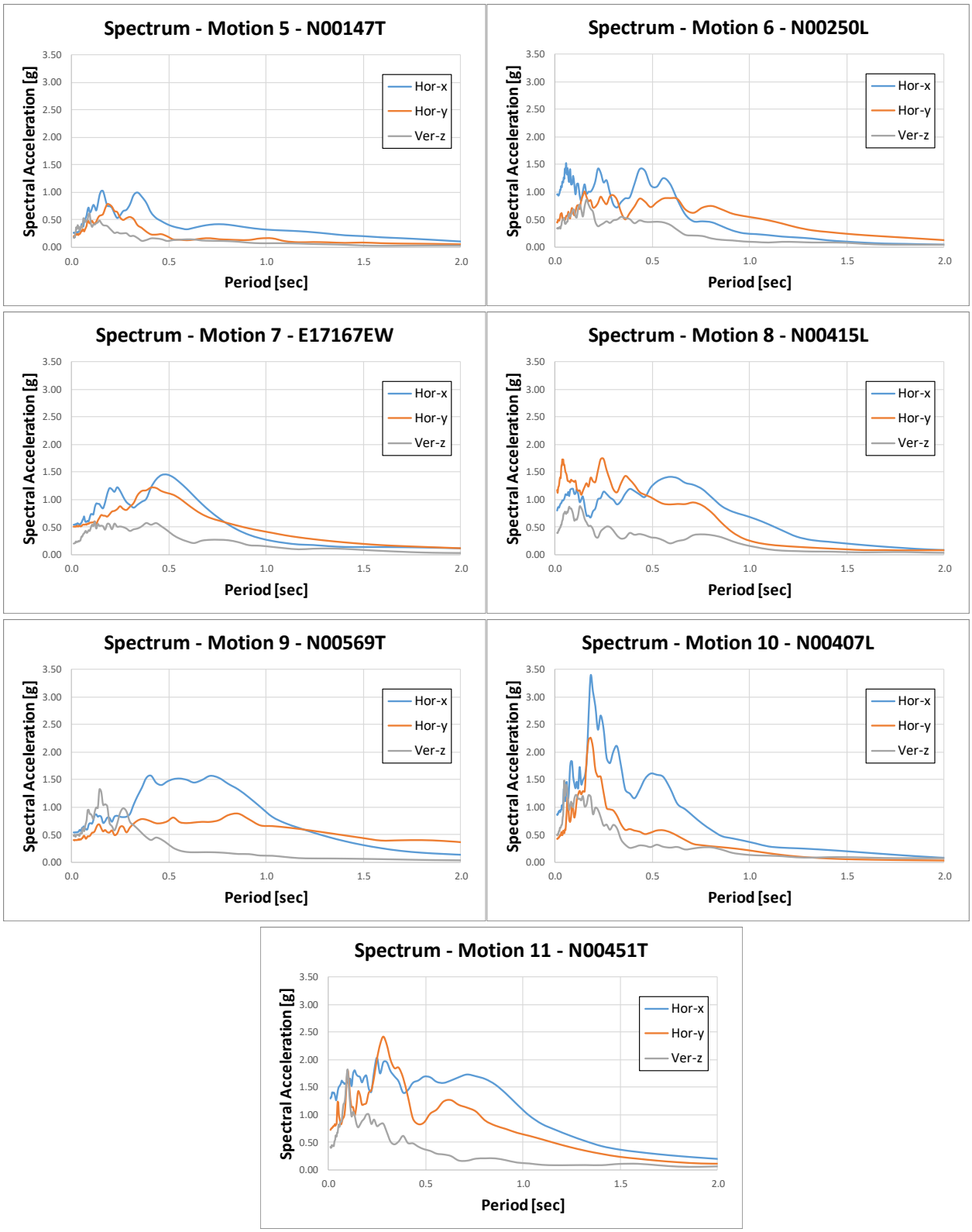

Figure B2. Response Spectra of the seven applied ground motions.

Appendix C – Material properties

The following material properties have been used in the numerical simulations with Diana FEA 10.4. The Engineering Masonry Model [20] is used as material model for piers, bank, spandrel and gables. Local y axis is aligned to the global Z axis in order to define the bed joint orientation. For the NLTH calculations the elastic properties are halved in order to properly capture the cyclic strength degradation, not explicitly described by the EMM. Besides, the same assumption has been already employed in other calibration/validation studies of URM buildings to overcome the global rigidity given by local connections which results in over stiff results.

1. Clay brick masonry (brickwork pre 1945): Engineering Masonry Model (EMM)

Elasticity parameters			
E_x = 2500 N/mm^2	E_y = 2500 N/mm^2	Gxy = 1250 N/mm^2	ρ = 1980 kg/m^3
Cracking parameters			
Head-joint failure type: tensile strength head-joint defined by friction			
f_{ty} =0.15 N/mm^2	$f_{tx,min}$ = 0.45 N/mm^2	G_{fI} = 0.01 N/mm	α = 0.60 rad
Crushing parameters			
f_c = 8.5 N/mm^2	G_c = 20 N/mm	n = 3	λ = 1
Shear failure parameters			
φ = 0.64 rad	c_0 = 0.30 N/mm^2	G_{fII} = 0.1 N/mm	Crack bandwidth: Rots

More detailed information on the meaning of the parameters and the constitutive model can be found in [20]

2. Clay brick masonry (brickwork post 1945): Engineering Masonry Model (EMM)

Elasticity parameters			
E_x = 1500 N/mm^2	E_y = 3000 N/mm^2	Gxy = 1250 N/mm^2	ρ = 1980 kg/m^3
Cracking parameters			
Head-joint failure type: tensile strength head-joint defined by friction			
f_{ty} =0.30 N/mm^2	$f_{tx,min}$ = 0.90 N/mm^2	G_{fI} = 0.01 N/mm	α = 0.50 rad
Crushing parameters			
f_c = 10 N/mm^2	G_c = 15 N/mm	n = 3	λ = 1
Shear failure parameters			
φ = 0.64 rad	c_0 = 0.40 N/mm^2	G_{fII} = 0.2 N/mm	Crack bandwidth: Rots

3. Calcium Silicate masonry: Engineering Masonry Model (EMM)

Elasticity parameters			
E_x = 1333 N/mm^2	E_y = 2000 N/mm^2	Gxy = 825 N/mm^2	ρ = 1850 kg/m^3
Cracking parameters			
Head-joint failure type: tensile strength head-joint defined by friction			
f_{ty} =0.15 N/mm^2	$f_{tx,min}$ = 0.30 N/mm^2	G_{fI} = 0.01 N/mm	α = 0.62 rad
Crushing parameters			
f_c = 7 N/mm^2	G_c = 15 N/mm	n = 3	λ = 1
Shear failure parameters			
φ = 0.54 rad	c_0 = 0.25 N/mm^2	G_{fII} = 0.1 N/mm	Crack bandwidth: Rots

4. Timber planks: orthotropic elastic behaviour

Linear material parameters		
E_x = 1.5 N/mm^2	E_y = 11 N/mm^2	E_z = 400 N/mm^2
v_{xy} = 0	v_{yz} = 0	v_{xz} = 0
G_{xy} = 1100 N/mm^2	G_{yz} = 1100 N/mm^2	G_{xz} = 500 N/mm^2

$\rho = 10^{-20}$ T/mm^3: the mass of the timber floor is applied directly to the timber joists.

5. Timber beams and lintels: isotropic elastic behaviour

Linear material parameters 'Metselwerk 1'		
E = 9000 N/mm^2	v = 0.35	ρ = 380 kg/m^3
Linear material parameters 'Metselwerk 7'		
E = 12000 N/mm^2	v = 0.40	ρ = 450 kg/m^3

6. Pocket connection timber-masonry: Coulomb-Friction ('Metselwerk 7' only)

Elasticity parameters			
k_n = 1000 N/mm^3	k_{t1} = 100 N/mm^3	k_{t2} = 100 N/mm^3	
Coulomb friction parameters			
φ = 0.54 rad	c_0 = 0.02 N/mm^2	ψ = 0.0 rad	Opening: No opening

7. Reinforced concrete: isotropic elastic behaviour

Linear material parameters 'Metselwerk 1'		
E = 27000 N/mm^2	v = 0.15	ρ = 2500 kg/m^3

8. Nehobo floor: isotropic elastic behaviour

Linear material parameters 'Metselwerk 1'		
E = 2000 N/mm^2	v = 0.15	ρ = 1700 kg/m^3

Appendix D – hysteretic and backbone curves for NLTHA of EUC-BUILD-2

Variation #01 - OOP Criteria 100 mm

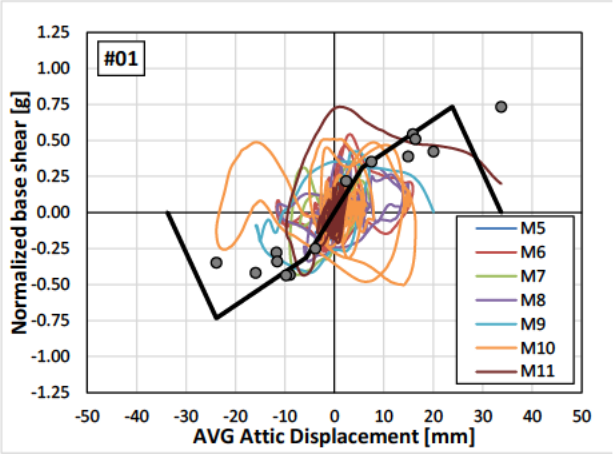

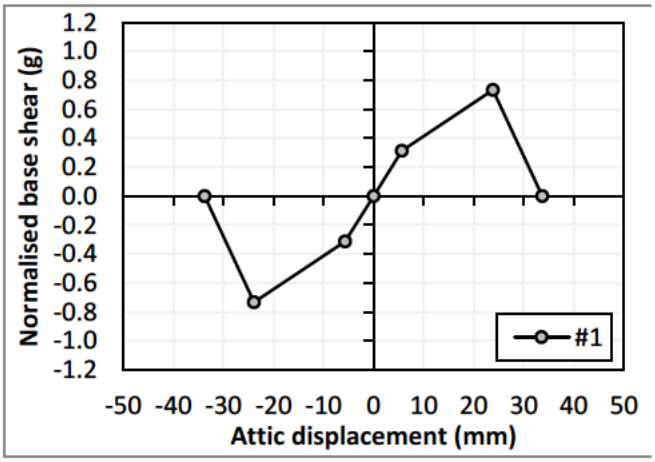

Variation #02 - OOP Criteria 100 mm

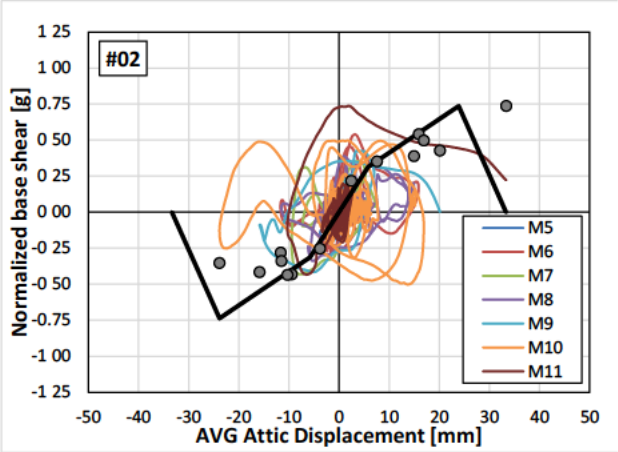

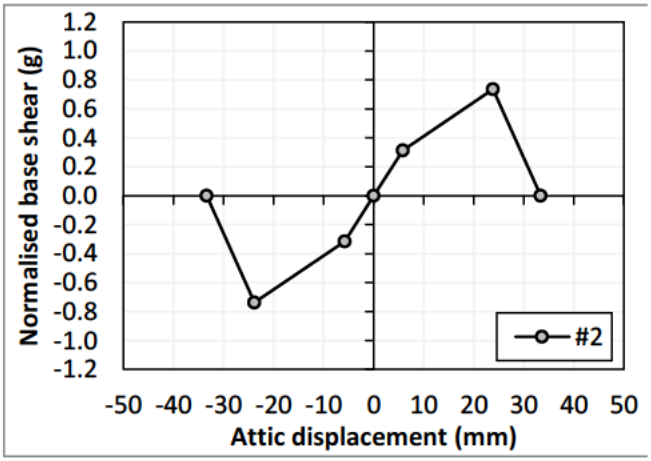

Variation #03 - OOP Criteria 100 mm

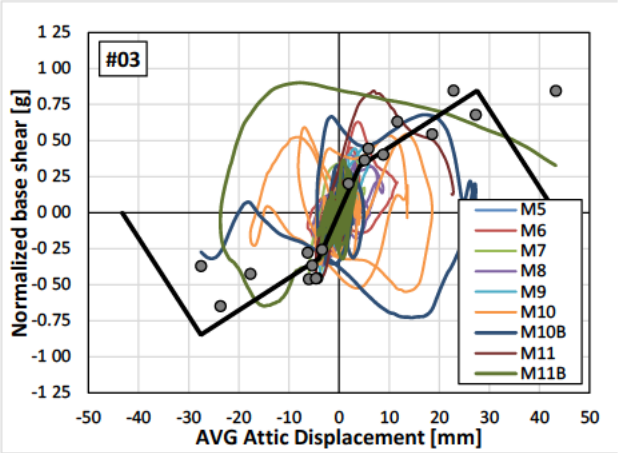

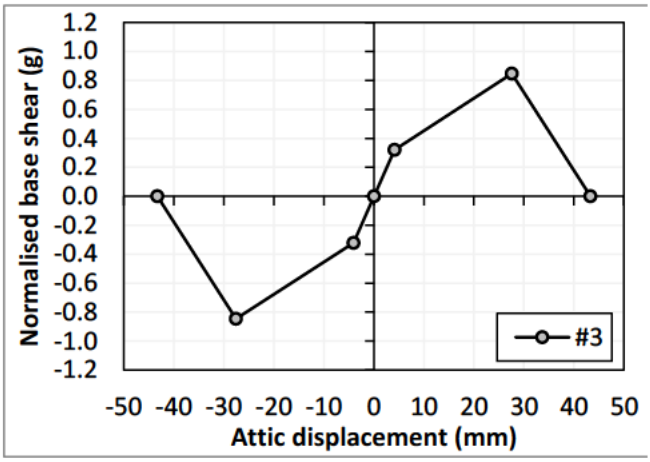

Variation #04 - OOP Criteria 100 mm

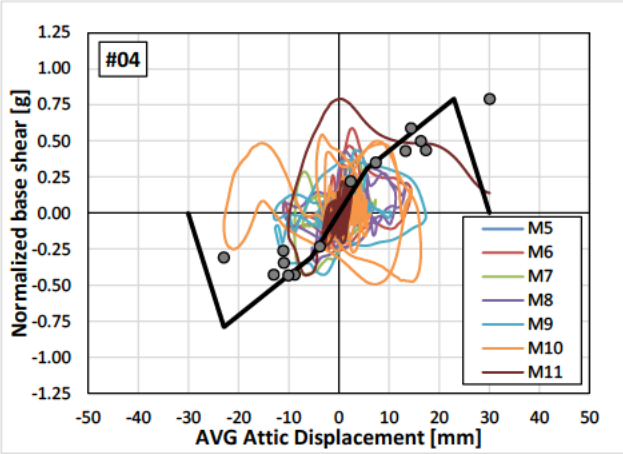

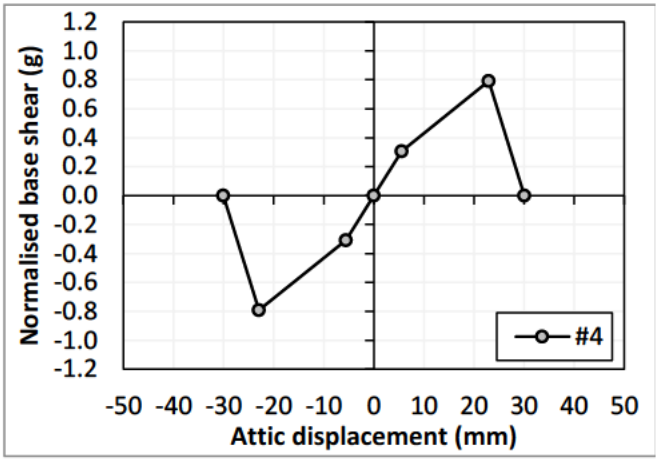

Variation #05 - OOP Criteria 100 mm

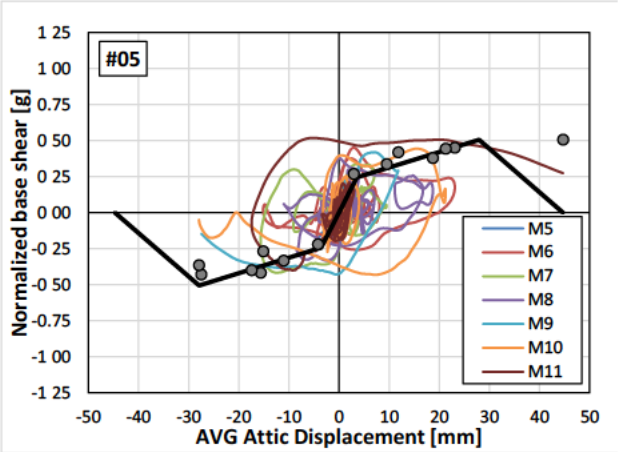

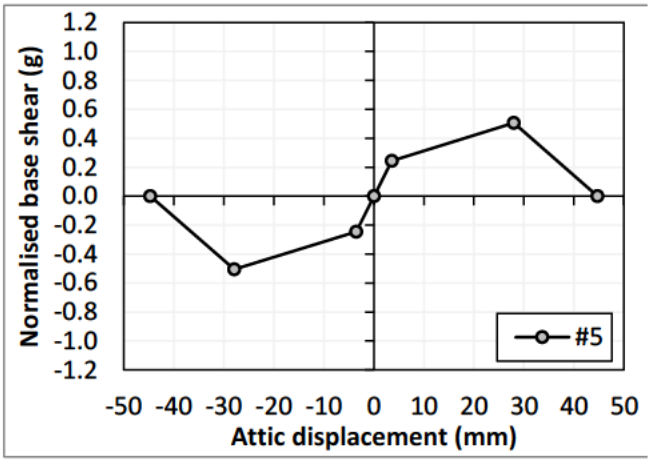

Variation #06 - OOP Criteria 100 mm

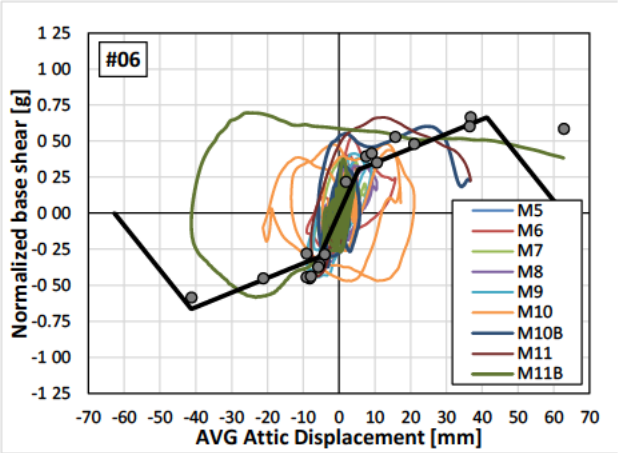

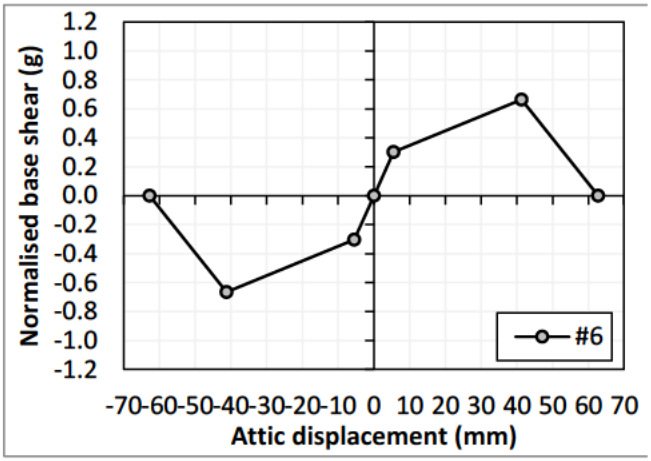

Variation #07 - OOP Criteria 100 mm

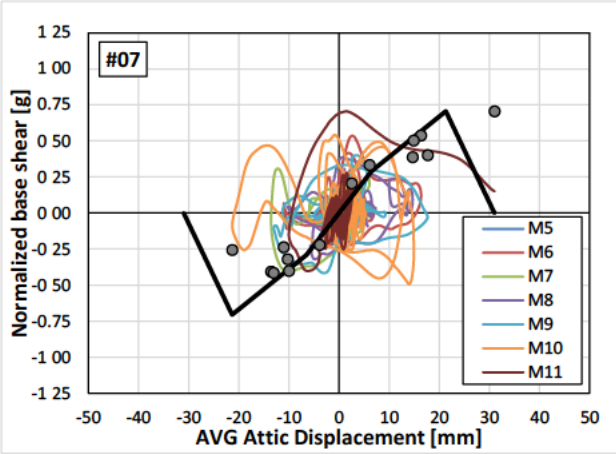

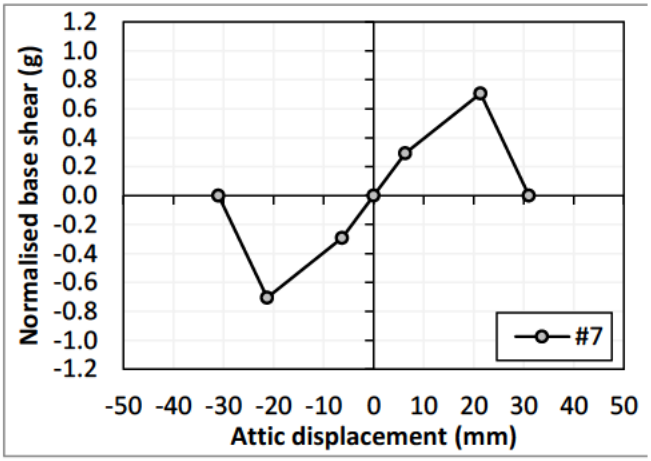

Variation #08 - OOP Criteria 100 mm

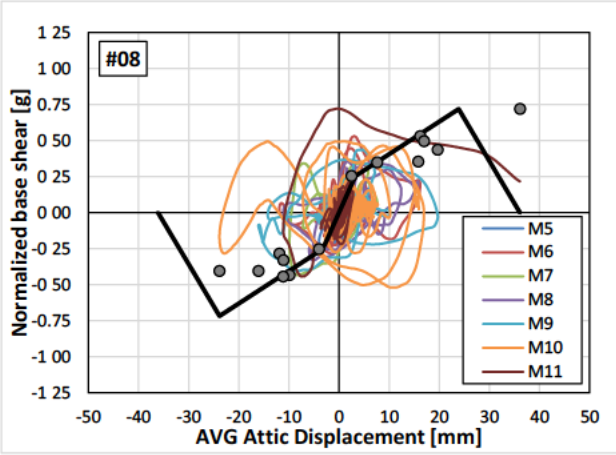

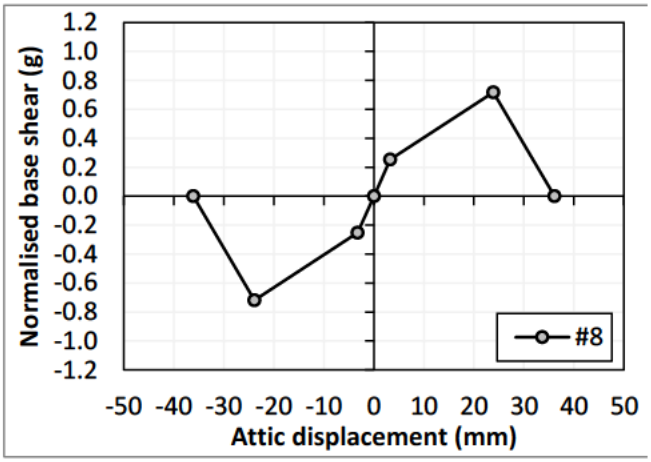

Variation #09 - OOP Criteria 100 mm

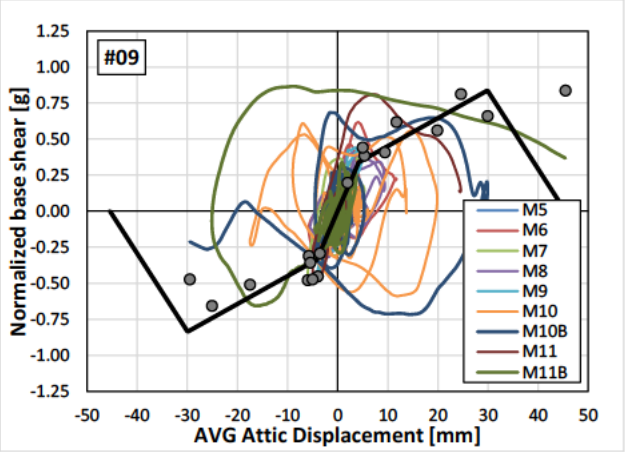

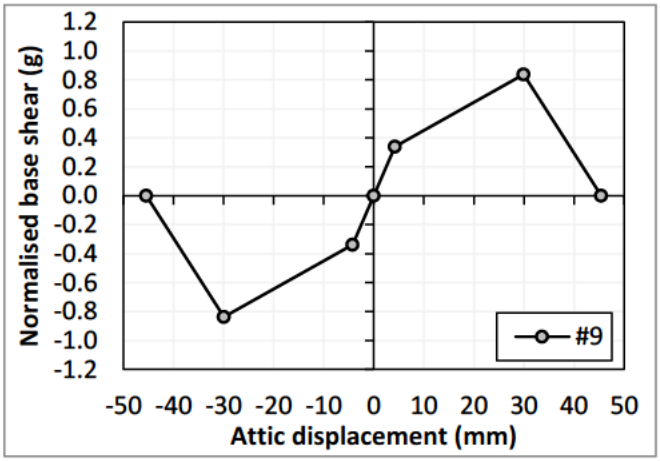

Variation #01

Table D1. Time step of the analyses when the failure criteria is reached for EUC-BUILD-2 #01 building.

Failure Time [s]	M5	M6	M7	M8	M9	M10	M11	M10B	M11B

OOP-060	/	4.7350	/	3.4925	2.1975	2.3100	3.7950	NA	NA
OOP-100	/	/	/	/	2.8025	/	3.8375	NA	NA
OOP-110	/	/	/	/	/	/	3.8500	NA	NA
OOP-120	/	/	/	/	/	/	3.8625	NA	NA
OOP-200	/	/	/	/	/	/	/	NA	NA

Table D2. Average backbone curves of EUC-BUILD-2 #01 for each stop criteria.

OOP-060		**OOP-100**		**OOP-110**		**OOP-120**		**OOP-200**		**No OOP**	
d [mm]	**v_a [g]**	**d [mm]**	**v_a [g]**	**d [mm]**	**v_a [g]**	**d [mm]**	**v_a [g]**	**d [mm]**	**v_a [g]**	**d [mm]**	**v_a [g]**
-25.36	0.00	-40.05	0.00	-42.15	0.00	-44.13	0.00	-77.53	0.00	-79.78	0.00
-17.26	-0.72	-26.94	-0.73	-27.62	-0.73	-28.07	-0.73	-28.09	-0.73	-30.88	-0.73
-4.89	-0.30	-4.89	-0.30	-4.91	-0.30	-4.91	-0.30	-4.91	-0.30	-4.91	-0.30
0.00	0.00	0.00	0.00	0.00	0.00	0.00	0.00	0.00	0.00	0.00	0.00
4.89	0.30	4.89	0.30	4.91	0.30	4.91	0.30	4.91	0.30	4.91	0.30
17.26	0.72	26.94	0.73	27.62	0.73	28.07	0.73	28.09	0.73	30.88	0.73
25.36	0.00	40.05	0.00	42.15	0.00	44.13	0.00	77.53	0.00	79.78	0.00

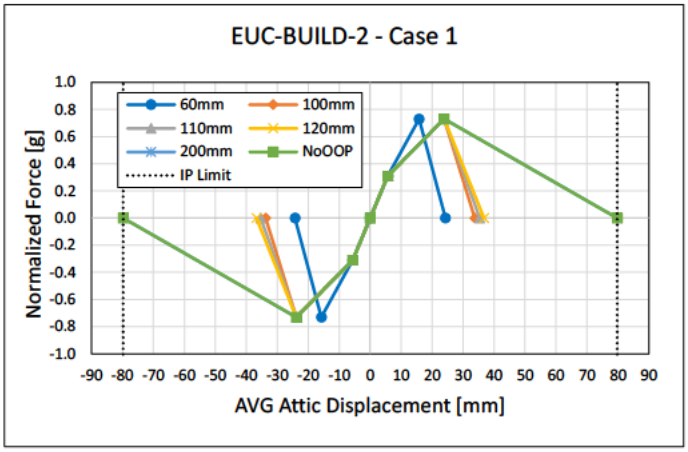

Variation #02

Table D3. Time step of the analyses when the failure criteria is reached for EUC-BUILD-2 #02 building.

Failure Time [s]	**M5**	**M6**	**M7**	**M8**	**M9**	**M10**	**M11**	**M10B**	**M11B**
OOP-060	/	4.7375	/	3.4900	2.1975	2.3100	3.7975	NA	NA
OOP-100	/	/	/	/	2.8025	/	3.8325	NA	NA
OOP-110	/	/	/	/	/	/	3.8450	NA	NA
OOP-120	/	/	/	/	/	/	3.8550	NA	NA
OOP-200	/	/	/	/	/	/	/	NA	NA

Table D4. Average backbone curves of EUC-BUILD-2 #02 for each stop criteria.

OOP-060		**OOP-100**		**OOP-110**		**OOP-120**		**OOP-200**		**No OOP**	
d [mm]	**v_a [g]**	**d [mm]**	**v_a [g]**	**d [mm]**	**v_a [g]**	**d [mm]**	**v_a [g]**	**d [mm]**	**v_a [g]**	**d [mm]**	**v_a [g]**
-25.28	0.00	-33.34	0.00	-35.21	0.00	-36.45	0.00	-79.78	0.00	-79.78	0.00

-15.81	-0.74	-23.85	-0.74	-23.85	-0.74	-23.85	-0.74	-23.85	-0.74	-23.85	-0.74
-5.80	-0.31	-5.80	-0.31	-5.80	-0.31	-5.80	-0.31	-5.80	-0.31	-5.80	-0.31
0.00	0.00	0.00	0.00	0.00	0.00	0.00	0.00	0.00	0.00	0.00	0.00
5.80	0.31	5.80	0.31	5.80	0.31	5.80	0.31	5.80	0.31	5.80	0.31
15.81	0.74	23.85	0.74	23.85	0.74	23.85	0.74	23.85	0.74	23.85	0.74

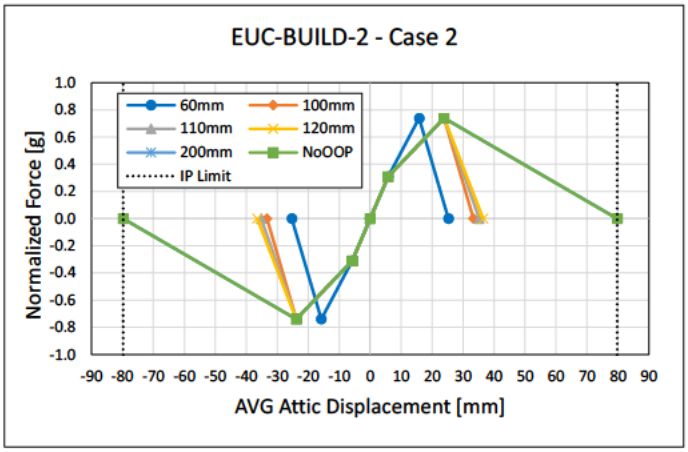

Variation #03

Table D5. Time step of the analyses when the failure criteria is reached for EUC-BUILD-2 #03 building.

Failure Time [s]	M5	M6	M7	M8	M9	M10	M11	M10B	M11B
OOP-060	/	/	/	/	/	2.5725	3.7875	2.2550	3.5375
OOP-100	/	/	/	/	/	/	3.8600	2.6300	3.8325
OOP-110	/	/	/	/	/	/	4.4225	2.6575	3.8400
OOP-120	/	/	/	/	/	/	/	/	3.8500
OOP-200	/	/	/	/	/	/	/	/	3.9375

Table D6. Average backbone curves of EUC-BUILD-2 #03 for each stop criteria.

OOP-060		**OOP-100**		**OOP-110**		**OOP-120**		**OOP-200**		**No OOP**	
d [mm]	**v_a [g]**	**d [mm]**	**v_a [g]**	**d [mm]**	**v_a [g]**	**d [mm]**	**v_a [g]**	**d [mm]**	**v_a [g]**	**d [mm]**	**v_a [g]**
-23.17	0.00	-43.25	0.00	-45.78	0.00	-48.85	0.00	-67.36	0.00	-79.78	0.00
-19.08	-0.85	-27.55	-0.85	-30.69	-0.85	-31.82	-0.85	-31.82	-0.85	-31.82	-0.85
-4.10	-0.32	-4.10	-0.32	-4.10	-0.32	-4.10	-0.32	-4.10	-0.32	-4.10	-0.32
0.00	0.00	0.00	0.00	0.00	0.00	0.00	0.00	0.00	0.00	0.00	0.00
4.10	0.32	4.10	0.32	4.10	0.32	4.10	0.32	4.10	0.32	4.10	0.32
19.08	0.85	27.55	0.85	30.69	0.85	31.82	0.85	31.82	0.85	31.82	0.85

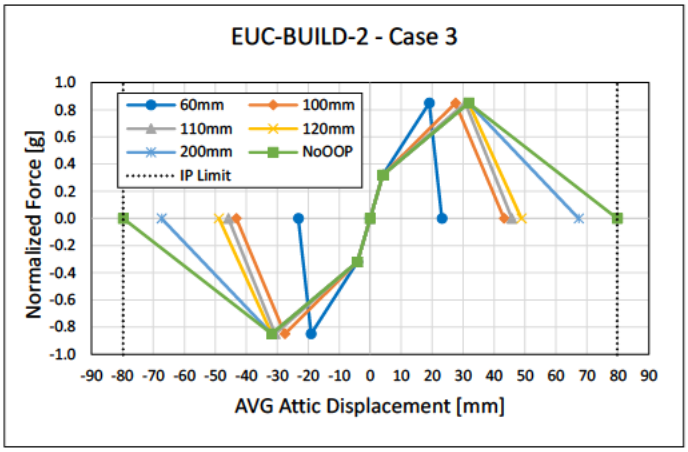

Variation #04

Table D7. Time step of the analyses when the failure criteria is reached for EUC-BUILD-2 #04 building.

Failure Time [s]	M5	M6	M7	M8	M9	M10	M11	M10B	M11B
OOP-060	/	/	/	/	2.2175	2.5575	3.7925	NA	NA
OOP-100	/	/	/	/	/	/	3.8425	NA	NA
OOP-110	/	/	/	/	/	/	3.8550	NA	NA
OOP-120	/	/	/	/	/	/	3.8675	NA	NA
OOP-200	/	/	/	/	/	/	/	NA	NA

Table D8. Average backbone curves of EUC-BUILD-2 #04 for each stop criteria.

OOP-060		OOP-100		OOP-110		OOP-120		OOP-200		No OOP	
d [mm]	v_a [g]	d [mm]	v_a [g]	d [mm]	v_a [g]	d [mm]	v_a [g]	d [mm]	v_a [g]	d [mm]	v_a [g]
-20.16	0.00	-30.06	0.00	-31.63	0.00	-33.00	0.00	-79.78	0.00	-79.78	0.00
-14.59	-0.79	-22.95	-0.79	-22.95	-0.79	-22.95	-0.79	-22.95	-0.79	-22.95	-0.79
-5.57	-0.31	-5.57	-0.31	-5.57	-0.31	-5.57	-0.31	-5.57	-0.31	-5.57	-0.31
0.00	0.00	0.00	0.00	0.00	0.00	0.00	0.00	0.00	0.00	0.00	0.00
5.57	0.31	5.57	0.31	5.57	0.31	5.57	0.31	5.57	0.31	5.57	0.31
14.59	0.79	22.95	0.79	22.95	0.79	22.95	0.79	22.95	0.79	22.95	0.79

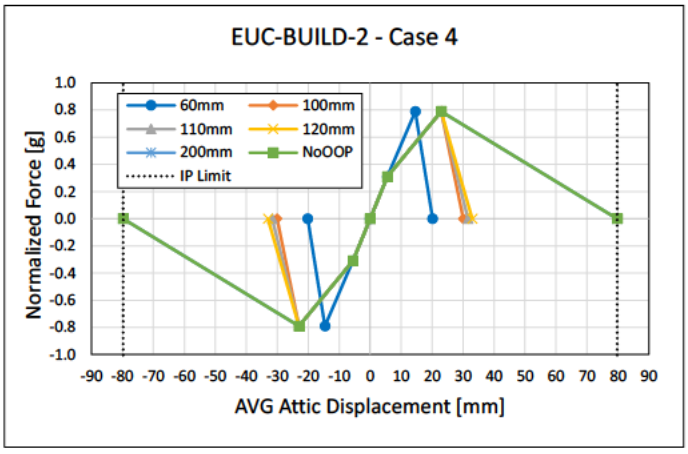

Variation #05

Table D9. Time step of the analyses when the failure criteria is reached for EUC-BUILD-2 #05 building.

Failure Time [s]	M5	M6	M7	M8	M9	M10	M11	M10B	M11B
OOP-060	/	4.7225	/	3.4725	2.1875	2.2900	3.8075	NA	NA
OOP-100	/	/	/	/	2.2625	2.6775	3.8475	NA	NA
OOP-110	/	/	/	/	2.3025	/	3.8600	NA	NA
OOP-120	/	/	/	/	/	/	3.8700	NA	NA
OOP-200	/	/	/	/	/	/	/	NA	NA

Table D10. Average backbone curves of EUC-BUILD-2 #05 for each stop criteria.

OOP-060		OOP-100		OOP-110		OOP-120		OOP-200		No OOP	
d [mm]	v_a [g]	d [mm]	v_a [g]	d [mm]	v_a [g]	d [mm]	v_a [g]	d [mm]	v_a [g]	d [mm]	v_a [g]
-32.52	0.00	-44.70	0.00	-47.12	0.00	-48.77	0.00	-79.78	0.00	-79.78	0.00
-21.47	-0.51	-27.93	-0.51	-28.96	-0.51	-30.25	-0.51	-30.25	-0.51	-30.25	-0.51
-3.56	-0.24	-3.56	-0.24	-3.56	-0.24	-3.56	-0.24	-3.56	-0.24	-3.56	-0.24
0.00	0.00	0.00	0.00	0.00	0.00	0.00	0.00	0.00	0.00	0.00	0.00
3.56	0.24	3.56	0.24	3.56	0.24	3.56	0.24	3.56	0.24	3.56	0.24
21.47	0.51	27.93	0.51	28.96	0.51	30.25	0.51	30.25	0.51	30.25	0.51

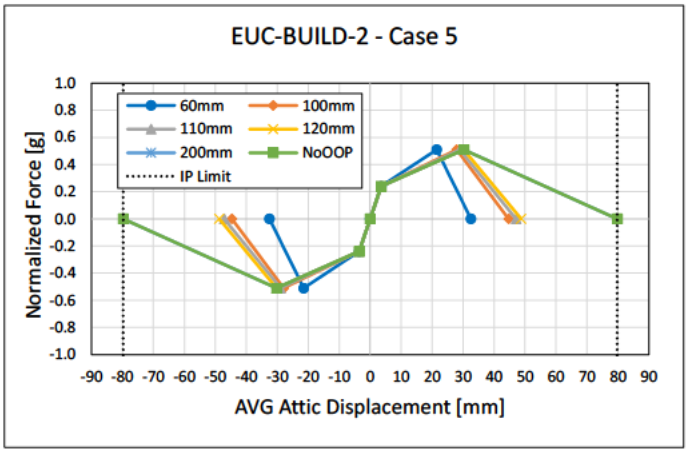

Variation #06

Table D11. Time step of the analyses when the failure criteria is reached for EUC-BUILD-2 #06 building.

Failure Time [s]	M5	M6	M7	M8	M9	M10	M11	M10B	M11B
OOP-060	/	/	/	/	/	2.3250	3.7925	2.2525	3.4800
OOP-100	/	/	/	/	/	/	3.8600	2.3125	3.8625
OOP-110	/	/	/	/	/	/	3.9000	2.3375	3.8700
OOP-120	/	/	/	/	/	/	4.4100	2.6750	3.8775
OOP-200	/	/	/	/	/	/	/	/	3.9500

Table D12. Average backbone curves of EUC-BUILD-2 #06 for each stop criteria.

OOP-060		OOP-100		OOP-110		OOP-120		OOP-200		No OOP	
d [mm]	v_a [g]	d [mm]	v_a [g]	d [mm]	v_a [g]	d [mm]	v_a [g]	d [mm]	v_a [g]	d [mm]	v_a [g]
-29.84	0.00	-62.76	0.00	-65.83	0.00	-68.76	0.00	-79.78	0.00	-79.78	0.00
-17.23	-0.66	-41.27	-0.66	-41.27	-0.66	-41.31	-0.66	-41.51	-0.66	-61.26	-0.66
-5.49	-0.30	-5.49	-0.30	-5.49	-0.30	-5.49	-0.30	-5.49	-0.30	-5.49	-0.30
0.00	0.00	0.00	0.00	0.00	0.00	0.00	0.00	0.00	0.00	0.00	0.00
5.49	0.30	5.49	0.30	5.49	0.30	5.49	0.30	5.49	0.30	5.49	0.30
17.23	0.66	41.27	0.66	41.27	0.66	41.31	0.66	41.51	0.66	61.26	0.66

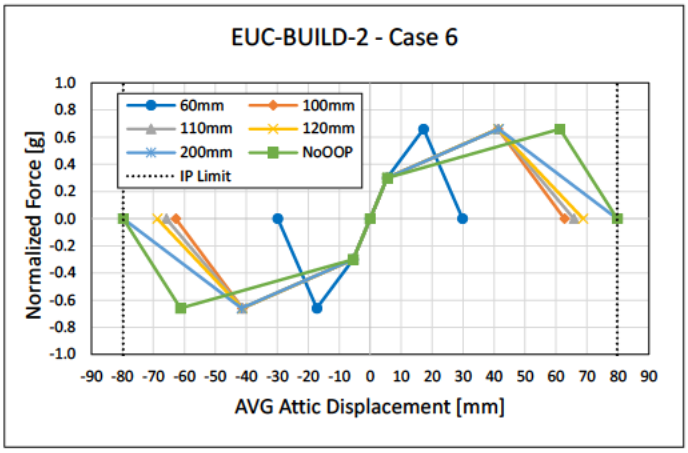

Variation #07

Table D13. Time step of the analyses when the failure criteria is reached for EUC-BUILD-2 #07 building.

Failure Time [s]	M5	M6	M7	M8	M9	M10	M11	M10B	M11B
OOP-060	/	4.7125	3.6725	3.4825	2.2125	2.5575	3.7925	NA	NA
OOP-100	/	/	/	/	/	/	3.8400	NA	NA
OOP-110	/	/	/	/	/	/	3.8525	NA	NA
OOP-120	/	/	/	/	/	/	3.8675	NA	NA
OOP-200	/	/	/	/	/	/	/	NA	NA

Table D14. Average backbone curves of EUC-BUILD-2 #07 for each stop criteria.

OOP-060		OOP-100		OOP-110		OOP-120		OOP-200		No OOP	
d [mm]	v_a [g]	d [mm]	v_a [g]	d [mm]	v_a [g]	d [mm]	v_a [g]	d [mm]	v_a [g]	d [mm]	v_a [g]
-21.26	0.00	-31.01	0.00	-32.54	0.00	-34.11	0.00	-79.78	0.00	-79.78	0.00
-15.32	-0.71	-21.32	-0.71	-21.32	-0.71	-21.32	-0.71	-21.32	-0.71	-21.32	-0.71
-6.32	-0.29	-6.32	-0.29	-6.52	-0.29	-6.52	-0.29	-6.52	-0.29	-6.52	-0.29
0.00	0.00	0.00	0.00	0.00	0.00	0.00	0.00	0.00	0.00	0.00	0.00
6.32	0.29	6.32	0.29	6.52	0.29	6.52	0.29	6.52	0.29	6.52	0.29
15.32	0.71	21.32	0.71	21.32	0.71	21.32	0.71	21.32	0.71	21.32	0.71

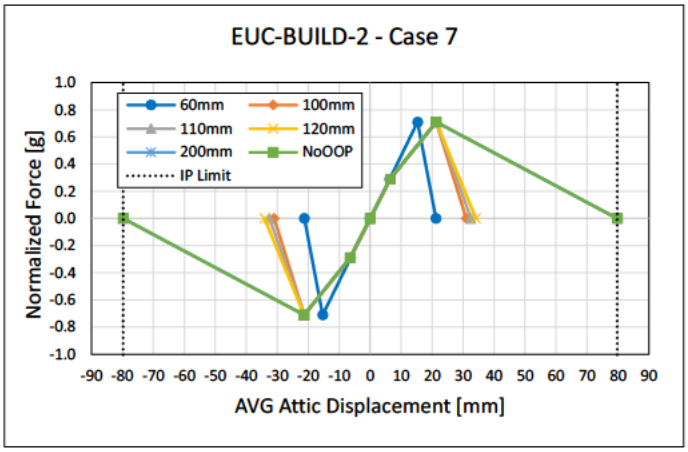

Variation #08

Table D15. Time step of the analyses when the failure criteria is reached for EUC-BUILD-2 #08 building.

Failure Time [s]	M5	M6	M7	M8	M9	M10	M11	M10B	M11B
OOP-060	/	4.7550	/	/	2.2100	2.3150	3.7975	NA	NA
OOP-100	/	/	/	/	/	/	3.8375	NA	NA
OOP-110	/	/	/	/	/	/	3.8475	NA	NA
OOP-120	/	/	/	/	/	/	3.8575	NA	NA
OOP-200	/	/	/	/	/	/	/	NA	NA

Table D16. Average backbone curves of EUC-BUILD-2 #08 for each stop criteria.

OOP-060		OOP-100		OOP-110		OOP-120		OOP-200		No OOP	
d [mm]	v_a [g]	d [mm]	v_a [g]	d [mm]	v_a [g]	d [mm]	v_a [g]	d [mm]	v_a [g]	d [mm]	v_a [g]
-25.94	0.00	-36.10	0.00	-37.75	0.00	-39.15	0.00	-79.78	0.00	-79.78	0.00
-16.18	-0.72	-23.86	-0.72	-23.86	-0.72	-23.86	-0.72	-23.86	-0.72	-23.86	-0.72
-3.25	-0.25	-3.25	-0.25	-3.25	-0.25	-3.25	-0.25	-3.25	-0.25	-3.25	-0.25
0.00	0.00	0.00	0.00	0.00	0.00	0.00	0.00	0.00	0.00	0.00	0.00
3.25	0.25	3.25	0.25	3.25	0.25	3.25	0.25	3.25	0.25	3.25	0.25
16.18	0.72	23.86	0.72	23.86	0.72	23.86	0.72	23.86	0.72	23.86	0.72

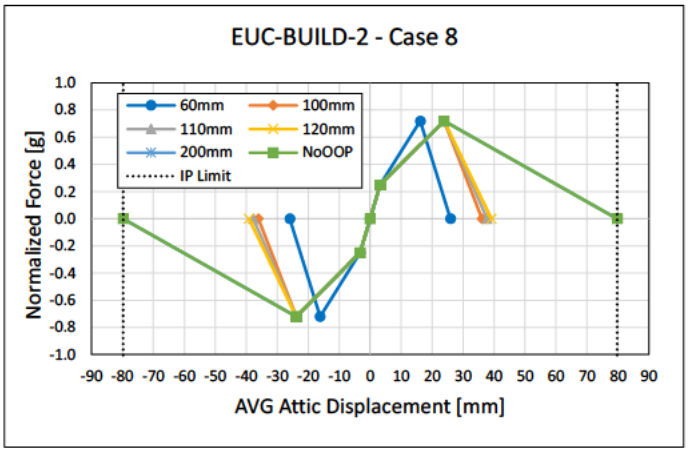

Variation #09

Table D17. Time step of the analyses when the failure criteria is reached for EUC-BUILD-2 #09 building.

Failure Time [s]	M5	M6	M7	M8	M9	M10	M11	M10B	M11B
OOP-060	/	/	/	/	/	2.5600	3.7875	2.2600	3.5275
OOP-100	/	/	/	/	/	/	3.8625	2.6375	3.8325
OOP-110	/	/	/	/	/	/	/	2.6550	3.8400
OOP-120	/	/	/	/	/	/	/	2.6850	3.8500
OOP-200	/	/	/	/	/	/	/	/	3.9500

Table D18. Average backbone curves of EUC-BUILD-2 #09 for each stop criteria.

OOP-060		OOP-100		OOP-110		OOP-120		OOP-200		No OOP	
d [mm]	v_a [g]	d [mm]	v_a [g]	d [mm]	v_a [g]	d [mm]	v_a [g]	d [mm]	v_a [g]	d [mm]	v_a [g]
-25.75	0.00	-45.44	0.00	-48.12	0.00	-51.34	0.00	-71.96	0.00	-79.78	0.00
-19.93	-0.81	-29.92	-0.84	-31.83	-0.84	-33.44	-0.84	-33.44	-0.84	-38.80	-0.84
-4.21	-0.34	-4.21	-0.34	-4.21	-0.34	-4.21	-0.34	-4.21	-0.34	-4.21	-0.34
0.00	0.00	0.00	0.00	0.00	0.00	0.00	0.00	0.00	0.00	0.00	0.00
4.21	0.34	4.21	0.34	4.21	0.34	4.21	0.34	4.21	0.34	4.21	0.34
19.93	0.81	29.92	0.84	31.83	0.84	33.44	0.84	33.44	0.84	38.80	0.84

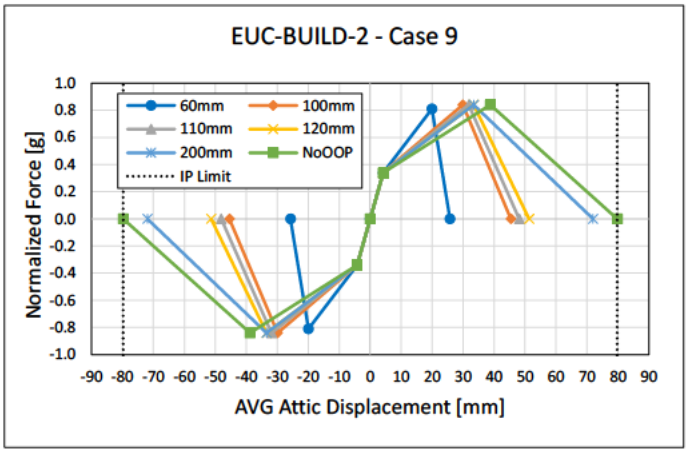

Appendix E – Hysteretic curves for NLTHA of LNEC-BUILD-3

Variation #10 - OOP Criteria 100 mm

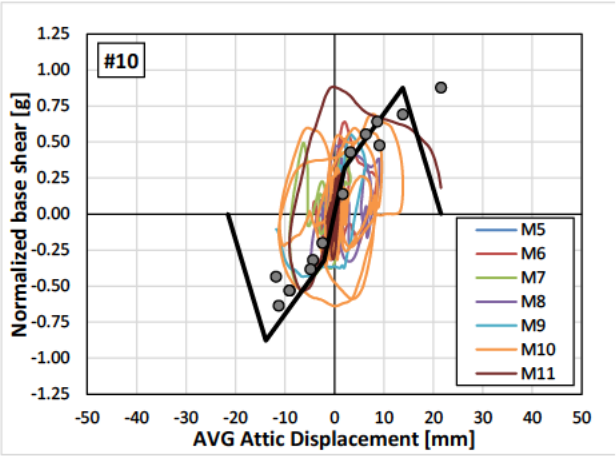

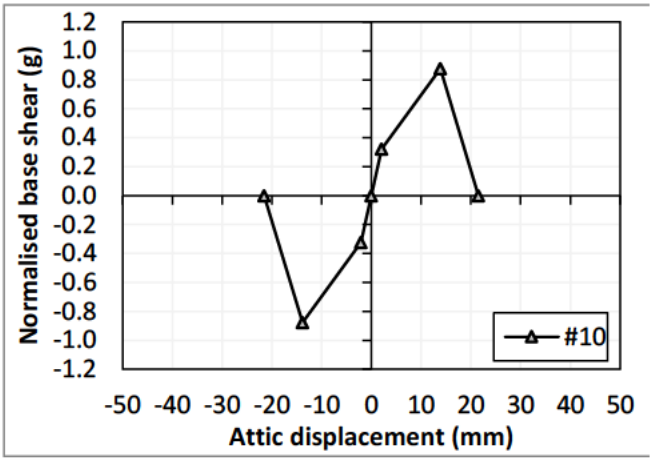

Variation #11 - OOP Criteria 100 mm

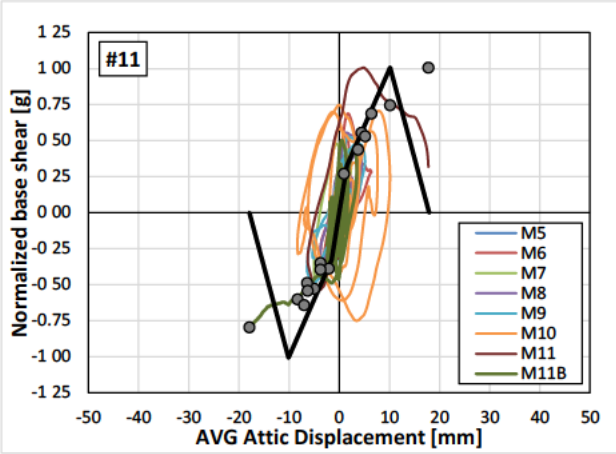

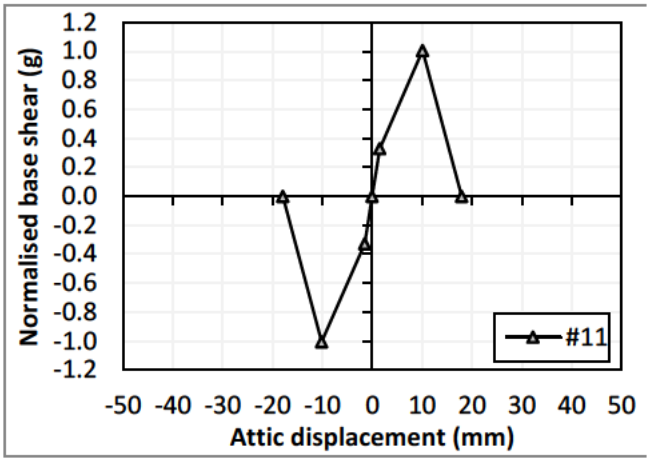

Variation #12 - OOP Criteria 100 mm

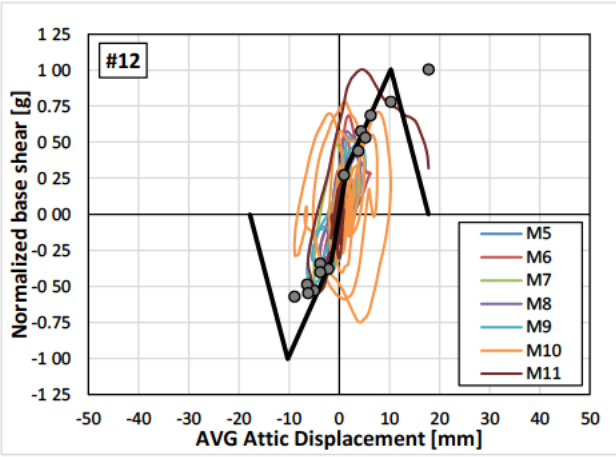

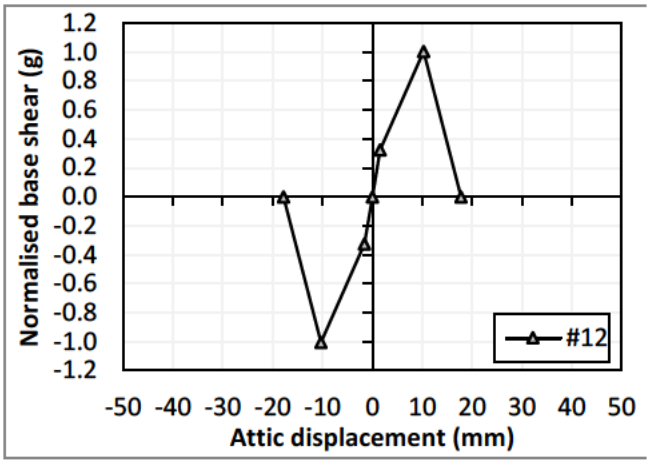

Variation #13 - OOP Criteria 100 mm

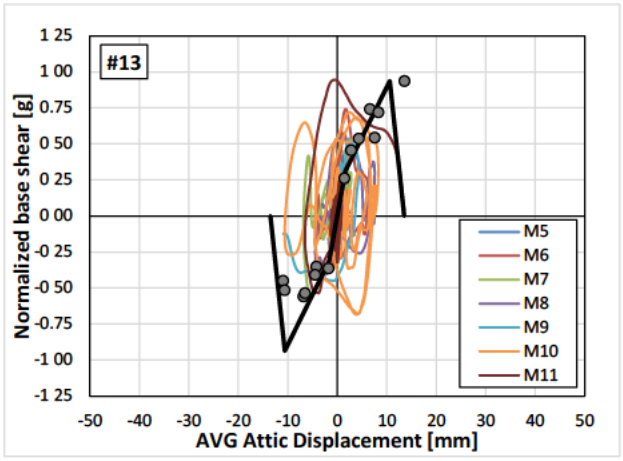

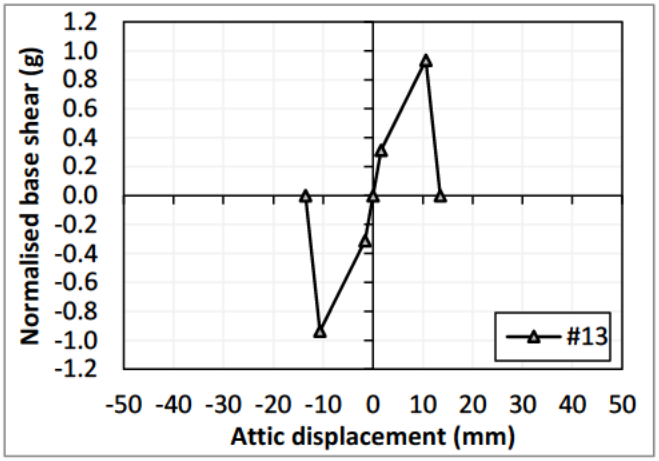

Variation #14 - OOP Criteria 100 mm

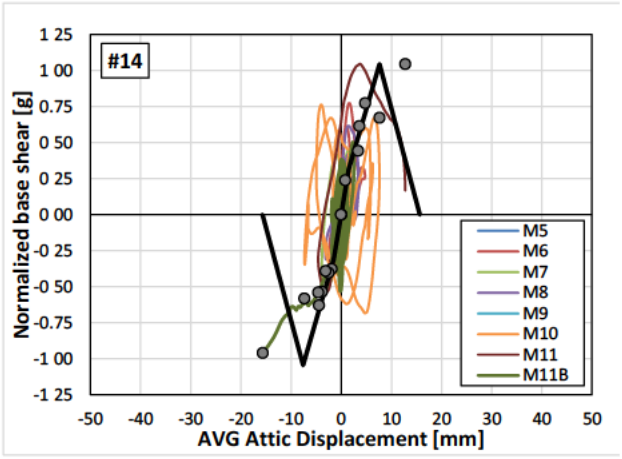

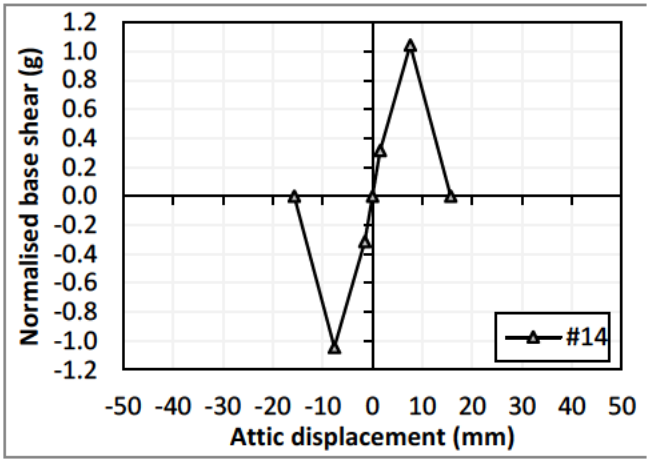

Variation #15 - OOP Criteria 100 mm

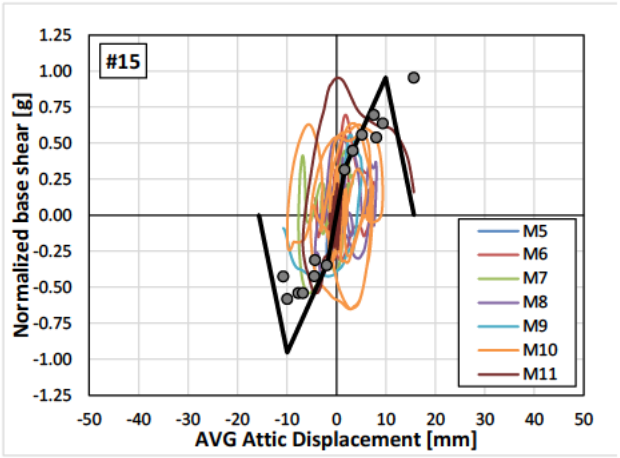

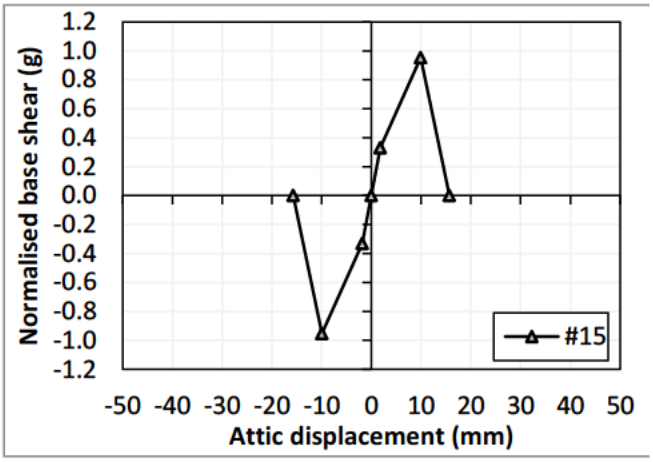

Variation #16 - OOP Criteria 100 mm

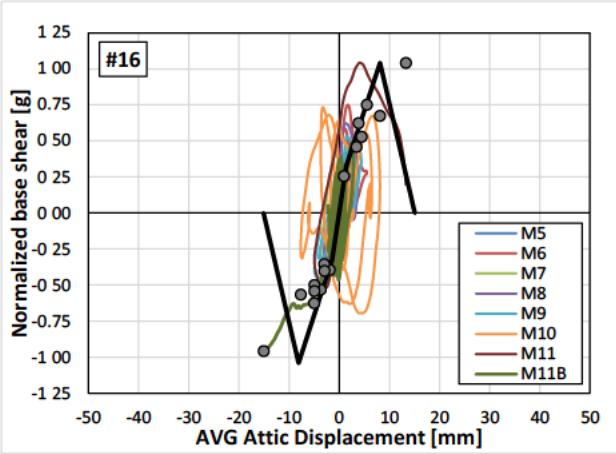

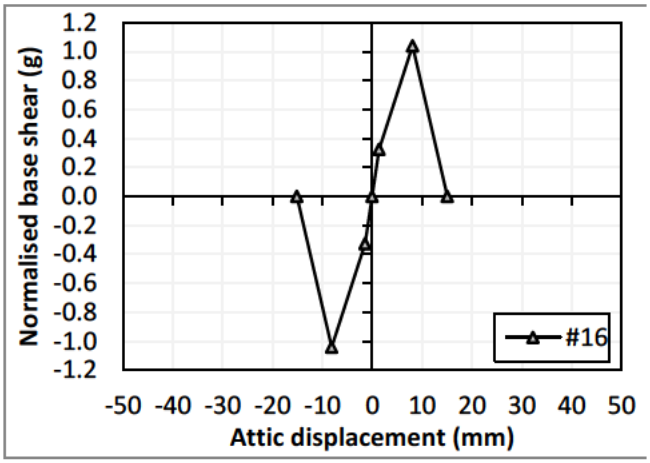

Variation #10

Table E1. Time step of the analyses when the failure criteria is reached for LNEC-BUILD-3 #10 building.

Failure Time [s]	M5	M6	M7	M8	M9	M10	M11
OOP-060	/	4.8075	3.7250	3.5425	2.2400	2.3275	3.8600
OOP-100	/	/	/	/	2.3275	/	3.8950
OOP-110	/	/	/	/	2.3950	/	3.9050
OOP-120	/	/	/	/	/	/	3.9150
OOP-200	/	/	/	/	/	/	4.0400

Table E2. Average backbone curves of LNEC-BUILD-3 #10 for each stop criteria.

OOP-060		OOP-100		OOP-110		OOP-120		OOP-200		No OOP	
d [mm]	v_a [g]	d [mm]	v_a [g]	d [mm]	v_a [g]	d [mm]	v_a [g]	d [mm]	v_a [g]	d [mm]	v_a [g]
-19.57	0.00	-21.55	0.00	-21.76	0.00	-21.97	0.00	-25.52	0.00	-72.22	0.00
-8.61	-0.88	-13.85	-0.88	-13.85	-0.88	-13.85	-0.88	-13.85	-0.88	-25.64	-0.88
-2.06	-0.32	-2.06	-0.32	-2.06	-0.32	-2.06	-0.32	-2.06	-0.32	-2.06	-0.32
0.00	0.00	0.00	0.00	0.00	0.00	0.00	0.00	0.00	0.00	0.00	0.00
2.06	0.32	2.06	0.32	2.06	0.32	2.06	0.32	2.06	0.32	2.06	0.32
8.61	0.88	13.85	0.88	13.85	0.88	13.85	0.88	13.85	0.88	25.64	0.88

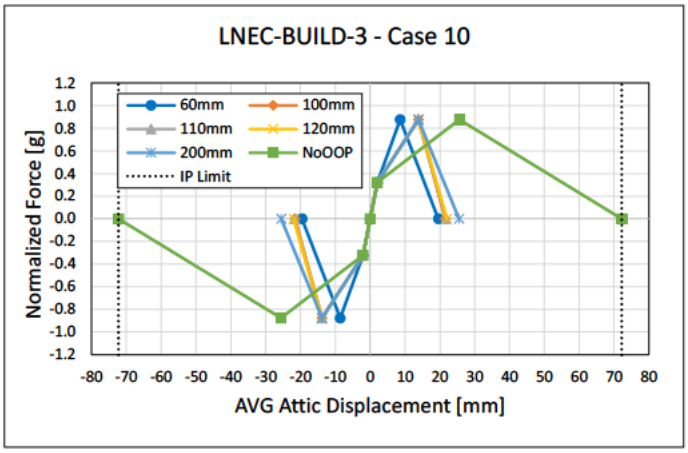

Variation #11

Table E3. Time step of the analyses when the failure criteria is reached for LNEC-BUILD-3 #11 building.

Failure Time [s]	M5	M6	M7	M8	M9	M10	M11
OOP-060	/	/	/	/	/	2.6000	3.8225
OOP-100	/	/	/	/	/	/	3.8650
OOP-110	/	/	/	/	/	/	3.8800
OOP-120	/	/	/	/	/	/	3.8950
OOP-200	/	/	/	/	/	/	/

Table E4. Average backbone curves of LNEC-BUILD-3 #11 for each stop criteria.

OOP-060		OOP-100		OOP-110		OOP-120		OOP-200		No OOP	
d [mm]	v_a [g]	d [mm]	v_a [g]	d [mm]	v_a [g]	d [mm]	v_a [g]	d [mm]	v_a [g]	d [mm]	v_a [g]
-13.63	0.00	-17.78	0.00	-17.80	0.00	-17.80	0.00	-72.22	0.00	-72.22	0.00
-9.01	-1.01	-10.12	-1.01	-10.12	-1.01	-10.12	-1.01	-17.80	-1.01	-17.80	-1.01
-1.53	-0.33	-1.53	-0.33	-1.53	-0.33	-1.53	-0.33	-1.53	-0.33	-1.53	-0.33
0.00	0.00	0.00	0.00	0.00	0.00	0.00	0.00	0.00	0.00	0.00	0.00
1.53	0.33	1.53	0.33	1.53	0.33	1.53	0.33	1.53	0.33	1.53	0.33
9.01	1.01	10.12	1.01	10.12	1.01	10.12	1.01	17.80	1.01	17.80	1.01

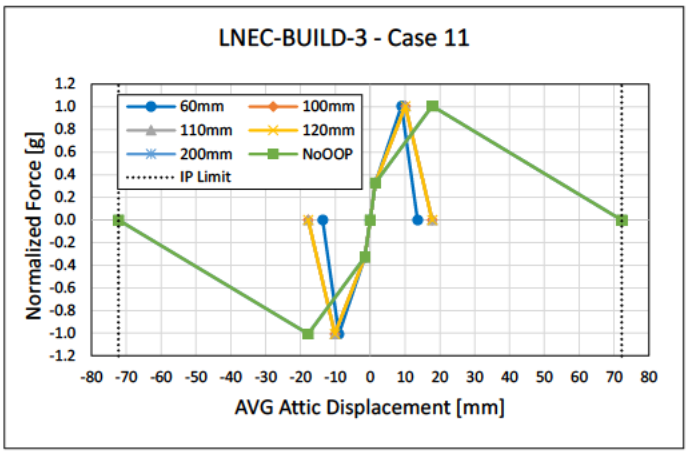

Variation #12

Table E5. Time step of the analyses when the failure criteria is reached for LNEC-BUILD-3 #12 building.

Failure Time [s]	M5	M6	M7	M8	M9	M10	M11
OOP-060	/	/	/	/	/	2.6000	3.8250
OOP-100	/	/	/	/	/	/	3.8650
OOP-110	/	/	/	/	/	/	3.8775
OOP-120	/	/	/	/	/	/	3.8950
OOP-200	/	/	/	/	/	/	/

Table D6. Average backbone curves of LNEC-BUILD-3 #12 for each stop criteria.

OOP-060	OOP-100	OOP-110	OOP-120	OOP-200	No OOP

d [mm]	v_a [g]	d [mm]	v_a [g]	d [mm]	v_a [g]	d [mm]	v_a [g]	d [mm]	v_a [g]	d [mm]	v_a [g]
-14.01	0.00	-17.80	0.00	-17.84	0.00	-17.84	0.00	-72.22	0.00	-72.22	0.00
-9.23	-1.00	-10.27	-1.00	-10.27	-1.00	-10.27	-1.00	-17.74	-1.00	-17.74	-1.00
-1.56	-0.33	-1.56	-0.33	-1.56	-0.33	-1.56	-0.33	-1.56	-0.33	-1.56	-0.33
0.00	0.00	0.00	0.00	0.00	0.00	0.00	0.00	0.00	0.00	0.00	0.00
1.56	0.33	1.56	0.33	1.56	0.33	1.56	0.33	1.56	0.33	1.56	0.33
9.23	1.00	10.27	1.00	10.27	1.00	10.27	1.00	17.74	1.00	17.74	1.00

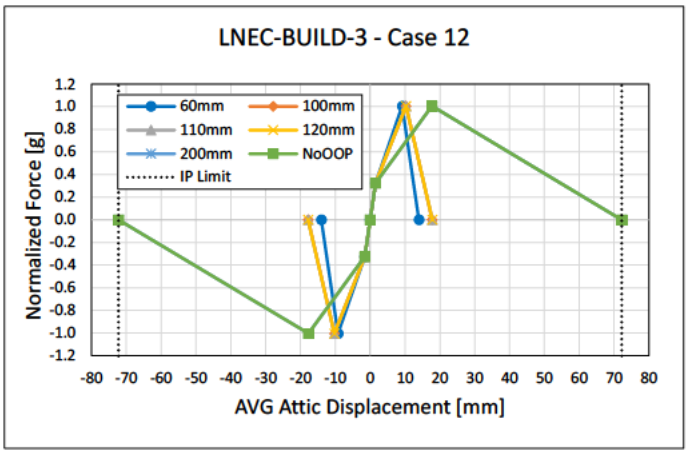

Variation #13

Table E7. Time step of the analyses when the failure criteria is reached for LNEC-BUILD-3 #13 building.

Failure Time [s]	M5	M6	M7	M8	M9	M10	M11
OOP-060	/	/	3.7425	3.5325	2.2375	2.3250	3.8575
OOP-100	/	/	/	/	2.3200	/	3.8950
OOP-110	/	/	/	/	2.3925	/	3.9050
OOP-120	/	/	/	/	/	/	3.9200
OOP-200	/	/	/	/	/	/	/

Table E8. Average backbone curves of LNEC-BUILD-3 #13 for each stop criteria.

OOP-060		OOP-100		OOP-110		OOP-120		OOP-200		No OOP	
d [mm]	v_a [g]	d [mm]	v_a [g]	d [mm]	v_a [g]	d [mm]	v_a [g]	d [mm]	v_a [g]	d [mm]	v_a [g]
-12.27	0.00	-13.53	0.00	-13.81	0.00	-14.40	0.00	-72.22	0.00	-72.22	0.00
-6.75	-0.94	-10.63	-0.94	-10.63	-0.95	-11.90	-0.95	-20.62	-0.95	-20.62	-0.95
-1.61	-0.31	-1.61	-0.31	-1.61	-0.31	-1.61	-0.31	-1.61	-0.31	-1.61	-0.31
0.00	0.00	0.00	0.00	0.00	0.00	0.00	0.00	0.00	0.00	0.00	0.00
1.61	0.31	1.61	0.31	1.61	0.31	1.61	0.31	1.61	0.31	1.61	0.31
6.75	0.94	10.63	0.94	10.63	0.95	11.90	0.95	20.62	0.95	20.62	0.95

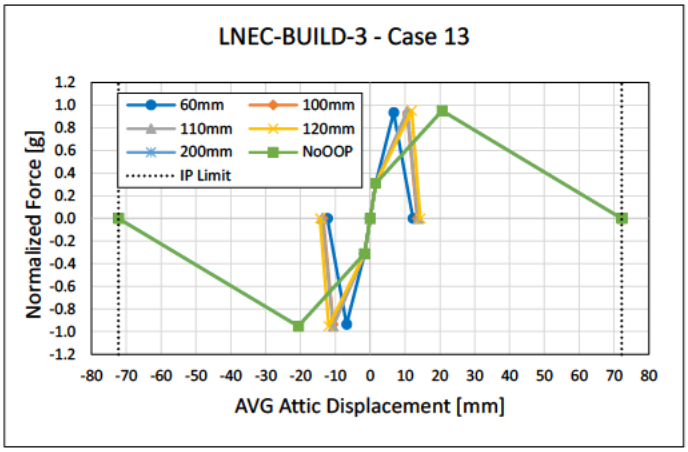

Variation #14

Table E9. Time step of the analyses when the failure criteria is reached for LNEC-BUILD-3 #14 building.

Failure Time [s]	M5	M6	M7	M8	M9	M10	M11
OOP-060	/	/	/	/	/	2.5975	3.8225
OOP-100	/	/	/	/	/	/	3.8650
OOP-110	/	/	/	/	/	/	3.8775
OOP-120	/	/	/	/	/	/	3.8975
OOP-200	/	/	/	/	/	/	/

Table E10. Average backbone curves of LNEC-BUILD-3 #14 for each stop criteria.

OOP-060		OOP-100		OOP-110		OOP-120		OOP-200		No OOP	
d [mm]	v_a [g]	d [mm]	v_a [g]	d [mm]	v_a [g]	d [mm]	v_a [g]	d [mm]	v_a [g]	d [mm]	v_a [g]
-9.96	0.00	-12.74	0.00	-12.76	0.00	-12.76	0.00	-72.22	0.00	-72.22	0.00
-6.70	-1.06	-7.61	-1.06	-7.61	-1.06	-7.61	-1.06	-14.88	-1.06	-14.88	-1.06
-1.37	-0.31	-1.37	-0.31	-1.37	-0.31	-1.37	-0.31	-1.37	-0.31	-1.37	-0.31
0.00	0.00	0.00	0.00	0.00	0.00	0.00	0.00	0.00	0.00	0.00	0.00
1.37	0.31	1.37	0.31	1.37	0.31	1.37	0.31	1.37	0.31	1.37	0.31
6.70	1.06	7.61	1.06	7.61	1.06	7.61	1.06	14.88	1.06	14.88	1.06

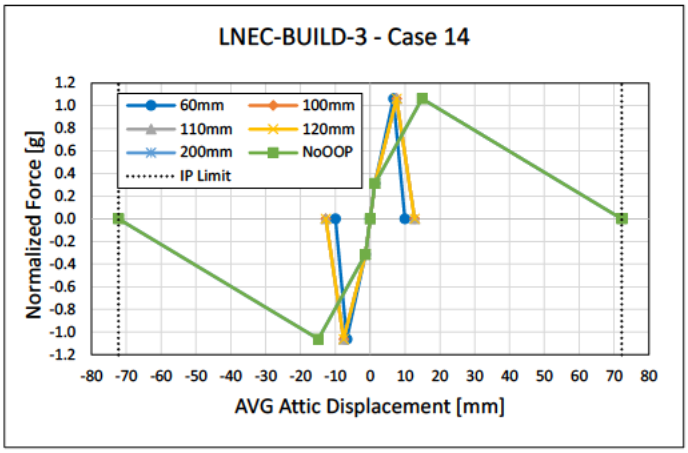

Variation #15

Table E11. Time step of the analyses when the failure criteria is reached for LNEC-BUILD-3 #15 building.

Failure Time [s]	M5	M6	M7	M8	M9	M10	M11
OOP-060	/	4.8000	3.7175	3.5350	2.2425	2.3375	3.8500
OOP-100	/	/	/	/	2.3150	/	3.8825
OOP-110	/	/	/	/	2.3525	/	3.8900
OOP-120	/	/	/	/	/	/	3.9000
OOP-200	/	/	/	/	/	/	4.0325

Table E12. Average backbone curves of LNEC-BUILD-3 #15 for each stop criteria.

OOP-060		OOP-100		OOP-110		OOP-120		OOP-200		No OOP	
d [mm]	v_a [g]	d [mm]	v_a [g]	d [mm]	v_a [g]	d [mm]	v_a [g]	d [mm]	v_a [g]	d [mm]	v_a [g]
-13.60	0.00	-15.67	0.00	-15.86	0.00	-16.11	0.00	-22.78	0.00	-72.22	0.00
-7.15	-0.97	-9.94	-0.97	-9.94	-0.97	-12.64	-0.97	-12.64	-0.97	-23.58	-0.97
-1.80	-0.33	-1.80	-0.33	-1.80	-0.34	-1.80	-0.34	-1.80	-0.34	-1.80	-0.34
0.00	0.00	0.00	0.00	0.00	0.00	0.00	0.00	0.00	0.00	0.00	0.00
1.80	0.33	1.80	0.33	1.80	0.34	1.80	0.34	1.80	0.34	1.80	0.34
7.15	0.97	9.94	0.97	9.94	0.97	12.64	0.97	12.64	0.97	23.58	0.97

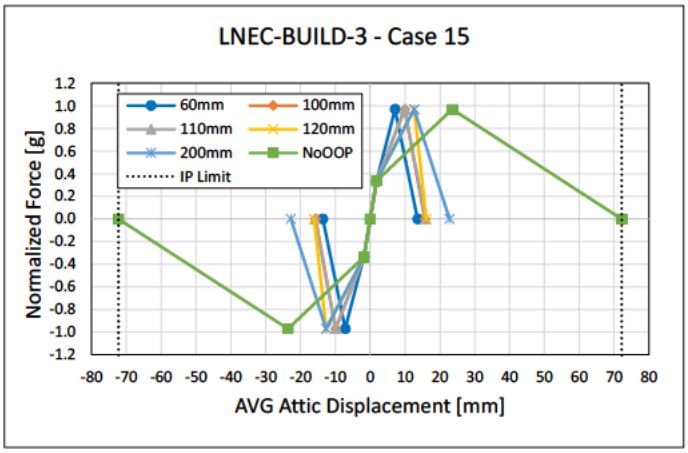

Variation #16

Table E13. Time step of the analyses when the failure criteria is reached for LNEC-BUILD-3 #16 building.

Failure Time [s]	M5	M6	M7	M8	M9	M10	M11
OOP-060	/	/	/	/	/	2.6075	3.8225
OOP-100	/	/	/	/	/	/	3.8650
OOP-110	/	/	/	/	/	/	3.8800
OOP-120	/	/	/	/	/	/	3.9000
OOP-200	/	/	/	/	/	/	/

Table E14. Average backbone curves of LNEC-BUILD-3 #16 for each stop criteria.

OOP-060		OOP-100		OOP-110		OOP-120		OOP-200		No OOP	
d [mm]	v_a [g]	d [mm]	v_a [g]	d [mm]	v_a [g]	d [mm]	v_a [g]	d [mm]	v_a [g]	d [mm]	v_a [g]
-10.37	0.00	-13.27	0.00	-13.32	0.00	-13.32	0.00	-72.22	0.00	-72.22	0.00

-7.68	-1.04	-8.12	-1.04	-8.12	-1.06	-8.12	-1.06	-15.15	-1.06	-15.15	-1.06
-1.41	-0.33	-1.41	-0.33	-1.41	-0.33	-1.41	-0.33	-1.41	-0.33	-1.41	-0.33
0.00	0.00	0.00	0.00	0.00	0.00	0.00	0.00	0.00	0.00	0.00	0.00
1.41	0.33	1.41	0.33	1.41	0.33	1.41	0.33	1.41	0.33	1.41	0.33
6.50	1.04	8.12	1.04	8.12	1.06	8.12	1.06	15.15	1.06	15.15	1.06

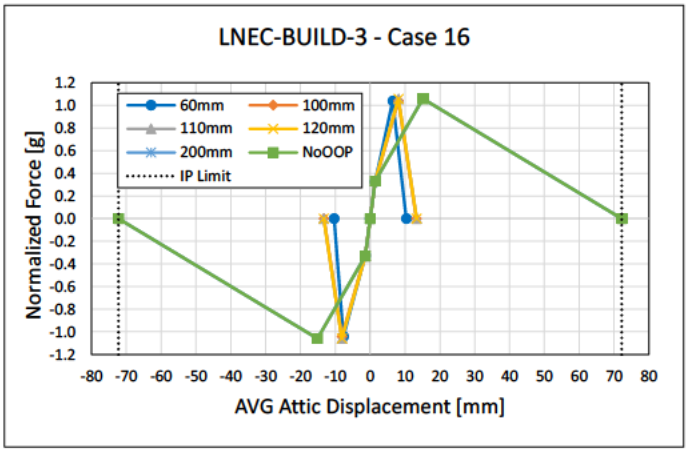

Appendix F – Results of NLTHA of Bleeksteen building

M08

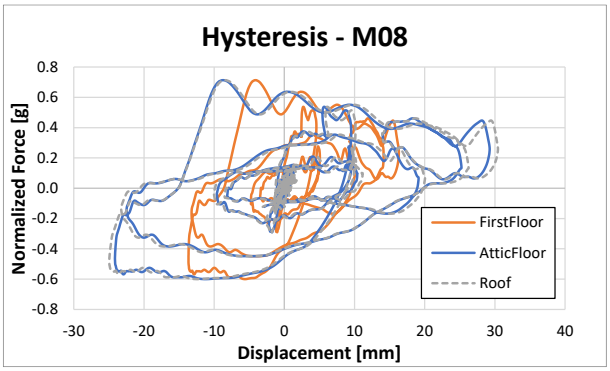

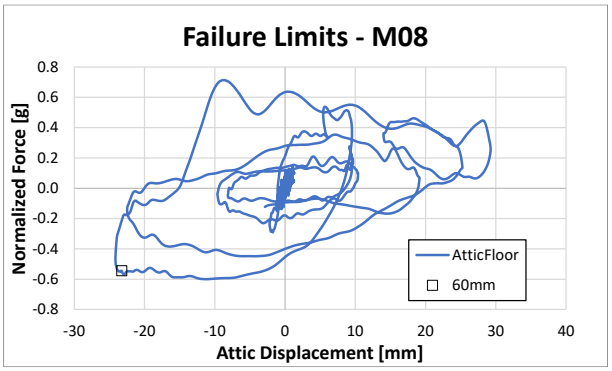

M08 – PGA x2

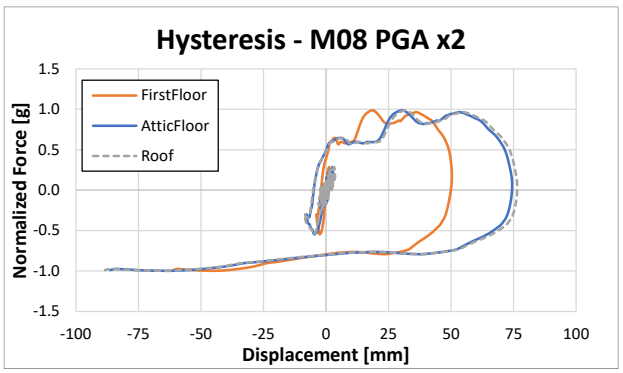

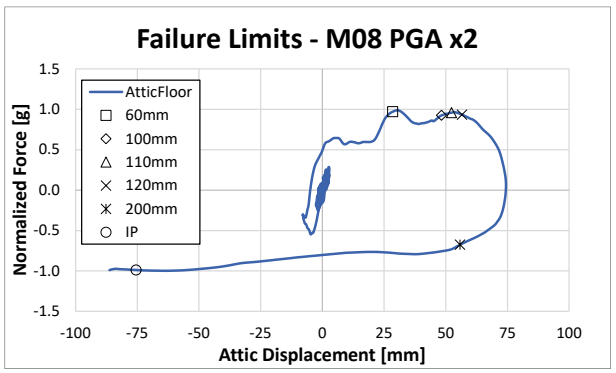

M09

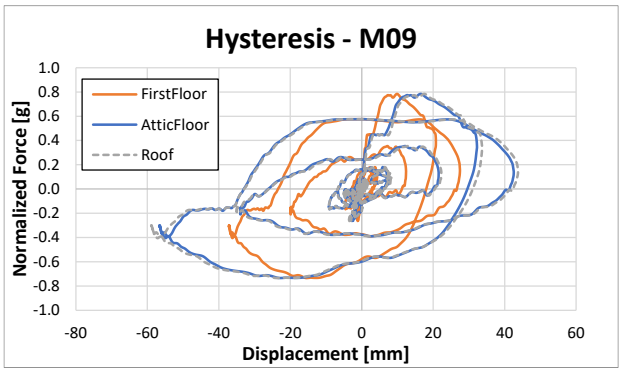

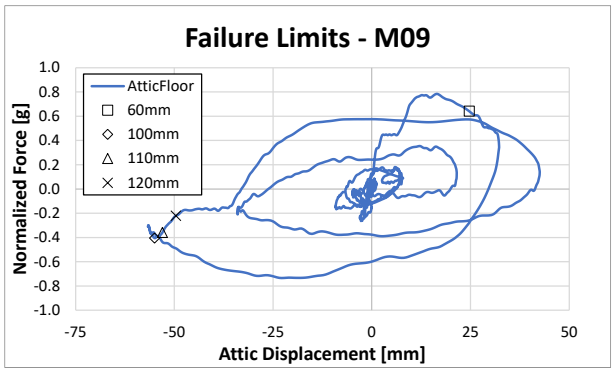

M09 – PGA x2

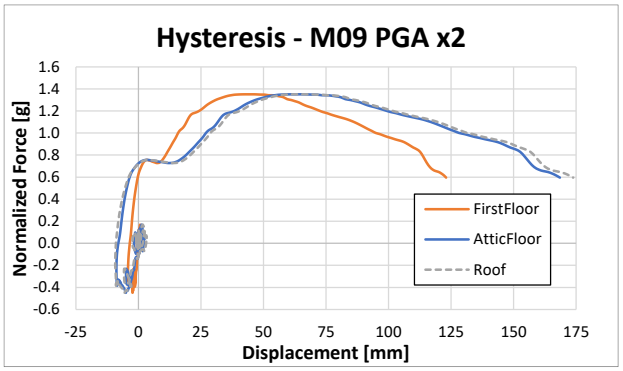

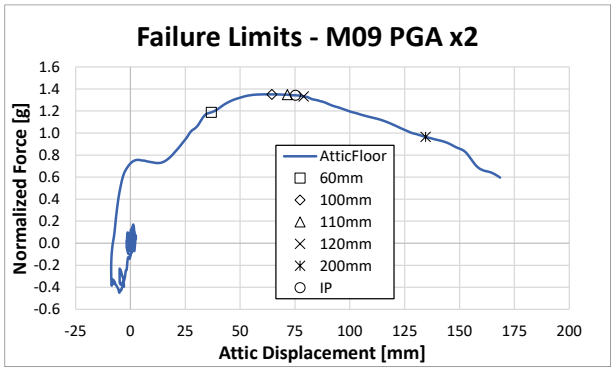

M10

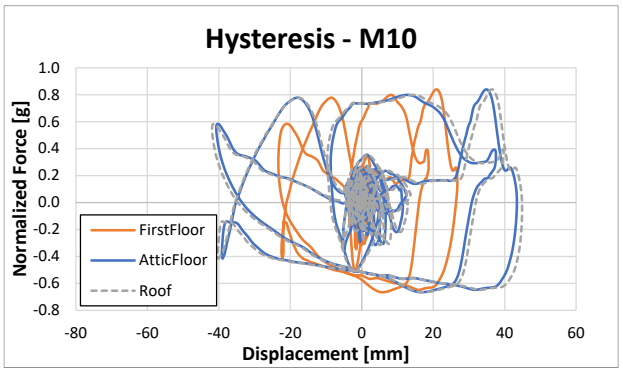

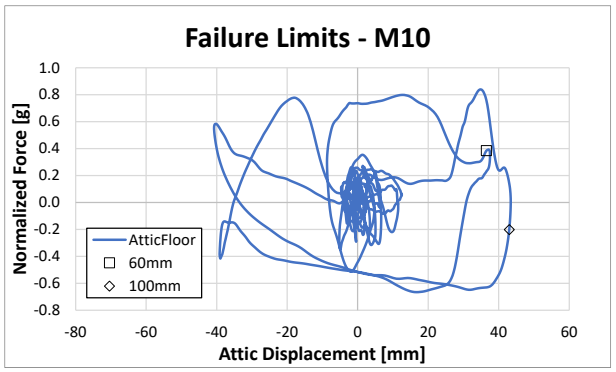

M10 – PGA x2

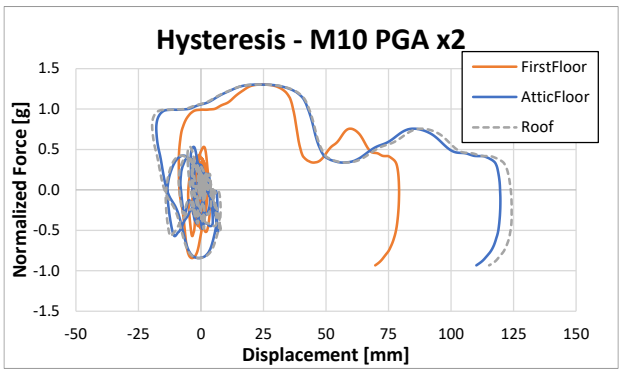

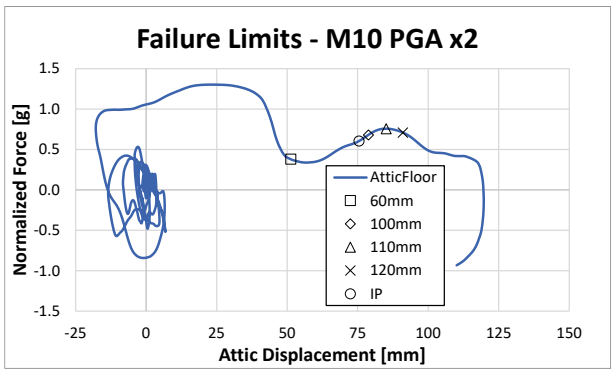

M11

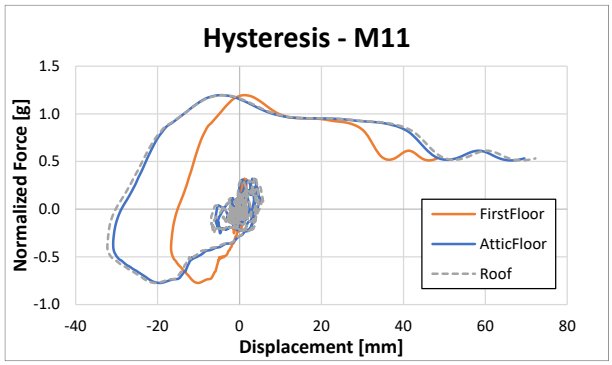

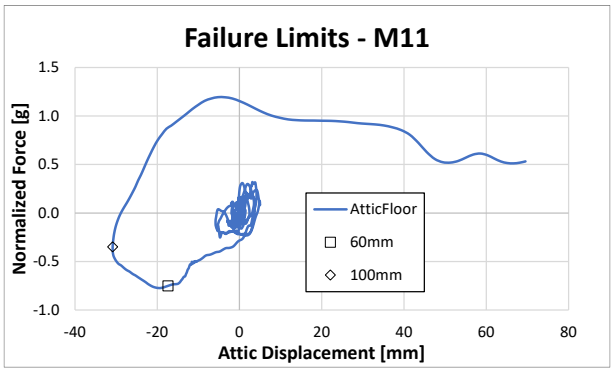

M11 – PGA x1.5

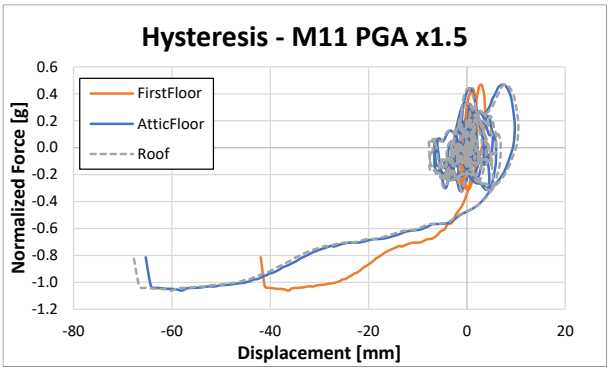

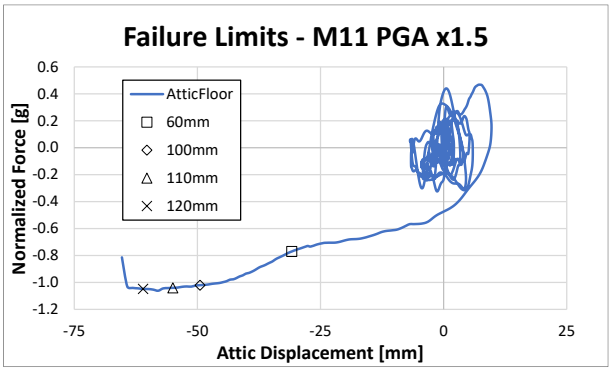

Table F1. Time step of the analyses when the failure criteria is reached for Bleeksteen building.

Failure Time [s]	**M8**	**M9**	**M10**	**M11**	**M8 PGA x2**	**M9 PGA x2**	**M10 PGA x2**	**M11 PGA x1.5**
OOP-060	3.1550	1.9350	2.2875	3.5175	2.7975	1.8325	2.2475	3.4300
OOP-100	/	2.3375	2.9825	3.6400	2.8650	1.8800	2.2825	3.5100
OOP-110	/	2.3600	/	/	2.8775	1.8900	2.2925	3.5250
OOP-120	/	2.3900	/	/	2.8900	1.9000	2.3025	3.5400
OOP-200	/	/	/	/	3.0250	1.9675	/	/
IP	/	/	/	/	3.1800	1.8950	2.2775	/